December 2012

Modeling Energy Production of Solar Thermal Systems and Wind Turbines for Installation at Corn Ethanol Plants

Elizabeth Ehrke
University of Wisconsin-Milwaukee

MODELING ENERGY PRODUCTION OF SOLAR THERMAL SYSTEMS AND WIND TURBINES FOR INSTALLATION AT CORN ETHANOL PLANTS

by

Elizabeth Ehrke

A Thesis Submitted in

Partial Fulfillment of the

Requirements for the Degree of

Master of Science

in Engineering

at

The University of Wisconsin-Milwaukee

December 2012

ABSTRACT

MODELING ENERGY PRODUCTION OF SOLAR THERMAL SYSTEMS AND WIND TURBINES FOR INSTALLATION AT CORN ETHANOL PLANTS

by

Elizabeth Ehrke

The University of Wisconsin-Milwaukee, 2012
Under the Supervision of Dr. John Reisel

Nearly every aspect of human existence relies on energy in some way. Most of this energy is currently derived from fossil fuel resources. Increasing energy demands coupled with environmental and national security concerns have facilitated the move towards renewable energy sources. Biofuels like corn ethanol are one of the ways the U.S. has significantly reduced petroleum consumption. However, the large energy requirement of corn ethanol limits the net benefit of the fuel. Using renewable energy sources to produce ethanol can greatly improve its economic and environmental benefits. The main purpose of this study was to model the useful energy received from a solar thermal array and a wind turbine at various locations to determine the feasibility of applying these technologies at ethanol plants around the country. The model calculates thermal energy received from a solar collector array and electricity generated by a wind turbine utilizing various input data to characterize the equipment. Project cost and energy rate inputs are used to evaluate the profitability of the solar array or wind turbine. The current state of the wind and solar markets were examined to give an accurate representation of the economics of each industry.

Eighteen ethanol plant locations were evaluated for the viability of a solar thermal array and/or wind turbine. All ethanol plant locations have long payback periods for solar thermal arrays, but high natural gas prices significantly reduce this timeframe. Government incentives will be necessary for the economic feasibility of solar thermal arrays. Wind turbines can be very profitable for ethanol plants in the Midwest due to large wind resources. The profitability of wind power is sensitive to regional energy prices. However, government incentives for wind power do not significantly change the economic feasibility of a wind turbine. This model can be used by current or future ethanol facilities to investigate or begin the planning process for a solar thermal array or wind turbine. The model is meant to aide in the planning stages of a renewable energy project, and advanced investigation will be needed to move forward with that project.

TABLE OF CONTENTS

LIST OF FIGURES

LIST OF TABLES

LIST OF ABBREVIATIONS

AC	Alternating Current
ACE	American Coalition for Ethanol
AWEA	American Wind Energy Association
Btu	British thermal unit
CFDC	Clean Fuels Development Coalition
DDG	Dry distillers grain
DOE	United States Department of Energy
DSIRE	Database of State Incentives for Renewables & Efficiency
DWG	Distillers wet grain
EIA	U.S. Energy Information Administration
EPA	Environmental Protection Agency
ESIA	Energy Independence and Security Act
GHG	Greenhouse gas
GWEC	Global Wind Energy Council
IEA	International Energy Agency
IEA SHC	International Energy Agency's Solar Heating and Cooling Programme
IPCC	Intergovernmental Panel on Climate Change
ITC	Investment Tax Credit
MMBtu	Million British thermal units
MTBE	Methyl Tertiary Butyl Ether

NASA	National Aeronautics and Space Administration
NREL	National Renewable Energy Laboratory
O&M	Operational and maintenance
ODEC	Organization for Economic Co-operation and Development
POWER	Prediction of Worldwide Energy Resource Project
PPA	Power Purchase Agreement
PTC	Production Tax Credit
RFA	Renewable Fuel Association
RFS	Renewable Fuel Standard
RPM	Revolutions per Minute
SSE	Surface meteorology and Solar Energy
SPF	Institut für Solartechnik (Institute for Solar Technology)
TSR	Tip speed ratio
USDA	United States Department of Agriculture

LIST OF SYMBOLS

a_1	Solar efficiency coefficient 1 (W/m^2K)
a_2	Solar efficiency coefficient 2 (W/m^2K^2)
A_a	Aperture area of solar collector (m^2)
A_c	Total area of solar collector (m^2)
A_s	Swept area of wind turbine (m^2)
C_f	Capacity factor of wind turbine
C_{fa}	Actual capacity factor of wind turbine
C_P	Coefficient of power of wind turbine
C_{pa}	Actual coefficient of power of wind turbine
C_{pd}	Design coefficient of power of wind turbine
CS_s	Cumulative cost savings for solar array
CS_w	Cumulative cost savings for wind turbine
D_R	Diameter of rotor (m)
E_{Btu}	Energy generated by wind turbine (MMBtu/yr)
E_w	Energy generated by wind turbine (kWh/yr)
E_{wt}	Theoretical energy generated by ideal wind turbine (kWh/yr)
ER	Ethanol plant electricity requirement (kWh/gal-ethanol)
$F_R(\tau\alpha)$	Collector heat removal factor times transmittance-absorptance product
F_RU_L	Collector heat removal factor times collector heat loss coefficient (W/m^2-^oC)
G	Solar irradiation (W/m^2)

G_t	Solar insolation on a tilted surface (kWh/m^2/day)
G_{ta}	Yearly average solar insolation on a tilted surface (kWh/m^2/day)
H_{day}	Number of hours per day (h/day)
H_y	Number of hours in one year (h/yr)
IC_{sc}	Installed cost per square foot of solar collector ($/ft^2)
IC_{wt}	Installed cost per kilowatt of wind turbine ($/kW)
L_f	Load factor of solar array
MW_B	Boiler makeup water requirement (gal-water/gal-ethanol)
MW_{total}	Total ethanol plant makeup water requirement
n_E	Annual percent increase of electricity price
n_{NB}	Annual percent increase of natural gas price
N_c	Number of collectors in solar array
N_d	Number of days
N_p	Number of solar panels
P_C	Ideal power capacity of a wind turbine (kW)
P_w	Power output of wind turbine (kW)
PC	Plant capacity (MGY)
PP_s	Simple payback period for solar array (years)
PP_w	Simple payback period for wind turbine (years)
Q_{AE}	Total heating requirement per gallon ethanol (Btu/gal-ethanol)
Q_{AE}^{Cook}	Energy to cook ethanol (Btu/gal-ethanol)
Q_{AE}^{D}	Energy to distill ethanol (Btu/gal-ethanol)
Q_{MW}	Total heating requirement of the boiler makeup water (Btu/gal-ethanol)

Q_{Total}	Total heating requirement of ethanol production (MMBtu)
Q_u	Useful solar energy (MJ/yr)
Q_{ut}	Useful solar energy (MMBtu/yr)
R_E	Electricity rate ($/kWh)
R_{NG}	Natural gas rate ($/MMBtu)
S_E	Yearly electricity cost savings ($/yr)
S_{NG}	Yearly natural gas cost savings ($/yr)
SC	Solar array total installed cost ($)
T_a	Average ambient temperature (^oC)
T_i	Average inlet temperature of the working fluid (^oC)
T_m	Mean temperature of working fluid in collector (^oC)
V_w	Wind speed (m/s)
V_a	Actual wind speed at wind turbine hub height (m/s)
V_d	Design wind speed for wind turbine (m/s)
WC	Wind turbine total installed cost ($)
η_a	Efficiency of solar array based on aperture area
η_{ap}	Efficiency of panel based on aperture area
η_c	Efficiency of solar array based on gross collector area
η_{cp}	Efficiency of panel based on gross collector area
η_o	SPF solar efficiency coefficient
η_{spf}	Solar panel efficiency using SPF coefficients
ρ_a	Density of air (kg/m^3)
$\%S_{MW}$	Percent shift from natural gas to solar energy for the boiler makeup water

$\%S_w$	Percent shift from conventional electricity to wind energy
$\%S_s$	Percent shift from natural gas to solar energy
$\%W_B$	Percent of makeup water used by the boiler

CHAPTER 1: INTRODUCTION

Energy is a global concern. There are limited sources of conventional energy like fossil fuels, and alternatives are generally expensive, limited in capacity, or represent technology still in need of development. Growing concerns over global climate change and energy security have lead to expanded use of renewable energy sources like fuel ethanol, wind power, and solar energy. These technologies are expected to grow in capacity to meet rising global energy requirements to help offset fossil fuel use. One of the benefits of wind and solar energy is that it is available to everyone. Unlike a coal-fired power plant that must be continually managed, a wind turbine can generate energy in a cornfield with little supervision. Solar thermal installations require slightly more oversight, but the use of modern control systems makes a solar thermal array easy to manage.

Both wind power and solar energy can be used to offset the copious fossil fuel consumption at an ethanol plant. One of the main drawbacks of corn ethanol is the energy requirement to produce the fuel. Ethanol is considered a renewable fuel because it is made from corn that uses the sun's energy to grow, but the current production methods of ethanol represent a non-renewable process. Increasing the amount of renewable energy used for the production of ethanol will reduce fossil fuel use, decrease greenhouse gas emissions, and ultimately reduce the ethanol plant's energy costs.

The economics of a wind or solar energy project is not as straightforward as it may seem. There are many factors that determine the economic feasibility of a renewable energy project. Wind and solar resources vary widely across the country and

not every location is an ideal candidate for either technology. The type and size of the equipment influence costs and potential energy savings. The current cost of energy plays a major role in the financial advantage of a renewable energy project as well. All of these factors make it difficult to give a good estimate for the initial costs, payback period, and cost savings of a wind turbine or solar thermal system. General assumptions about wind and solar energy are not applicable to a wide range of locations and project specifications.

The main purpose of this project is to create a model that can be used to evaluate the feasibility of installing a wind turbine or solar thermal array at a corn ethanol plant. The model can be used with plant-specific information to accurately estimate the useful energy produced by a wind turbine and solar array at that location. Cost estimates for the renewable energy installation along with the current price of natural gas and electricity are then used to find the payback period and cost savings of each project. Numerous variables can be changed to simulate different conditions for the renewable energy technology, energy prices, and government incentives. This allows a wide range of projects to be considered by the same model. It also enables the user to compare several project options or different financial circumstances.

The estimated energy output of the model was verified by using experimental and operational data for solar thermal panels and utility-scale wind turbines. Experimental test data from the Institute for Solar Technology (SPF 2012) was used to compare the model outputs to the real performance of the average solar thermal panel. Wind turbine model outputs were compared to the averaged yearly output of hundreds of large-scale wind turbines in the U.S. for 2011 (Wiser and Bolinger 2012).

The model was then used to assess the solar and wind resources at 18 different U.S. ethanol plant locations. The economic feasibility of a solar thermal array and a wind turbine was evaluated for each plant. The locations were chosen to represent a wide variety of conditions to find the best areas for wind power and solar energy systems. Various inputs were changed to determine the effects on payback period and cost savings. Current federal tax incentives were also considered to determine their financial influence on wind and solar projects. Realistic conditions were chosen to represent an accurate estimate of costs and energy savings. Recommendations are then given for the best areas for the application of solar energy and wind power.

This project continues the work of Kumar (2009), in which he created a model for the energy requirements of a dry mill ethanol plant. Numerous design characteristics of an ethanol plant can be entered to determine the natural gas requirements of a dry mill corn ethanol plant. The ethanol model was also verified for its accuracy. The energy requirement output for a specific corn ethanol plant from Kumar's model can be used as an input for this model to determine the percent shift to solar energy. Kumar's model also calculates the payback period and cost savings of a solar and wind project. His solar and wind calculations are limited due to few design inputs and inadequate information to help guide the user on realistic values for the solar energy and wind power calculations. The wind calculations were not based on the available equipment on the market. Instead of using a turbine of known dimensions, the dimensions were calculated depending on the percent shift to wind power. This created a problem, because there are only certain dimensions commercially available and wind turbine prices are based on design size not actual power generated. The model created for this project improves the methods for

calculating useful solar energy and wind power. This project takes Kumar's research even further by not only creating a model, but also using that model to evaluate solar and wind resources at ethanol plants across the country.

The renewable energy market is quickly growing and is expected to continue expanding due to decreasing equipment prices, energy security concerns, and environmental policy. A growing market means lower costs and better technology. This indicates that wind and solar installations cost less and perform better than past equipment. The current state of the solar thermal and wind industries is discussed in the following chapters. Market projections for fossil fuels and renewable energy are also included to show what the future of energy and energy costs might look like in the next 20 years.

Ethanol, wind power, and solar energy will all be a part of the energy matrix over the next 20 years. Using wind and solar energy to produce ethanol can increase ethanol's sustainability and reduce overall energy costs. Not only can these renewable energy resources save money, but they can also contribute to America's goals of reducing fossil fuel use, decreasing greenhouse gas emissions, and increasing energy security.

CHAPTER 2: BACKGROUND

2.1 Introduction

As the world economies advance, the demand for energy continues to increase. Many agree that fossil fuels alone will not be able to sustain this level of consumption. Fossil fuels like petroleum, coal, and natural gas must soon give way to greener technologies like ethanol, wind, and solar energy. It is imperative that economic analysis be made available to ease this transition from the old to the new age of energy. Though we are most likely more than a half century away from depleting our fossil fuel resources (Fay and Golomb 2012), action must be taken now to avoid energy shortages later. Ethanol, wind, and solar energy will not be the only solution to the energy problem, but they provide a viable option to reduce fossil fuel use right now.

The following sections will examine relevant historical and predictive market information to characterize the current and future state of conventional and renewable energy sources. Fuel ethanol, wind power, and solar energy are described in detail to provide general background information and illustrate how each technology fits into the U.S. energy market. Global energy and economic issues are briefly discussed as well. The main focus is to provide background information for the study of the feasibility of wind and solar installations at ethanol plants to reduce fossil fuel consumption.

2.2 Ethanol Background

Ethanol has been used for years as a fuel additive as a way to reduce gasoline consumption, raise the octane level of fuel, and reduce pollution (CFDC 2010). Ethanol

is a clean burning, biodegradable fuel additive that acts as an oxidizer to facilitate a more complete combustion of gasoline. Most of the ethanol produced in the U.S. comes from corn crop in the Midwest. Cellulosic ethanol and advanced biofuel production have shown promising advantages over corn ethanol for reducing greenhouse gas (GHG) emissions and energy inputs, but obstacles still exist to large-scale development of this technology. Since much of the energy contained in corn and cellulosic materials comes from the sun, these are considered renewable fuels. One of the main reasons corn ethanol is not completely renewable is the energy required to cook and distill the corn feedstock. Producing ethanol requires process heat and electricity is needed to run the plant. Over 90% of U.S. facilities use natural gas for process heat (RFA 2012a) and use electricity generated mainly from coal and natural gas. Reducing fossil fuel use in the production of ethanol will make the process more sustainable.

The majority of ethanol plants are located throughout the Midwest where corn is most plentiful. This ensures adequate supply and reduces transportation costs between the farm and the ethanol production facility. A map of U.S. corn production and ethanol plant locations is shown in Figure 2.1. Some of the ethanol plants located in areas seemingly devoid of corn crop actually have corn production, but the corn crop was not estimated for this figure. In addition, there are several plants that use feedstock other than corn. About 90% of the ethanol plants in the U.S. use the dry mill process to produce ethanol from corn (RFA 2012a). This study focuses on corn ethanol produced from dry mill plants using natural gas for process heat. The wind and solar resources at the current locations of ethanol plants will be used to assess the viability of using these renewable energy sources.

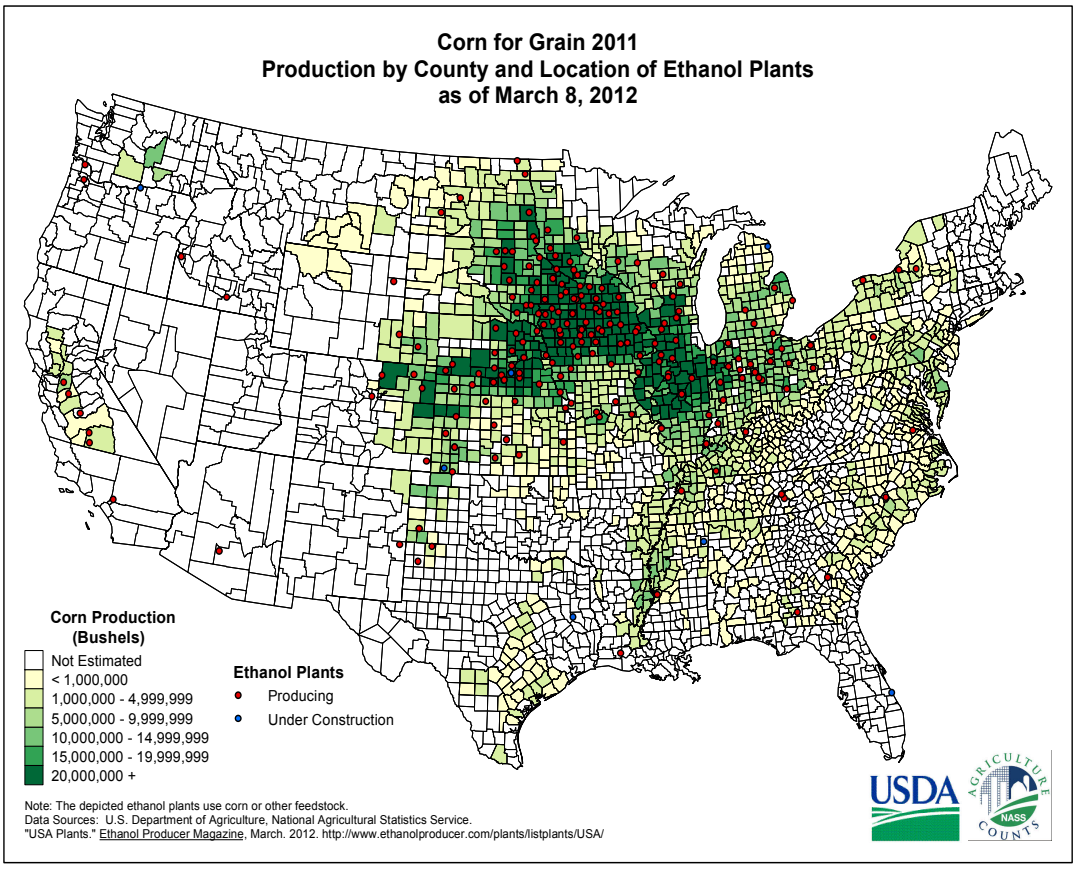

Figure 2.1: U.S. map of ethanol plant locations as of March 2008 and estimated number of bushels of corn produced in 2011 (USDA 2011).

Another advantage to placing ethanol plants near farmland is the proximity to livestock. The main co-product of ethanol plants, distillers grains, is sold as an additive to livestock feed. Wet and dry distillers grains have high protein content and are used in animal feed for the dairy, beef, swine, and poultry industries. If the ethanol plant is close enough to the livestock farm, the co-products can be sold as wet distillers grains, which significantly reduces the energy required to dry the grains for transportation. In 2011, ethanol co-products accounted for 12% of net corn use in the U.S., which amounted to 39.4 million metric tons of livestock feed (RFA 2012a). The corn used to produce

ethanol was 26% of the net corn use in 2011 or 3,437.5 million bushels of corn. The sale of co-products for animal feed greatly improves the economics and energy balance of ethanol production.

The ethanol industry has seen rapid growth due to energy, fuel, and pollution regulations. The industry has grown to 13.9 million gallons of ethanol produced in 2011 from just 1.6 million gallons in 2000 (EIA 2012a). This growth was a result of rising gas prices and government subsidies. Some of these incentives for corn ethanol are expiring naturally as the industry matures, but the ethanol market as a whole is expected to expand with tax incentives and energy mandates to accelerate the growth of cellulosic and advanced biofuels (RFA 2012a).

The amount of energy to produce this ethanol has decreased through numerous efficiency improvements and the use of waste heat. A survey of dry mill corn ethanol plants shows that the average energy and corn requirements to produce one gallon of ethanol have significantly decreased from 2001 to 2008 (Mueller 2010). Dry mill plants made up 86% of corn ethanol plants in 2008 and represented 9.27 billion gallons of operating capacity. In 2001, the average plant used 36,000 Btu of heating, 1.09 kWh of electricity, and 0.38 bushels of corn to produce one gallon of ethanol. The average plant in 2008 only used 28,859 Btu of heating, 0.74 kWh of electricity, and 0.36 bushels of corn to produce that same gallon of ethanol. This is 28% less thermal energy, 32.1% less electricity and 5.3% less corn required to produce the same gallon of anhydrous ethanol. The study included 90 of the 150 operating dry mill plants in 2008, and was a good representation of the industry because it included plants of all ages. The resource reduction in the production of ethanol was over the course of only 7 years. It is likely

that energy usage and corn requirements will continue to decrease moderately as data from newer plants are considered and existing plants incorporate energy saving equipment and procedures.

The U.S. government and the Department of Energy (DOE) have been long time supporters of increased production of fuel ethanol. The DOE succinctly sums up this support through their biofuels mission statement:

> The U.S. Department of Energy (DOE) is committed to advancing technological solutions to promote and increase the use of clean, abundant, affordable, and domestically- and sustainably-produced biofuels to diversify our nation's energy sources, reduce greenhouse gas emissions, and reduce our dependence on oil (DOE 2008).

They stress the importance of continued development of biofuels such as ethanol in order to meet the growing energy demand instead of relying on volatile foreign energy markets. Not only does ethanol reduce oil imports, but also reduces GHG emissions and creates American jobs.

Opponents of ethanol claim that it pollutes more than gasoline, but the DOE states that the average life cycle of ethanol production, when compared to the life cycle of gasoline production, significantly reduces greenhouse gas emissions. The average GHG reduction of corn ethanol compared to gasoline was 19% in a DOE report (2008). This value is dramatically increased when cleaner energy sources are used. Using natural gas for process heating reduces lifecycle GHG emissions by 28-39% according to Wang, Wu, and Huo (2007). Liska et al. (2008) show that GHG emissions can be reduced by 48-59% when modern farming methods, production practices and co-product sales are

considered. Cellulosic ethanol production can reduce GHG emissions by 86% if biomass is used for process heating (DOE 2008). The use of renewable energy sources for the production of corn ethanol will further reduce lifecycle GHG emissions when compared to gasoline.

The assertions of the DOE can be corroborated by Farrell et al. (2006) study that examined 6 reports and created 3 of their own models of the energy life cycle of ethanol to determine parameters used, assumptions made, and then standardize them using a new evaluation technique to reproduce their results to within a half percent. They found that the calculations are highly sensitive to the assumptions made in the parameters of the study, boundaries of the calculations, and differences in the various types of fossil fuels. They argue that the two studies that reported a negative energy balance for the ethanol life cycle misrepresented key variables in their calculations and ignored the energy consumption of the co-products of ethanol production. The largest disparities between the studies stem from the treatment of co-products that replace items like corn and soybean meal in animal feed, which inherently take energy to produce. There are several limiting factors to the study due to large differences in reported energy consumption, however the best estimate for corn ethanol is that it reduces petroleum use by about 95% and reduces GHG emissions by 13%. These values are similar to the data reported by the DOE. Farrell et al.'s study also found a dramatic environmental advantage to cellulosic ethanol, but concluded more research is needed to investigate the feasibility of large-scale cellulosic ethanol production. The study also found that agriculture practices account for 34-44% of GHG emissions and 45-85% of the petroleum inputs to the production of corn ethanol. Concluding that improving agriculture practices could significantly improve the

energy balance and GHG emissions in ethanol production. The article suggests that advancements in sustainable agriculture and cellulosic ethanol will grow the biofuels industry to ultimately reduce energy consumption and reduce negative environmental impacts.

There is some concern about the sustainability of increasing corn crop and other ethanol feedstock to meet the demand for increased biofuels. The DOE and the U.S. Department of Agriculture (USDA) conducted a study that concluded the U.S. could grow enough biomass to replace about 30% of current gasoline use without drastic changes to current land use (Perlack 2005). The report asserts this is more than adequate to meet the standards set by the Energy Independence and Security Act of 2007, which requires that 36 billion gallons of renewable transportation fuels be in use by 2022. Advancing technologies are increasing crop output per acre and reducing resource inputs. The act also caps the amount of corn ethanol to limit strain on the corn market. It is clear that the DOE has high hopes for cellulosic ethanol and its role in the future of ethanol.

Many ethanol opponents claim ethanol has a negative energy balance (Pimentel 2003) (Keeney and DeLuca 1992), but others specifically disprove these claims (Shapouri et al. 2002) (Farrel et al. 2006). The DOE (2008) reports that gasoline takes about 1.23 Btu to produce per 1 Btu of energy delivered. This is called a negative energy balance because it takes more non-renewable energy to produce than is delivered by the gasoline. Corn ethanol energy balance is about 0.73 Btu in per Btu delivered, while cellulosic ethanol energy balance is about 0.1 Btu in per Btu delivered. The report shows that gasoline is produced using energy derived almost solely from petroleum products, while ethanol uses almost entirely coal and natural gas. Natural gas and coal are more

abundant resources and are domestically available. Studies that show a negative energy balance typically ignore the co-products that are a result of ethanol production (Farrell et al. 2006) (Shapouri et al. 2002). The co-products from ethanol can be used as animal feed and replace other ingredients that take energy to produce. The studies also site technological advancements that have improved agricultural practices. Better farming methods have increased energy efficiency and reduced pollution. All of these factors lead to a positive energy balance for corn ethanol, which consumes less non-renewable energy than gasoline.

Another myth the DOE would like to dispel is the notion that 10% ethanol-gasoline blends significantly reduce the fuel economy of the vehicle. Since modern cars are designed to run on a 10% blend, there is no measurable reduction in vehicle fuel economy (ACE 2005). Since ethanol is generally less expensive than gasoline the slight reduction in fuel efficiency with ethanol blended gasoline is offset by the lower cost. Knoll (2009) concludes that 10% ethanol blends reduce fuel efficiency by 3-4%. Gasoline burns more completely when using an oxygenate like ethanol, which reduces some harmful pollutants. Ethanol replaced MTBE as a fuel oxygenate after MTBE was found to contaminate groundwater (DOE 2012). There is some disagreement about ethanol's ability to reduce harmful tailpipe emissions and reduce pollution (Niven 2004), but Knoll (2009) finds that most agree 10% ethanol blends reduce carbon monoxide by 15% and non-methane hydrocarbons by 12%. Even though tailpipe emissions are only moderately reduced, ethanol currently displaces 485 million barrels of imported oil a year (RFA 2012a). This supports the U.S. economy and reduces fuel use required to transport the oil to America. The DOE asserts that further advancement of agriculture practices

combined with increased use of renewable energy sources in the production of ethanol will continue to reduce GHG emissions. It is clear that although ethanol may have some drawbacks, ethanol is reducing GHG emissions and petroleum use. By substituting fossil fuel with renewable energy sources in the production of ethanol, the negative environmental impacts can be dramatically reduced.

2.3 Energy and Economic Concerns

Energy runs our cities and powers our cars, but that energy is coming at an ever-increasing cost. Not only is the cost of energy rising, but also the growing need for energy is creating tension in global relations and straining the environment. According to the U.S. Energy Information Administration (EIA 2012b), 82% of the energy consumed in the United States in 2011 was in the form of fossil fuels. In addition, the total energy consumed in the U.S. has steadily increased over the past 60 years, with 2.8 times the amount of energy consumed in 2011 as compared to 1950. Global demand for energy is expected to continue to rise as China and other non-OECD countries substantially increase their energy use over the next 25 years. There is a finite amount of fossil fuel on our planet, which means there is a looming deadline to implement the widespread use of sustainable and renewable energy.

It is not clear how long the Earth's reserves of oil, coal, and natural gas will last, but everyone agrees they will not last indefinitely at the current rate of consumption. Estimating the lifespan of fossil fuels is complicated due to an ever-changing energy market and numerous supplies of unconventional resources that are not yet proven. Fay and Golomb's (2012) best estimate for the useful lifespan of the fossil fuel resources is

170-190 years for coal, 50-60 years for oil, and 60-65 years for natural gas. They note that unconventional resources may be able to significantly extend these timeframes, but the cost of recovering those fossil fuels will dramatically change the cost of energy.

The global energy market is inherently unstable, which will continue to cause conflicts as the demand for energy increases. The first indication of an unstable energy market was the 1973 oil crisis, which brought gas shortages, an economic recession, and widespread energy conservation in the United States. Further motivation for energy independence and conservation came when the second oil crisis hit in 1979. In response to the oil crisis, the U.S. government eliminated a federal fuel tax on gasoline blended with 10% ethanol in 1978. Tax incentives for ethanol-blended gasoline continues today as a method of reducing petroleum consumption and increasing the energy independence of the United States.

The demand for all types of energy, including liquid fuels like petroleum and ethanol, is expected to increase globally over the next 25 years. This puts even more importance on U.S. energy independence as competition for fossil fuel reserves increase. The EIA (2012a) predicts global energy use to increase by over 52% between 2008 and 2035 through their extensive modeling of the energy market. This report projected that China and the other non-OECD countries will account for most of this growth as shown in Figure 2.2. Petroleum and other liquid fuels continue to be the largest source of energy worldwide through the year 2035, with most of the growth of liquid fuel consumption attributed to the transportation sector, according to the model. The rising growth of energy consumption in the transportation sector verifies the need for continued

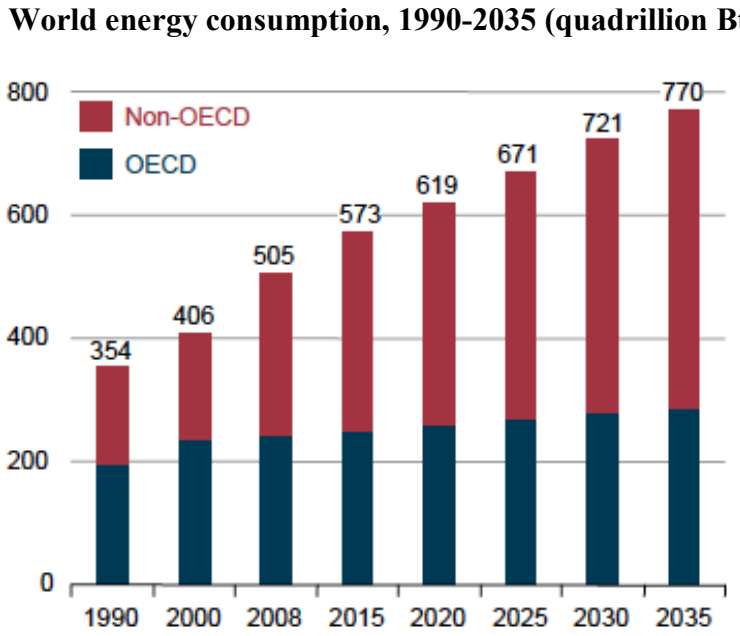

Figure 2.2: World energy consumption in quadrillion Btu with historical data for 1990-2008 and projections for 2015-2035 (EIA 2011, 1).

development of affordable renewable energy sources for transportation. This will help offset some petroleum consumption and decrease U.S. dependence on foreign oil.

Petroleum is the United States' largest import, export, and most-consumed single form of energy. The U.S. is highly dependent on the use of petroleum, which made up 36% of the total domestic energy use and 85% of the energy imports in 2011 (EIA 2012b). The transportation sector used the largest portion of petroleum, consuming 71% of the petroleum, which made up 93% of the energy consumed by the transportation sector. Only 4% of the energy used by the transportation sector came from renewable energy sources, which includes fuel ethanol. With this type of energy distribution, it is clear that petroleum has a major influence on America's economy and must be considered in all discussions of U.S. energy security.

The development of gasoline alternatives has been motivated by the instability of the oil industry. The price of oil is anything but stable. Predictions for the price of oil are highly dependent on global relations, new oil discovery and refinement, as well as the state of the global economy. The EIA (2012a) has projected the price of oil in three future conditions, which is shown in Figure 2.3. The historical spike in oil prices as a result of the two oil crises in the 1970's can be seen in the first half of the 1980's. Oil prices rose through the 2000's and dropped as a result of the worldwide economic downturn in 2008. The price of oil is recovering and is expected to steadily increase for the next 20 years in addition to inflation. The high and low oil price cases represent high demand and low demand for oil respectively. It is clear that oil prices in the future will be highly variable and hard to predict. This is one of the many reasons to reduce oil consumption by use of biofuels thus reducing dependence on foreign oil and depletion of reserves.

Average annual world oil prices in three cases, 1980-2035 (2010 dollars per barrel)

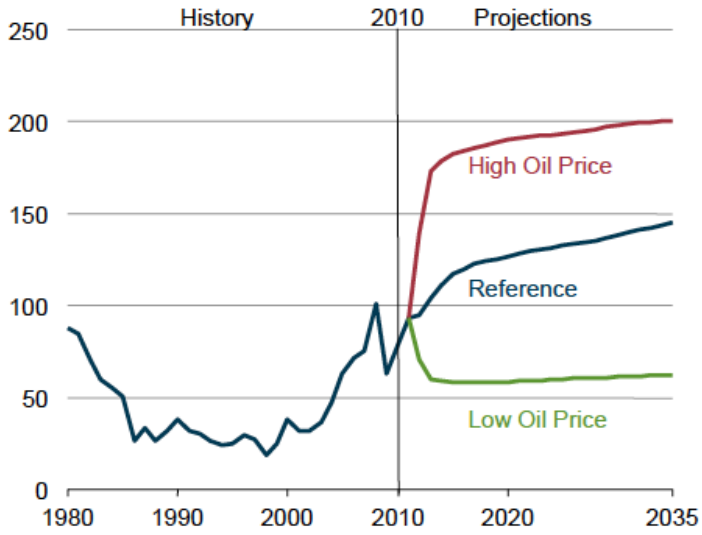

Figure 2.3: World oil prices in 2010 dollars per barrel for the EIA reference, high oil price and low oil price cases (EIA 2012a, 24).

The United States has taken a strong stance supporting the production and expanded development of renewable fuels. The Energy Policy Act of 2005 created the Renewable Fuel Standard (RFS), which mandates the amount of renewable fuels that are blended with transportation fuel. The policy was expanded in 2007 to create renewable fuel standards through 2022. Much of the expanded production of renewable fuels mandated by the RFS must reduce GHG emissions by 50% or more, which eliminates conventional corn ethanol as a possibility. This does not indicate that corn ethanol is being phased out but merely limits vast expansion of the industry. Corn ethanol production is still expected to grow over the next 10 years. However, cellulosic and advanced biofuels are anticipated to dramatically expand over this same period. The RFS transportation biofuels mandates are illustrated in Figure 2.4. The graph shows rapid growth of the biofuels industry, with increasing production required across all types of

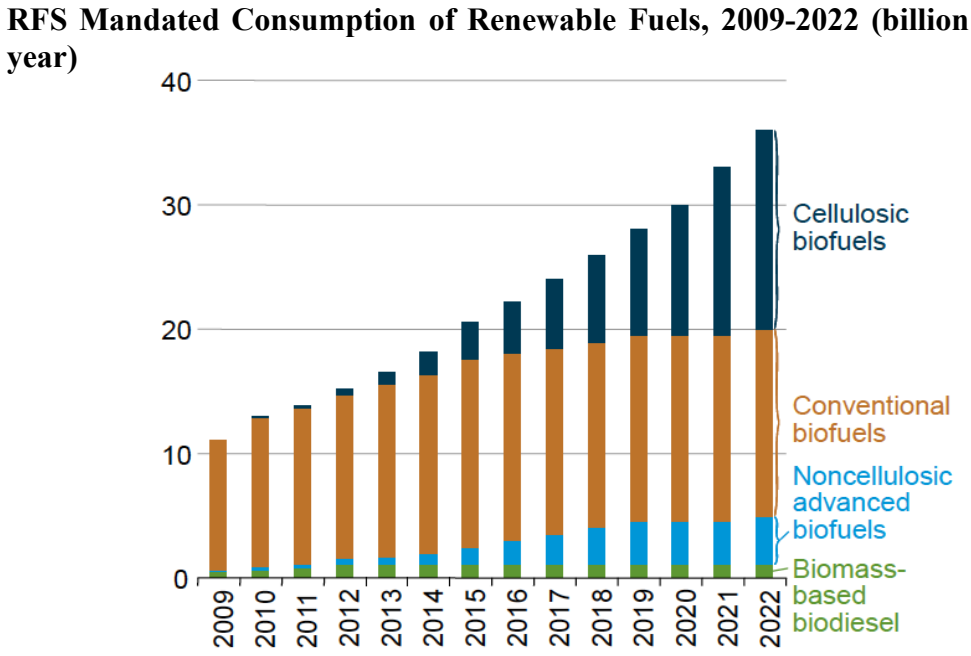

Figure 2.4: RSF renewable fuels mandates through 2022 (EIA 2012a, 4)

renewable fuels. Most of the increase in renewable fuel production is assigned to cellulosic biofuels with more moderate growth in noncellulosic advanced biofuels, conventional biofuels, and Biomass-based biodiesel.

Actual production of cellulosic biofuels has not met the original RSF standards, which has resulted in the EPA lowering renewable fuel requirements in 2010, 2011 and 2012. This will significantly delay the full realization of the RSF mandates, but the EIA 2012 projections estimate the original standards will by met by 2035. The EIA projections are displayed in Figure 2.5, which shows delayed production of cellulosic ethanol and biomass-to-liquids. Rapid growth of these industries after technological and financial barriers are overcome allows the production of renewable fuels to meet the RSF standards before 2035.

EISA 2007 RFS credits earned in selected years, 2010-2035 (billion credits)

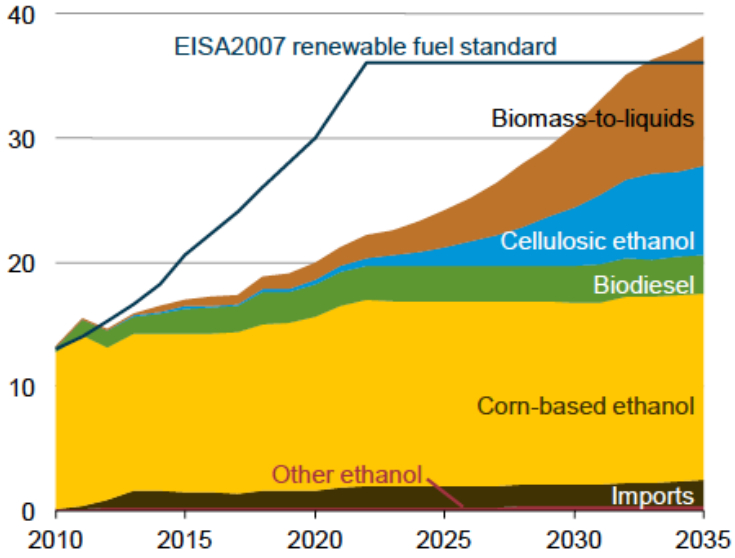

Figure 2.5: Projections of renewable fuel production in billions of gallons through the year 2035 compared to 2007 RFS mandates (EIA 2012a, 97).

The motivation behind the RSF mandates is two-fold. Increasing biofuels production reduces gasoline consumption which in turn reduces oil imports. This improves U.S. energy independence and reduces the effects of fluctuations in global oil prices. Domestic production of biofuels creates jobs and supports local economies, while importing foreign oil does little to support the U.S. economy. Another desired effect of the biofuel mandates was a more rapid reduction of GHG emissions. When biofuels are compared to petroleum transportation fuels on a life-cycle basis, they can significantly reduce GHG emissions.

The burning of these fossil fuels produces large quantities of carbon dioxide and other greenhouse gases. The intergovernmental panel on climate change concludes that:

> Most of the observed increase in global average temperature since the mid-20th century is very likely due to the observed increase in anthropogenic greenhouse gas concentrations… Recent data confirm that consumption of fossil fuels accounts for the majority of global anthropogenic greenhouse gas concentrations (Eidenhofer et al. 2011).

This report by the Intergovernmental Panel on Climate Change (IPCC) concludes that human consumption of fossil fuels has led to climate change. Among other suggestions, the IPCC recommends improving energy conservation and efficiency while developing renewable energy sources to mitigate climate change. Not only can renewable energy sources reduce GHG emissions, but they can also lead to economic development, greater energy independence, and reduce negative impacts on the environment and human health (Eidenhofer et al. 2011). Some of the effects of climate change are loss of glaciers, loss of species, increase in severe weather, and increased flooding. Renewable energy

sources like solar, wind, and biofuels have the potential to replace energy produced by fossil fuels, reduce GHG emissions, and increase U.S. energy independence while reducing contributions to climate change.

Energy is a complex problem and will not be solved with a single solution. Systematically reducing energy consumption and increasing the use of available renewable resources will extend the life of fossil fuel resources, reduce the vulnerability of the U.S. to uncertain global relations, and hopefully decrease the negative effects of global climate change by reducing GHG emissions.

2.4 Wind Energy

Wind power is a renewable source of electricity that is available across the country and across the globe. Power can be generated in large wind farms, distributed in community wind projects, or produced in large offshore installations. The versatility of wind power has lead to installations in 38 U.S. states and 75 countries worldwide (GWEC 2012). There are currently 5 U.S. states that generate at least 10% of their electricity from wind power, with North Dakota producing 22% of its electricity from wind power in 2011 (Roney 2012). Turbines do not produce GHG emissions nor do they have continuous fuel and water requirements like most forms of electricity generation. Individual turbines use very little space and can be placed on land used for other purposes including farmland or private businesses. Electricity production from wind turbines is rapidly increasing. The wind market has grown significantly due to government incentives and falling turbine prices. Wind is the fastest growing form of renewable electricity generation and is slated to continue to grow over the next 20 years

and beyond. Even though the number of wind projects has vastly increased over the last six years, electricity generation form wind only accounted for 3.3% of the U.S. electricity demand at the end of 2011 (Wiser and Bolinger 2012). There are still many avenues for expanded development of the wind market, but it is unlikely that wind power alone can solve the global energy problem.

Large-scale turbines are precisely designed to extract as much energy from the wind as possible. The growing demand for wind energy has broadened the market, which now includes turbines for a large range of wind speeds, conditions, and power capacities. Wind turbines convert the linear kinetic energy of the wind to rotational energy that turns a generator, which converts this energy into electricity. Precisely designed turbine blades are designed similar to an airplane wing in that the air has a longer distance to travel on one side of the blade as compared to the opposite side. Wind flows over the blade and creates lower pressure on the downside of the blade. The pressure difference causes the blades to rotate around a central shaft or rotor. The pitch of the blades can be adjusted with changing wind speeds to obtain the proper rotational speed. The direction the turbine is facing can also be adjusted as the wind direction changes. A brake is also included on the rotor to prevent damage from excessive wind speeds or allow maintenance. These adjustments are generally performed by the control system that receives information from an attached anemometer and wind vane to measure wind speed and direction.

The large size of the average utility scale wind turbine means that the rotor only completes about 6-18 revolutions per minute. The RPM is increased to around 1800 RPM by a system of gears, which is generally called the gearbox. This faster rotation

runs a generator that converts rotational energy to electricity. The generator and gearbox system is usually called the drive train. The drive train and shaft are contained within the nacelle, which sits on the tower. The tower can be as short as 30 meters tall for residential turbines to 200 meters tall for the largest offshore turbines. The average wind turbine in 2011 had a nameplate capacity of 1.97 MW with a hub height of 81 meters with a rotor diameter of 89 meters (Wiser and Bolinger 2012). The overall size of wind turbines is slowly increasing, with rotor diameter increasing more rapidly over the last three years. Higher wind speeds are available at higher altitudes and larger blades can sweep a larger area. The two largest factors in determining the power produced by a wind turbine are the wind speed and swept area of the rotor blades. The higher cost and additional logistics of a taller tower and larger rotor must be balanced by the additional power that can be generated with higher wind speeds and greater area.

The turbine must also be designed to work with the power grid in order to supply useful energy. An inverter is needed to produce AC current that is synchronized with the grid. Transmission lines need to be installed to convey the power to users. Metering and overcurrent protection are also vital to protect the system and verify output. In addition to standard power transmission equipment, wind turbines also benefit from predictive models that help the utility company adjust for changing wind speeds. This is one of the drawbacks of wind power, because the power generated depends on the environment and not power demand. The changes in power output of a large wind farm or many farms across a state must be compensated for using operating reserves. Small wind installments do not generally need predictive modeling due to the relatively low power input compared to the demand of the system. Wind turbines can produce anywhere from a few

kilowatts of power for residential sized systems or over 7 MW of power for the largest turbines available. The power ratings of turbines will be described in greater detail in the following sections.

The U.S. wind industry is showing large capacity additions despite a struggling economy. Over 70% of the total installed capacity was added in the past five years. Despite a substantial drop in new wind projects in 2010 due to economic uncertainty, the total installed wind capacity in 2011 was nearly 47 GW as compared to about 11 GW in 2006 (Wiser and Bolinger 2012). The average project price as well as the maintenance costs of new projects continues to decline according to Wiser and Bolinger. Many wind projects have benefited from renewables portfolio standards (RPS) in their respective states that require a certain percentage of electricity production come from renewable sources. State and federal incentives provide financial support, which has made wind power more favorable to investors that want to reduce the financial risks of a new project.

The two main incentives for wind projects are the Business Energy Investment Tax Credit (ITC) and the Renewable Electricity Production Tax Credit (PTC) (DSIRE 2012). The ITC provides a 30% tax credit on the installed cost of specific renewable energy projects. The PTC allots $0.022 per kWh generated by certain renewable electricity projects. Both of these credits are expiring for large-scale wind projects at the end of 2012 and may not be extended.

Wind resources are fairly consistent year-to-year and have been well-documented to aid the development of new projects. A map of the U.S. wind resources at a height of 80 meters is shown in Figure 2.6. Most of the wind resources are located in the center of the U.S., east of the Rocky Mountains. Hub heights of 80 meters are most common for

large and utility scale wind projects. Community wind projects have smaller turbines with hub heights of 50 meters, while residential hub heights are around 30 meters. Much of the installed wind capacity is located in areas with average wind speeds of 6.5 m/s or larger, which is considered suitable for wind large-scale wind development according to the DOE. A map of the locations and sizes of wind turbines installed in the U.S. as of the third quarter of 2012 is shown in Figure 2.7. The locations on the map are not exact to more clearly show the number of wind installations. Wind projects are spread across the country, but notably there are still large areas of the country that are suitable for wind installations that have not been utilized. This will allow expansion of the industry for years to come.

The growth of the wind industry in the U.S. has been rapid due in part to progressive energy standards and incentives, but the future of government support for wind power is uncertain. Federal and state incentives have contributed to increased wind installations, but many of these incentives have reached their distribution limits or are expiring at the end of 2012 (DSIRE 2012). Typical incentives reimburse part of the installed cost, guarantee the purchase price for electricity produced, or give tax credits for equipment depreciation. In particular, turbine manufacturers are waiting to see if the PTC will be extended beyond 2012. If this credit is not extended, industry experts predict dramatically reduced sales in 2013. Diminishing grants, incentives and tax credits are expected as the industry matures and moves into a more sustainable level of government support. Even with reduced funding for projects, wind power is profitable and will continue to grow. Growth in the U.S. may be slower than in recent years, but projections for the future of the industry all indicate robust expansion.

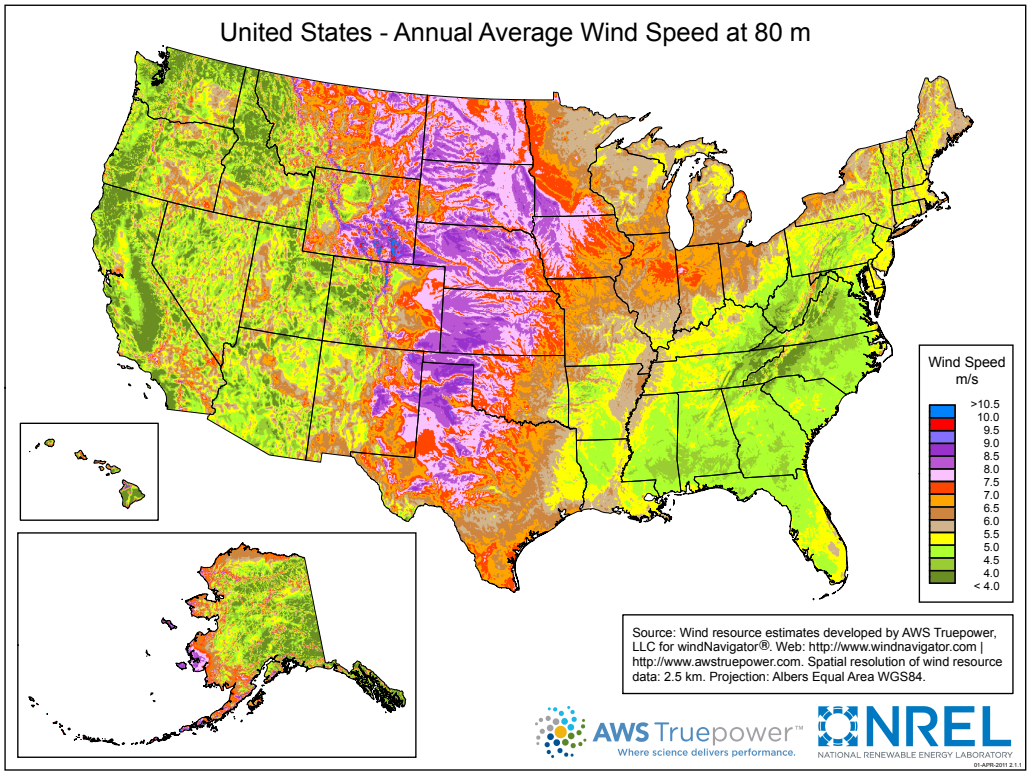

Figure 2.6: Average wind speed for the U.S. at a height of 80 meters (NREL 2012)

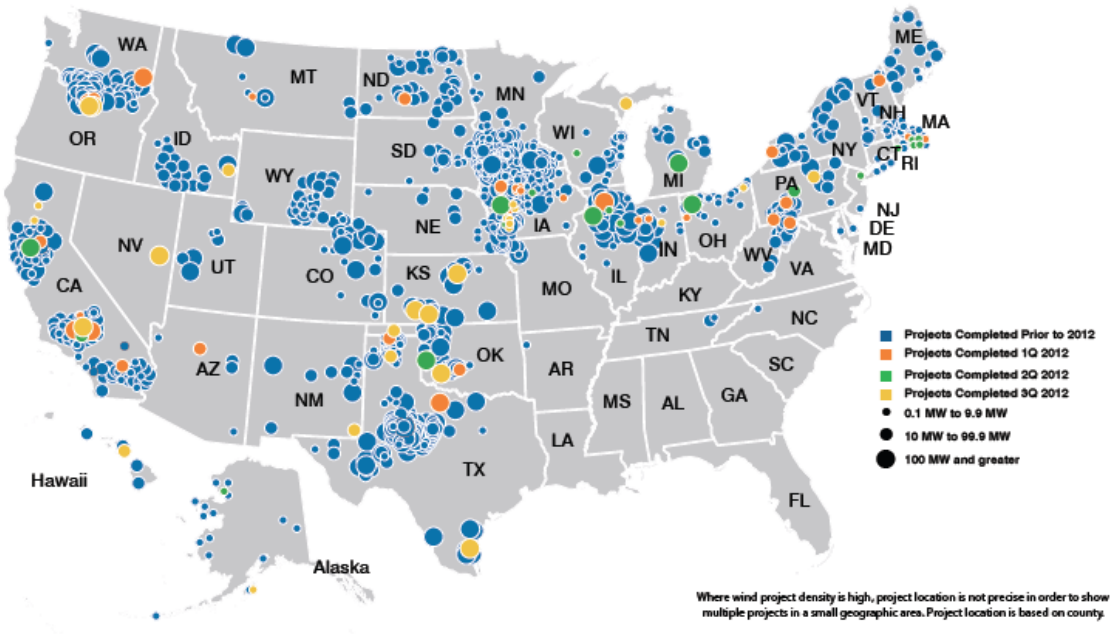

Figure 2.7: Map of the location and size of installed wind projects in the U.S. prior to 2012 and in the first three quarters of 2012 (AWEA 2012).

Despite short-term uncertainty in the U.S. wind market, global wind capacity is predicted to continue to expand through 2035. The EIA (2012a) projects that wind power will account for 60% of the non-hydropower renewable energy generation increases from 2010 to 2035. Hydropower remains the largest source of renewable electricity generation even with the dramatic expansion of wind capacity. Projections for the growth of wind power and other renewable sources of electricity are shown in Figure 2.8. The world generation of wind power was less than 400 billion kWh in 2010, but is projected to reach over 1,500 billion kWh by 2035 (EIA 2012a). Even with this significant increase in capacity, the EIA projections still have U.S. electricity generation from all renewable sources accounting for only 15% of the total demand in 2035. If renewable energy policies are extended, wind power will see increased growth over this reference case (EIA 2012a). From this prediction, it is clear that wind will make up a substantial portion of the worlds' energy mix in the future.

World renewable electricity generation by source, excluding hydropower 2005-2035 (billion kWh)

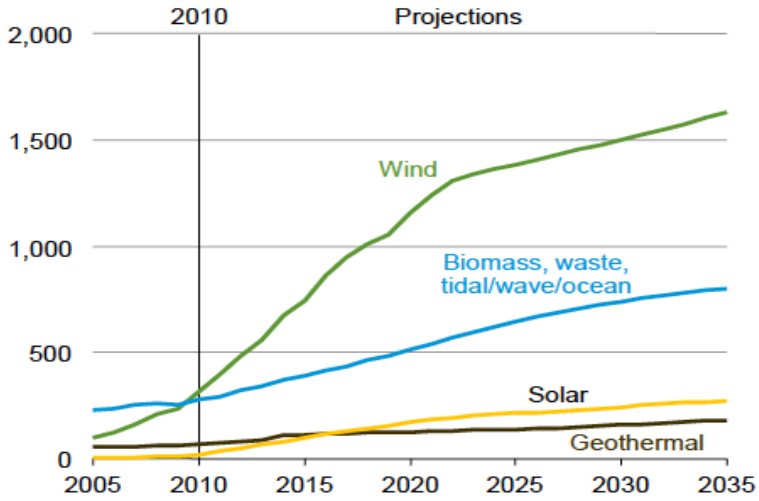

Figure 2.8: World renewable electricity generation by source without hydropower with historical data from 2005 to 2010 and projections from 2010 to 2035 in billion kWh (EIA 2012a, 75).

There are some obstacles that make large-scale wind power slightly more complicated. Wind turbines can obscure the landscape, produce noise, and cast shadows. Most of these issues are most severe within a half mile of the turbine. All of these things make it difficult to install turbines near communities and densely populated areas. Projects may require approval by the community before planning can continue. Fortunately, most ethanol plants are located away from towns with adequate space for a turbine in a cornfield. Despite the few negative aspects of wind turbines, 89% of Americans believe increasing wind power is a good idea (Swofford 2010). The negative impacts of wind turbines should be considered during the planning stages of a project, but widespread support for wind power should make project approval easier. Wind power will be a substantial part of U.S. electricity generation for many years to come.

2.5 Solar Thermal Energy

The use of solar energy for heating is not a new idea, but advancing technologies are making it possible to use solar thermal energy for large-scale applications for numerous end uses. Solar thermal collectors work on the general premise of using solar energy to heat a fluid, which can then be used to provide thermal energy. Low temperature applications (below 120^{o}C) can use non-concentrating flat plate or evacuated tube collectors. Higher temperatures can be achieved with concentrating collectors that use reflectors to greatly increase the temperature of the working fluid. Concentrating collectors are generally much more expensive and require more space to process the same amount of fluid as non-concentrating collectors. Since none of the processes in an ethanol plant require fluid above 120^{o}C and most of the ethanol plants are not located in

prime concentrating solar regions, only non-concentrating collectors will be considered for thermal energy production at ethanol plants.

Solar thermal energy is available year round across the United States. However, the overall efficiency of the solar collectors is greatly affected by location. Collector efficiency decreases as the temperature difference between the working fluid and ambient air increases. Efficiency is also negatively affected by decreasing solar insulation, which occurs during the winter months. This means that areas of the U.S. that have large temperature swings between summer and winter will see enormous differences in energy obtained from a solar thermal system throughout the year. The solar installation will also produce no energy overnight and may not produce energy on particularly overcast or cold days. All of these factors make solar thermal systems suitable for supplemental heat as opposed to the main source of process heat.

The solar thermal resources in the U.S. are concentrated in the Southwest, but solar thermal installations have been successful across the country. The map in Figure 2.9 shows the concentrating solar resources in the U.S., which can be used to evaluate non-concentrating thermal collectors as well. It is clear that some of the Midwest states may not be ideal locations for solar thermal installations, but that just signifies that each collector will produce less energy as compared to a state in the Southwest. The payback period for a solar thermal installation will certainly be longer in the Midwest compared to the Southwest, but both systems will supply thermal energy with nearly no GHG emissions or fuel consumption.

The two most common types of non-concentrating solar collectors are flat plate and evacuated tube. They have some notable differences that may make one or the other

more suitable for different areas of the country. A diagram of each type of collector is shown in Figure 2.10. Flat plate collectors use an absorber plate to transfer solar energy

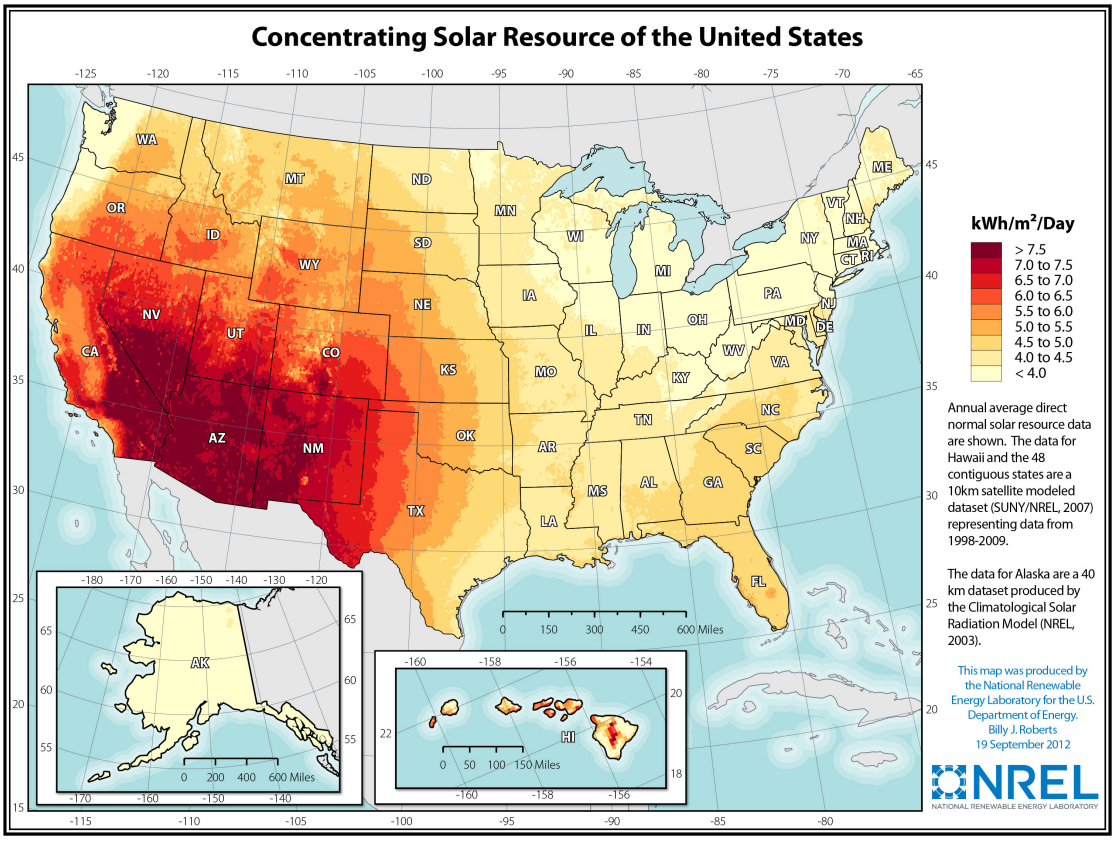

Figure 2.9: U.S. map of solar thermal resources in kWh/Day available per m^2 (NREL 2012).

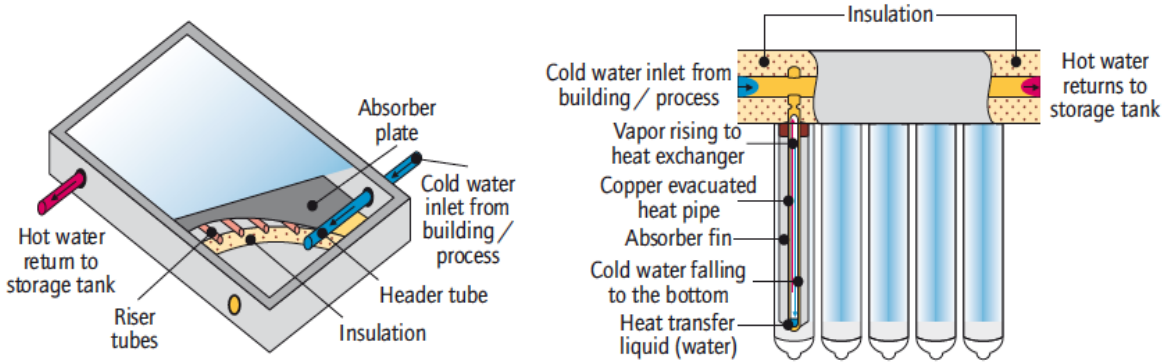

Source: Victoria Sustainability.

Figure 2.10: Simplified diagram of a flat plate and a evacuated tube solar thermal collector (IEA 2012).

to tubes of fluid that pass through the plate. The only protection from ambient conditions is the air gap between the absorber plate and the protective glass cover and the insulation on the back of the panel. This makes flat plate collectors susceptible to substantial heat loss in cold climates and may freeze if the temperature drops low enough. Evacuated tube collectors are generally less vulnerable to freezing and heat loss because the tubes around the working fluid are evacuated to reduce heat transfer to the ambient air. The advantages of flat plate collectors are that they are less expensive in the U.S. and have lower maintenance costs. Some of the tubes in an evacuated tube system will eventually lose their vacuum, which will require time and materials to repair.

A study completed by Ayompe et al. (2011) compared the performance of a flat plate collector and an evacuated tube collector with a closed glycol system over an entire year in the temperate climate of Dublin, Ireland. Most studies test panels under ideal conditions or more favorable ambient temperatures, but real-world experiments give a better representation of the actual energy output of a collector. The overall system performance averaged over the entire year for the flat plate was 37.9%, which was significantly less than the 50.3% efficiency for the evacuated tube system. The collectors themselves had efficiencies of 46.1% and 60.7% for the flat plate and evacuated tube panels respectively. The total system efficiency was decreased by pipe heat losses, which amounted to about 17% of the total energy collected. It is clear that even with pipe insulation, there will be significant heat losses in solar thermal arrays. Ireland has low solar resources, but the solar thermal arrays were able to provide hot water for the experiments. The solar resource in Ireland is about 2.68 kWh/m^2/day (Stackhouse 2012), which is over 30% lower than any of the locations considered for this study.

Solar thermal systems are an effective alternative to water heating using fossil fuels. They use very little energy to operate compared to a traditional natural gas or electric heater with nearly 100% reduction in GHG emissions and fossil fuel use. Large-scale water heating systems will be limited by the space available and capital required to install the equipment. The long lifespan of the equipment and low maintenance costs ensure low cost energy production for decades. Solar installations are generally not plagued by as many aesthetic issues as wind turbines. They do not produce any noise, cast large shadows, or obstruct the landscape. This makes project approval easier because the community is not usually as concerned about the decision.

2.6 Summary

The use of wind and solar energy to offset fossil fuel consumption at ethanol plants is conceptually viable and aligns with U.S. goals to increase production of biofuels, decrease fossil fuel use, and reduce greenhouse gas emissions. The ethanol, wind, and solar industries are well established and are projected to increase substantially over the next 20 years or more. Advancing technologies and increased production are making each of these sectors more economically viable and prime for increased development. The future of energy is uncertain, but ethanol, wind, and solar can help America reach its energy goals right now.

CHAPTER 3: MODELING TECHNIQUE AND APPROACH

3.1 Introduction to the Model

A model was created to investigate the viability of installing a wind turbine and/or a solar thermal array at various U.S. ethanol plant locations to reduce fossil fuel use. This model can be used in a variety of ways. The main focus was to determine if any U.S. ethanol plants are located in areas with sufficient solar and/or wind resources to provide a reasonable payback period and limited risks for specific renewable energy installations. The model can also be used to evaluate any location with user-entered meteorological and resource data. This allows the model to be used for other ethanol plant locations that were not considered or to investigate sites for future ethanol plants. Numerous input variables allow the model to be used for a wide range of projects and market conditions. The following sections discuss in detail the inputs for the model and assumptions made using current industry data and future projections.

The output data from this model can be used to evaluate a large range of projects and future conditions. Current and projected energy prices are used to estimate yearly cost savings and payback periods for modeled renewable energy installations. Projects can be compared using small or large specification changes to determine optimal or worst case system performance. Details of the output data and potential applications will be discussed in the subsequent sections.

The basic function of the model is to use input data to estimate realistic energy production of an installed solar array and wind turbine. This spreadsheet-based model uses operator-entered data to estimate yearly energy production, cost savings, and

lifetime savings of a given system. The user enters resource data for the location, wind turbine specifications, and solar array specifications. These values are used to find the yearly energy production of the renewable projects. Average electricity and gas rates are used to find payback periods and lifetime net savings of the solar and wind installations. These results can then be analyzed to determine if the location is suitable for wind or solar energy projects.

This model was designed to work with and expand upon the work completed by Kumar (2009) for his Master's thesis in which he developed a model to estimate the energy required to produce corn ethanol at dry mill plants using only natural gas for thermal energy. His model uses detailed inputs for the various processes required to cook and distill ethanol to determine the required thermal energy inputs. The energy estimates are then used to size a wind turbine and solar thermal array to replace a specified percentage of the energy inputs. The wind and solar estimates are very rudimentary and do not consider variations in wind and solar resources throughout the year, the use of commercially-available equipment, or reduced output of wind and solar installations due to low resources. Considerations for rising energy costs or the cost to install the systems were not completely studied as well. The model developed for this research project more accurately estimates useful energy production and payback periods for wind and solar thermal installations. The current model can use the thermal energy requirement for a specified ethanol plant calculated with the Kumar (2009) model and use it as an input. Another difference between the two models is that the current model is used to investigate solar and wind installations at 18 different ethanol plants across the country for their actual nameplate capacity. The ranges for the input variables are also

investigated to determine the effect on output data and the possible span of annual cost savings and payback periods. All of these improvements increase the accuracy and applicability of the model.

3.2 Energy Use by Ethanol Plant

The first section of the model requires input data for the capacity of the ethanol plant and energy usage. These values are used to determine the plant's thermal energy use and electricity use per year. The input field of the spreadsheet is shown in Figure 3.1. The input cells to the model are always green and the output cells are always red to aid understanding.

Ethanol Plant Inputs		
	Typical Values	**Input**
Ethanol Plant Capacity, PC (million gallons per year MGY)	1 - 130	
Electricity Requirement, ER (kWh/gal-ethanol)	0.74 kWh/gal	
Heating Energy Requirement, Q_{AE} (Btu/gal-ethanol)	29,000 Btu/gal	
Makeup Water Energy Requirement, Q_{MW} (Btu/gal-ethanol)	1,365 Btu/gal	

Figure 3.1: The spreadsheet inputs and typical values for the ethanol plant modeling section.

Nameplate ethanol production capacity of a given ethanol plant is the main factor in determining energy use for the facility. The first entry on the spreadsheet is the production capacity in million gallons per year (MGY) of anhydrous ethanol. All values for ethanol will be assumed to be anhydrous ethanol unless otherwise noted. Capacity

values are published for all currently operating plants online and in many ethanol publications (RFA 2012c). Most plants produce between 40 and 100 MGY. Equation (3.1) estimates the total thermal energy needed for an ethanol plant.

$$Q_{Total} = PC \times Q_{AE} \tag{3.1}$$

The total yearly heating requirement for the plant (Q_{Total}) in MMBtu is found by multiplying the plant capacity (PC) in MGY by the heating rate required to produce anhydrous ethanol (Q_{AE}) in Btu/gal-ethanol. Kumar's (2009) ethanol production energy model can be used to easily calculate Q_{AE} for various plant conditions by adding together the output values of the total energy to cook (Q_{AE}^{Cook}) and the total energy to distill (Q_{AE}^{D}) per unit anhydrous ethanol shown in Equation (3.2).

$$Q_{AE} = Q_{AE}^{Cook} + Q_{AE}^{D} \tag{3.2}$$

The value for Q_{AE} can also be found by using averages found from actual operational ethanol plants. A survey of 90 ethanol plants showed that the average dry mill corn ethanol plant used 28,859 Btu/gal-ethanol for plants using natural gas in 2008 (Mueller 2010). It is not essential that this number exactly matches a particular facility's energy consumption, because it is mainly used to determine the percent of total energy use that the wind and solar installations replace.

The electricity consumption of an ethanol plant can be obtained from actual plant operations or estimated using averages and rules of thumb. BBI International (2003) estimates an ethanol plant's electricity requirement at 0.8 kWh/gal-ethanol. Mueller's survey (2010) of 90 dry mill plants reported an average electricity usage of 0.74 kWh/gal-ethanol. Similar to the thermal energy requirement of ethanol plants, the

electricity requirement (ER) is used to find the percentage of electricity replaced by wind power so precise values are not required.

The percent shift for the total natural gas heating requirement of the ethanol plant to solar thermal energy is most likely going to be very small. Ethanol requires substantial amounts of energy to cook and distill, primarily due to the shear volume of water and mash that must be heated. Most plants reuse most or all of the process water to take advantage of the residual heat remaining after the ethanol has been distilled out. This means there will be much smaller amounts of makeup water necessary to replace boiler water than the total water requirement of the ethanol production process. The average fresh water requirement of a survey of 73 dry mill natural gas plants was 2.72 gallons of water per gallon of ethanol produced (Mueller 2010). Aden (2007) reports that most of the fresh water use in ethanol plants is makeup water for the boiler and cooling tower due to nearly complete reuse of process water. This report also specifies that about 68% of the makeup water goes to the cooling tower and 32% goes to the boiler with estimated water use of 3 - 4 gallons of water per gallon of ethanol for dry mill plants (Aden 2007). The boiler makeup water requirement in gallons of water per gallon of ethanol (MW_B) is given by Equation (3.3).

$$MW_B = MW_{total}\,\%W_B \tag{3.3}$$

The total makeup water requirement (MW_{total}) for the plant is multiplied by the percent of the makeup water going to the boiler ($\%W_B$). If the average value of 3 gal-water/gal-ethanol were used for MW_{total}, then the necessary boiler makeup water would be about 0.96 gal/gal-ethanol. Heating requirements for the boiler makeup water will be significantly less than the total heating requirement of the plant. The heating requirement

for the boiler makeup water will be found to determine the amount of heat the solar array would need to provided to heat the boiler makeup water from the ground water temperature (T_{gw}) to the boiler input water temperature (T_B). The makeup water heating requirement (Q_{MW}) in kJ/gal-ethanol is determined by Eq. (3.4).

$$Q_{MW} = MW_B \times c_{p,w} \times \left(T_B - T_{gw}\right) \times \frac{1{,}000\ kg}{m^3} \times \frac{1\ m^3}{264.2\ gal,water} \tag{3.4}$$

Using the specific heat of water ($c_{p,w}$ = 4.19 kJ/kg-^oC), a boiler inlet temperature of 100^{o}C, and a ground water temperature of 15^{o}C, the heating requirement for the makeup water is 1,294 kJ/gal-ethanol or 1,365 Btu/gal-ethanol. This is significantly less than the total thermal energy of 28,859 Btu/gal-ethanol reported by the average dry mill plant in Mueller's survey (2010). The boiler makeup water heating requirement is less than 5% of the total heating requirement of the plant.

Using the makeup water heating requirement significantly increases the percentage of heating a solar thermal array can replace. Kumar (2009) did not consider the difference between reheating recycled process water and preheating boiler makeup water. The biggest difference between these two methods is the inlet temperature to the panels. Recycled process water will be much warmer than makeup ground water, which will increase the temperature of the solar array working fluid and increase heat loss from the collectors. Using low temperature ground water increases the efficiency of the solar array by reducing heat loss, which increases the total energy the solar array can provide.

3.3 Resource and Meteorological Inputs

This model can be used with monthly or yearly averages for solar insolation on a tilted surface, wind speed, temperature, and daylight hours. These values are used to

calculate the available resources for a solar array and wind turbine. Figure 3.2 shows the input format of the spreadsheet model for meteorological and resource values. The averaged monthly values were obtained from a NASA sponsored web site (Stackhouse 2012) that provides measured and calculated values averaged from 22 years of data. These values generally agree with the wind and solar resource maps shown in Figure 2.6

Location:												
Resource and Meteorological Inputs												
	Jan	**Feb**	**Mar**	**Apr**	**May**	**Jun**	**Jul**	**Aug**	**Sep**	**Oct**	**Nov**	**Dec**
Solar Insolation on a tilted surface, G_t (kWh/m^2/day)												
Monthly Average Air Temperature, T_a (^{o}C)												
Monthly Average Wind Speed, V_a (m/s)												
Average daylight hours per day, H_{day}												

Figure 3.2: Spreadsheet model input field for monthly averaged resource and meteorological data.

and Figure 2.9 produced by NREL (2012), which can also be a source for yearly average wind and solar resource values. The values from the NASA website provide greater detail than the resource maps provided by NREL, which is important because monthly values for solar and wind resources vary significantly from month-to-month. These two sources of wind and solar resources provide slightly different values, which can drastically affect model outputs. The best inputs would be from data collected near the

plant site. To obtain values from the NASA website (Stackhouse 2012), the user enters the latitude and longitude of the location and then selects the desired datasets. The datasets used for the model are "Daylight Hours" (H_{day}), "Radiation on equator-pointed tilted surfaces" (G_t), "Daily Temperature Range at 10m" (T_a), and "2) Gripe Power Law used to adjust Wind Speed at 50 m to other heights" (V_a). The Gripe Power Law dataset requires a height input for the desired wind speed at a specified height above the ground. All of the ethanol plant locations were compared using wind speeds at 80 meters, which is the most common height for wind turbines. This model will also work for any desired wind turbine height. The data obtained from this website (Stackhouse 2012) for each ethanol plant location are included in Table A.1 through A.19 in Appendix A.

The radiation on a tilted surface dataset provides values for various tilt angles. The tilt angle closest to 25^o was chosen to compare the different plant locations, but any tilt angle can be used for the user location input section. The angle between the ground and the collector is defined as the tilt angle and is used to optimize the incident radiation on a solar collector's surface. Tilt angles should be adjusted for each location to give a balance between radiation during the summer and winter. Higher tilt angles provide more radiation in the winter and less radiation in the summer than lower tilt angles. Higher radiation in the winter can help guard against freezing, but this will also reduce the energy available in the summer. The NASA dataset (Stackhouse 2012) also calculates the optimal tilt angle for each month of the year and the average optimal tilt angle. This information could be used to optimize designs for a solar thermal array.

Monthly resource data for solar installations is much more useful than yearly values because the range of solar insulation throughout the year can vary widely from

summer to winter. This is especially true in northern states when the temperature and solar insulation drops during the winter. During the winter, solar energy is reduced, heat loss of the solar array increases, and daylight hours are shortened which all leads to dramatic reductions in the available energy from the solar array. Preliminary evaluations of a proposed solar thermal array must take into account the large variation in available solar energy throughout the year and how this will be managed by the planned system. The large variations in solar energy, particularly in Midwestern states where most of the ethanol plants are located, is another reason to use the solar installations to preheat process water or makeup water instead of producing steam or high temperature water. The lower temperatures of makeup water reduce heat loss to the environment in colder climates. This will also aid integration into the existing system, because the solar array can be connected before the process to eliminate the need for major changes in plant operation. The model can use either monthly averages or a yearly average for solar resources, but monthly data will give a more complete picture of available thermal energy.

Wind resources also vary throughout the year, but do not have as great an effect on plant operations. Most wind projects are grid connected, which eliminates negative effects on process operation of changing electricity generation throughout the day and year. It is still beneficial to calculate the changes in wind energy throughout the year to predict variations in energy and cost savings. Yearly or monthly average wind resources may be used with this model; however, monthly values show the range of available energy throughout the year more accurately.

3.4 Calculating Wind Power Generated

This model can be used employing two different methods to calculate the annual electricity generation of a reference wind turbine. Users can enter monthly wind resource data or an average yearly wind speed value in m/s. These values can either be actual wind averages for the location considered or the design values for the wind turbine. The type of data will determine how the operator uses the model. The individual input data required for each method is listed under the specific title. Monthly wind resource data is entered into the spreadsheet in the appropriate green cells shown in Figure 3.2. The input fields of the spreadsheet for specific wind turbine information are displayed in Figure 3.3.

Wind Inputs		
	Typical Values	**Input**
Design Wind Speed for Turbine, V_d (m/s)	8-15 m/s	
Installed Cost of Wind Turbine, IC_{wt} ($/kW)	$2,000/kW	
Diameter of Turbine Blade, D_R (m)	50-90m	
Monthly Wind Data		
Power Coefficient, C_{pa} or C_{pd}	Max: 0.59	
Capacity Factor, 1 or C_{fa}	1 or 0.2-0.55	
Yearly Wind Data		
Yearly Average Wind Speed, V_a or V_d	6.5-15	
Power Coefficient, C_{pa} or C_{pd}	Max: 0.59	
Capacity Factor, 1 or C_{fa}	1 or 0.2-0.55	

Figure 3.3: Illustration of the wind inputs for the spreadsheet model

Typical values are given for input values to aid the user in obtaining an accurate model of energy generation. Some of the input labels indicate that there are two possible variables that can be entered into that cell. This allows the model to perform different calculations depending on user needs. Notes are also included in the spreadsheet to help direct the user on the appropriate use of the model.

The main difference between the two types of calculations is whether the inputs are the design parameters of the wind turbine or the actual conditions at the turbine site. When a user enters a design wind speed (V_d) for the turbine, then a design power coefficient (C_{pd}) and an actual coefficient of power (C_{pa}) should be entered. If the user enters actual average wind resource values (V_a), then a realistic average power coefficient (C_{pa}) can be entered and the capacity factor should be set to 1.0 or something near one. Both methods are verified for their accuracy in predicting actual electricity generation.

The actual power delivered by the wind turbine will be substantially less that the total energy contained in the wind that flows past. The power output (P_w) of the wind turbine is calculated using the density of air (ρ_a), the particular turbine coefficient of power (C_P), the swept area of the rotor blades (A_s), and the wind speed (V_w), as shown in Equation (3.5).

$$P_w = \frac{1}{2}\,\rho_a\,C_P\,A_s\,V_w^3 \tag{3.5}$$

The density of air is generally assumed to be 1.23 kg/m^3 for this model. Determining the other values is discussed in detail subsequently.

The coefficient of power is unique to every turbine and will vary as the wind speed varies. This is why a turbine should be selected for a design wind speed that corresponds to wind speeds at the desired turbine location. Equation (3.6) defines the coefficient of power.

$$C_P = \frac{Power\ generated}{Wind\ Stream\ Power} \tag{3.6}$$

If the coefficient of power were one, the turbine would reduce the air speed of all the wind that crossed the swept area of the blades to zero. This is not theoretically possible,

and Albert Betz determined the maximum theoretical value of the coefficient of power was 59.3%, which is known as the Betz limit (Ragheb 2011). This means that at least 40.7% of the energy contained in the wind continues past the turbine. In general, real turbines have average coefficients of power lower than this theoretical value. Some turbine manufactures will publish coefficient of power information for a specific design wind speed, but average operational values will most certainly be lower than any design numbers. This is because the stated value is for a specific design wind speed when the turbine is most efficient.

This design wind speed results in the optimal tip speed ratio (TSR). The TSR is the ratio of the rotor tip speed to the free stream wind speed. Deviations from the optimal TSR reduce the coefficient of power. Typical values for coefficients of power for changing tip speed ratios are shown Figure 3.4. As seen in the Figure 3.4, the power coefficient peaks at an optimal TSR and is significantly lower at values far from this value. Typical values for the coefficient of power for commercial turbines are about 0.40 (Regheb 2011). Advanced designs and reduced losses have allowed large-scale turbines to achieve higher power coefficients for optimal wind speeds. Figure 3.5 shows the

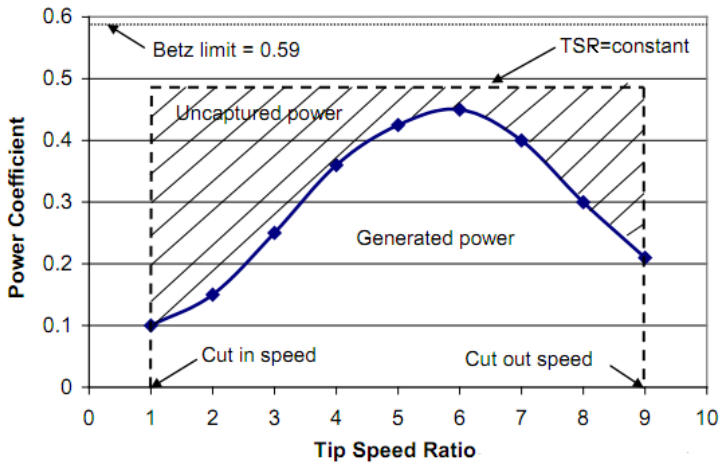

Figure 3.4: Power coefficient as a function of tip speed ratio for a two-bladed wind turbine rotor (Regheb 2011, 33).

power curve of a 2.0 MW turbine calculated by the turbine manufacturer ENERCON (2010). The maximum coefficient of power is 0.5 for this turbine. The graph also shows how the power produced by the turbine rapidly increases as the wind speed increases until it reaches its design power production. Once the wind speed increases above the design speed, the pitch of the blades adjusts to control the speed of the rotors. This slows the rotors down to maintain the desired power output. Maintaining the desired power output quickly reduces the power coefficient because more wind energy is flowing past the turbine without being collected. The coefficient of power is relatively stable for wind speeds near the design speed. This makes deciding on a capacity factor to use for

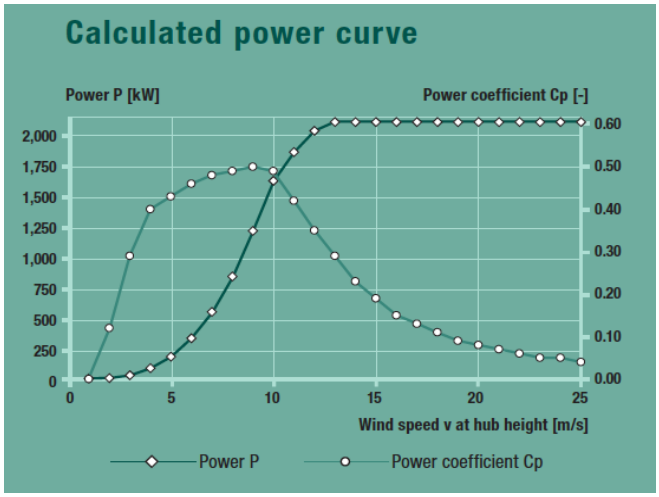

Figure 3.5: Calculated power curve and power coefficient for a 2MW wind turbine as a function of wind speed at hub height from the product brochure (ENERCON 2010).

calculations much easier. If the speed used for calculations is close to the design speed, but not larger, then the design power coefficient can be used with only small errors. Design wind speeds should always be larger than average wind speeds to take advantage of the additional energy available as the wind speed increases. From Eq. (3.5) it is clear that small increases in wind speed will lead to large increases in power, because the wind

speed is cubed. It is tempting to increase the design wind speed to maximize power production, but this will also decrease the coefficient of power at lower wind speeds. Care must be taken to install a turbine that is designed to work with the wind resources available at that particular site. A realistic coefficient of power to use to model the power produced by a new large-scale turbine would be in the range 0.40 to 0.50. Using the maximum value of 0.593 would overestimate power production.

The swept area in m^2 is found using the rotor diameter (D_R) in meters, as shown is Equation (3.7).

$$A_s = \pi \frac{D_R^2}{4} \tag{3.7}$$

The average wind speed for a particular location can be found from multiple sources. This model uses monthly data obtained from the Surface Meteorology and Solar Energy (SSE) website (Stackhouse 2012) sponsored by NASA using the latitude and longitude of selected ethanol plant locations. The wind speed data is calculated mainly using 50m airport data with some adjustments based on topography and known issues with certain regions. They report about 20-25% uncertainty for the mean monthly wind speed values due to specific location conditions. A yearly average wind speed can be obtained from Figure 2.6 or the individual state maps provided online by NREL (2012). In general, wind speeds will be lower in the summer and higher in the winter, which makes monthly averages more useful in predicting the variation of power generation throughout the year. If monthly wind speeds are entered into the model, a graph showing the useful electricity production each month is generated. This allows users to quickly see how the energy output of the turbine will vary throughout the year.

The yearly electricity production of a wind turbine can be calculated using two different methods. The first method uses monthly average wind speeds, a realistic coefficient of power, and a capacity factor of one. The model assumes the average wind speed will be below the turbine design levels, so the actual capacity factor will be far below unity. An actual capacity factor is calculated later in the model. This first method is used to compare the wind resources at the various ethanol plant locations. The user can also perform these calculations by entering monthly wind speed data into the spreadsheet as illustrated in Figure 3.2. The second method uses only one average wind speed for the entire year. This method can be used in two different ways. The first way is similar to the monthly data entry in that a realistic wind speed is used with a realistic coefficient of power and a capacity factor of unity. The second way to use the yearly wind speed method is to pick a design wind speed for a turbine with the design coefficient of power and a realistic capacity factor (C_f). The yearly electricity production of the modeled wind turbine (E_w) is calculated using Equation (3.8).

$$E_w = P_w \, C_f \, H_y \tag{3.8}$$

Yearly operating hours (H_y) in hours/year are assumed to be 8,760 h/yr for all simulations. The capacity factor is mainly used for design wind speeds and is defined by Equation (3.9).

$$C_f = \frac{Actual\ Yearly\ Energy\ Generation}{Yearly\ Energy\ Generation\ at\ Maximum\ Capacity} \tag{3.9}$$

The actual capacity factor of an individual wind turbine depends on numerous aspects of its operation, but average values are readily available. Data from 50 wind projects built in 2010 (Wiser and Bolinger 2012) with a total installed capacity of 4,989 MW showed that capacity factors ranged from 18% to 53% in 2011. This same report showed that the

weighted average of the capacity factors for 305 projects totaling 32.8 GW installed from 2004-2010 was about 34% for 2011 electricity generation data. An NREL technical report (Tegen 2012) uses 38% capacity factor for their reference case for a 1.5 MW land-based wind turbine. Capacity factors will be higher for projects with higher and more consistent wind speeds and lower for areas with lower wind speeds, less consistent wind, and areas that require curtailment of wind power to adjust for power demand. Capacity factors will generally fall between 20% and 50% and should be adjusted to project conditions.

The ideal energy and power generated by the turbine is calculated to determine the actual power factor and design capacity of the proposed system. The power capacity (P_C) of the system is determined using Equation (3.10).

$$P_C = \frac{1}{2} C_{pd} \rho_a A_s V_d^3 \tag{3.10}$$

This provides the nameplate capacity of the wind turbine. This capacity can be used to estimate the installation price of the wind turbine or determine maximum power production. Design wind speed (V_d) is used along with the turbine design coefficient of power (C_{pd}) to determine the maximum amount of power that can be produced by this turbine. Design wind speeds are generally in the 8-13 m/s range depending on location and height. Larger design wind speeds increase the maximum power the turbine can produce, but most often lower capacity factors. Lower design wind speeds limit the power production, but generally increase the capacity factor because the wind speed is close to the design wind speed more often. Equation (3.11) gives the theoretical electricity production (E_{wt}) of the wind turbine if it operated at ideal conditions 24 hours per day for the entire year.

$$E_{wt} = P_C \, H_y \tag{3.11}$$

The wind turbine capacity factor (C_{fa}) for simulations using actual wind speeds instead of design wind speeds is evaluated employing Equation (3.12).

$$C_{fa} = \frac{E_w}{E_{wt}} \tag{3.12}$$

Calculation of the actual capacity factor for the proposed wind turbine aids the user in verifying that the values used are consistent with industry standards. If the calculated value for the actual capacity factor is below 19% or above 53% then the proposed wind turbine is outside the known range of over 50 installed wind projects in 2011 (Wiser and Bolinger 2012).

The installed cost of a wind turbine (IC_{wt}) is based on the nameplate power capacity of the turbine. Average turbine prices fell from just under $1,400/kW in Jan 2011 to just over $1,200/kW in Jan 2012 (Wiser and Bolinger 2012). The turbine cost is only part of the total installed cost for the turbine. The allocation of total installed costs is show in Figure 3.6. Turbine costs account for about 68% of the installed cost of a wind

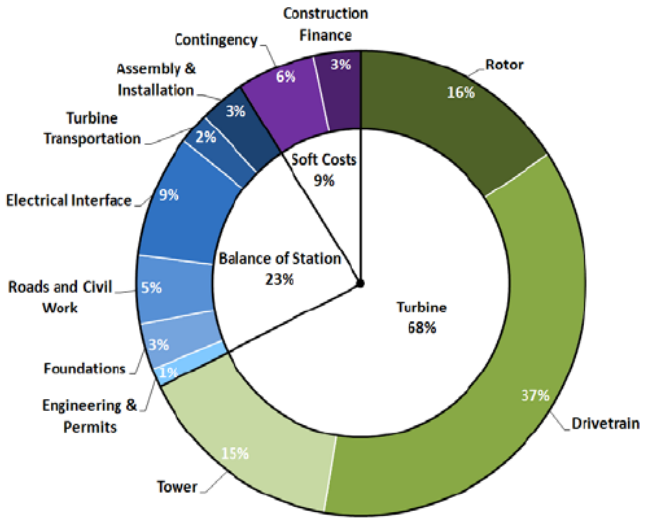

Figure 3.6: Average installed costs of land based wind turbine (Tegen et al. 2012)

project according to Tegen *et al*. (2012). Their report models the costs of wind energy in 2010, in which they use $2,155/kW as the installed cost of a 1.5MW turbine. Wiser and Bolinger (2012) report an average capacity weighted installed cost of $2,100/kW in 2011, and preliminary values for installed costs for 2012 projects may be well under $2,000/kW. The average installed costs of 584 wind projects constructed between 1982 and 2012 are shown in Figure 3.7 (Wiser and Bolinger 2012).

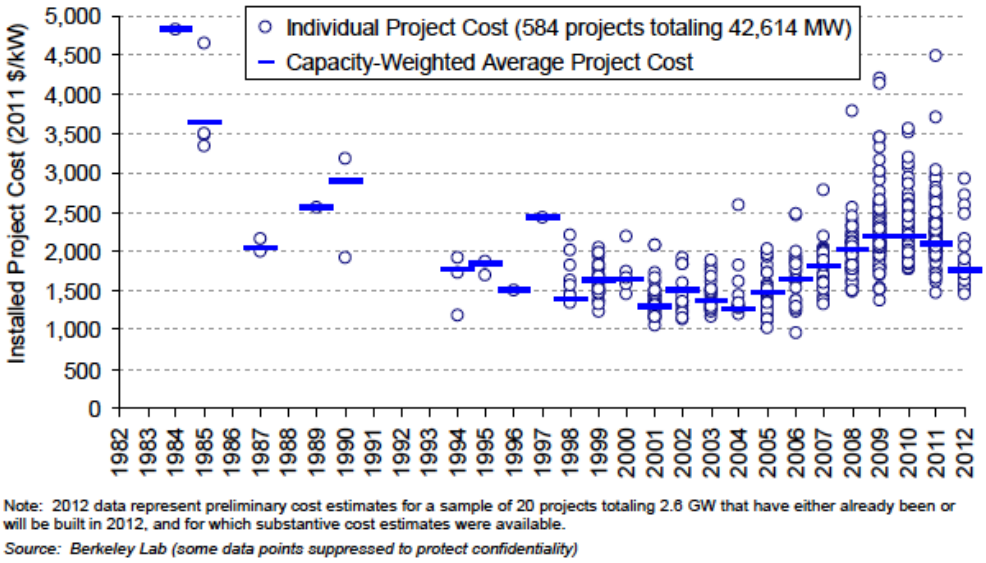

Figure 3.7: Installed project cost in 2011 $/kW for 584 projects installed between 1982 and 2012. The blue line shows weighted averages for project cost according to project size (Wiser and Bolinger 2012).

Installed costs peaked in 2009 and 2010 and fell in 2011 and 2012. Even though the average installed cost is dropping, the range for total installed costs is still rather large. The most expensive project surveyed in 2011 was about $4,500/kW while the least expensive project was $1,500/kW, though the vast majority of the wind projects were between $1,500 and $3,100/kW. For a 1.5 MW turbine this would result in a difference in installed costs of $2.4 million, which is more than the cost of the cost of the

$1,500/kW project. It is likely that the more expensive projects have more difficult installations and longer planning periods, which should not be an issue for ethanol plants. Ethanol plants are typically located away from densely populated areas with abundant land for a wind turbine. Another factor to consider in determining installed cost is the size of the project. Wind turbines benefit from economies of scale, which means larger projects generally have a lower installed cost on a $/kW basis. A comparison of 275 projects between 2009 and 2011 show an average installed cost of nearly $2,500/kW for turbines greater than 0.1 MW and less than 1 MW, about $2,250 for turbines 1 MW to less than 1.75 MW, and about $2,100 for turbines from 1.75 MW to less than 3.25 MW (Wiser and Bolinger 2012). Due to decreasing price trends, this model will use an average installed cost of $1,800/kW to compare wind installations at ethanol plant locations. Simulations of varied installed costs will also be completed to account for possible price ranges.

The outputs for the wind energy calculations are shown in Figure 3.8. All of the wind outputs previously discussed are included, as well as the useful wind energy (E_{Btu}) in MMBtu/yr and the electricity generation percent of total. The useful wind energy is

Wind Outputs	
Design Turbine Power, P_d (MW)	
Theoretical Electricity Generation, E_{wt} (kWh/yr)	
Electricity Generation, E_w (kWh/yr)	
Useful Wind Energy, E_{Btu} (MMBtu/yr)	
Wind Turbine Capacity Factor, C_{fa}	
Percent Shift Electricity to Wind, $\%S_w$	

Figure 3.8: Spreadsheet model outputs for wind calculations

calculated by dividing the electricity generation value by the general conversion factor of 293.1 $\frac{kWh}{MMBtu}$. This allows comparisons across energy types. Equation (3.13) calculates the percent shift from traditional electricity to electricity generated by wind power ($\%S_w$).

$$\%S_w = \frac{E_w}{PC \times ER} \tag{3.13}$$

Percent shift is another factor that aids in verifying appropriate project input values and relative project size. If the percent shift from conventional wind energy is very low then the ethanol plant will not see a large reduction in energy costs, but will also have a manageable implementation cost relative to annual profits. If the percent shift is very large then the company will see dramatic reductions in annual electricity costs, but will most likely need extensive financing and project backing.

3.5 Calculating the Solar Energy Collected

The solar energy collected by a proposed solar thermal array can be calculated from monthly or yearly solar resource data. This model can estimate the thermal energy collected by both evacuated tube and flat plate collectors with adjustments to panel parameters. Just as with the wind resource data, average monthly solar insulation values in kWh/m^2/day are entered into the spreadsheet using the field shown in Figure 3.2. Monthly resource data will more accurately show the available thermal energy available throughout the year. The input field for solar data is shown in Figure 3.9. The total area of each collector (A_c) is the gross area of each of the collectors in the solar array. The aperture area of each collector (A_a) is the area of the collector that can absorb sunlight to transfer thermal energy to the working fluid. For flat plate collectors, the aperture area will be between about 85-95% of the gross area of the collector. Evacuated tube

Solar Inputs		
	Typical Values	**Input**
Total Area of Each Collector, A_c (m^2)	1-10	
Aperture Area of Each Collector, A_a (m^2)	60-95% A_C	
Number of Panels, N_p	3 - 5000	
Price per Square Meter, IC_{sc} ($/total m^2)	200 – 600	
$F_R(\tau\alpha)$	0.5 - 0.9	
F_RU_L (W/m^2-^oC)	0.7 - 15	
Average Input Temperature of Working Fluid, T_i (^oC)	15 -100	
Load Factor, L_f	≤ 1	
Yearly Solar Data		
Yearly Average Insulation, G_t (kWh/day/m^2)	2.0 - 9.0	
Yearly Average Air Temperature, T_a (^oC)	5.0 - 20	
Load Factor, L_f	≤ 1	

Figure 3.9: Illustration of the solar inputs for the spreadsheet model

collectors have slightly more variation, so the aperture area can be anywhere between 60-85% of the gross collector area. The aperture area is not essential to the operation of the model. It is used to calculate the efficiency of the collectors based on aperture area in addition to gross collector area. Typical residential panels are usually between 2 and 4 square meters and are readily available. Large industrial panels can have gross areas up to 10 m^2.

The installed cost per square meter (IC_{sc}) of the solar collectors will mainly depend on the type of collector and the size of installation. Installed costs can be hard to estimate, because they include costs for the design, permits, piping, panels, pumps, insulation, a heat exchanger, storage tank and installation. Larger systems will have a smaller cost per square meter due to economies of scale. The installation costs of large

projects make up a smaller percentage of the total installed cost. RETScreen International (2005) reports typical panel prices for flat plate collectors in the range of \$180-\$310/m^2 and evacuated tube collectors in the range of \$900-\$1,100/m^2. The lower price range is for large systems while the higher price range is for small systems. The price range for flat plate collectors agrees with prices reported by EIA (2012) for a 2009 survey of U.S. solar thermal collector manufacturers, which reported average prices for flat plate collectors at a rate of \$19.43/ft^2 and evacuated tube collectors at a rate of \$25.88/ft^2. These prices are equivalent to \$209/m^2 for flat plate collectors and \$279/m^2 for evacuated tube collectors. The RETScreen numbers may also include evacuated tube collectors with concentrators, which would dramatically increase the average price and account for the large disparity between manufacturer and RETScreen values. Installed costs are more difficult to estimate due to the large range of project specifications and locations. The IEA (2012) reports that installation costs for small-scale solar hot water systems can be up to 50% of the total cost, and large-scale systems generally have lower installation costs compared to the equipment costs. Model inputs for total installed costs for flat plate and evacuated tube arrays are estimated to be in the range \$314-\$418/m^2 and \$419-\$558/m^2 for each type of panel respectively. These values are between 1.5 and 2 times the 2009 panel prices reported by U.S. manufacturers from the EIA website (2012). Users can adjust these values to the specific project considered.

There are two collector performance variables that determine the amount of solar insolation the collector absorbs and the heat lost to the environment. The variable $F_R(\tau\alpha)$ determines the percentage of solar energy absorbed, and the variable F_RU_L determines the heat lost to the environment due to the temperature difference between the ambient air

(T_a) and the input fluid temperature (T_i). The total useful solar energy (Q_u) in MJ/yr transferred to the working fluid is calculated using Equation (3.14).

$$Q_u = L_f A_c N_p \left[F_R(\tau\alpha)\, G_t - F_R U_L\, (T_i - T_a) \times (H_{day} - 2)\right] \times \frac{3{,}600\ s}{1\ hour} \times N_d \quad (3.14)$$

Flat plate collectors have $F_R(\tau\alpha)$ values between 0.6 and 0.8, while evacuated tube collectors have values typically between 0.5 and 0.6 based on gross collector area (RETScreen 2005). This means that flat plate collectors will capture more solar energy than evacuated tube collectors due to a less reflective surface. Values of $F_R U_L$ for flat plate collectors range from 3.5 to 6 W/m^2-^{o}C and range from 0.7 to 3 W/m^2-^{o}C for evacuated tube collectors based on gross collector area (RETScreen 2005). Flat plate collectors will lose significantly more energy due to temperature differences between fluid temperature and ambient air temperature. Specific values of $F_R(\tau\alpha)$ and $F_R U_L$ may be available from collector manufactures, but can also be found through the RETScreen database (2012) of collector efficiency values. Average values for these performance variables were used to compare the performance of flat plate and evacuated tube collectors at various ethanol plant locations. The variables used to model flat plate collectors were 0.72 and 4.5 W/m^2-^{o}C, and the variables used for evacuated tube collectors were 0.59 and 1.5 W/m^2-^{o}C. Panels with higher values for $F_R(\tau\alpha)$ and lower values for $F_R U_L$ are usually more expensive because they have a higher efficiency. The model can simulate adjustments in price and performance variables to weigh the benefits and disadvantages of increased performance with increased cost.

The total useful energy available for water heating is reduced by a user defined load factor (L_f). The load factor can be less than or equal to 1.0 depending on anticipated heat losses and reduced capacity. This value accounts for additional heat loss from

piping or storage tanks as well as reduced operation time due to excessively cold temperatures or low solar energy days. Solar collector arrays will only operate when the collectors are receiving sufficient energy from the sun. This means that there will always be some solar energy that is wasted, because the energy received is too low to warrant operating the system. Flat plate collectors will have a lower load factor than evacuated tube collectors because they cannot utilize as much solar energy during the morning and evening hours when the incidence angle is not optimal. Flat plate collectors lose more heat due to extreme temperatures as well, which may not be accounted for if the user enters yearly averages for the solar insulation and ambient temperature. The load factor can also be adjusted to simulate non-ideal solar conditions or reach a desired solar collector efficiency.

The solar insolation incident on the tilted surface of the collector (G_t) in kWh/m^2/day is the total solar energy that hits the collector. Monthly values for G_t are entered in the spreadsheet field shown in Figure 3.2, while a yearly average value can be entered in the field shown in Figure 3.9. The user only needs to use one of these methods to model the proposed solar array.

The heat loss coefficient (U_L) in W/m^2-^{o}C is converted to J/m^2-^{o}C-day by multiplying by the number of hours the collector is in operation per day and the number of seconds per hour. For monthly solar data this value is the number of sunlight hours per day (H_{day}) minus two. Subtracting two from the sunlight hours accounts for the fact that early morning and evening solar energy is too weak to operate solar arrays. The collectors will only lose heat when the system is operating. If the user enters a yearly value for the solar resource, H_{day} is assumed to be 12.

Total useful solar energy per year shown in Eq. (3.14) is multiplied by the number of days (N_d) the array operates to find J/year. For monthly input data a separate value for useful solar energy is calculated for each month by using the average number of days in a month, 30.417 days/month. Then the monthly values are added together to give the yearly useful energy. Yearly input data uses 365 days per year to calculate the total useful energy. The useful solar energy per month is calculated for monthly user input data and each of the 18 ethanol plant locations on their respective worksheets of the model. These values are used to generate a graph each time the user runs a simulation that shows the monthly variation in useful energy output of the solar thermal array. The relative differences between solar energy throughout the year can help the user predict changing thermal energy throughout the year. It can also be used to help size the array to ensure peak summer output will not be too large.

The performances of solar thermal collectors are often compared on the basis of efficiency. There is some debate on the best way to measure efficiency, so this model calculates the efficiency of the total solar array and modeled panel based on gross collector area and aperture area. The efficiency measured by aperture area will always be larger than the efficiency measured by gross collector area, but evacuated tubes usually benefit more from aperture efficiencies. This is because a lower percentage of their total area can collect solar energy. Equation (3.16) determines the total solar energy incident on the tilted surface of a collector array. Equation (3.17) gives the total energy incident on the aperture area of the solar array.

$$Q_c = A_c\, N_p\, G_{ta} \times \frac{3{,}600\ s}{h} \times \frac{365\ days}{year} \qquad (3.16)$$

$$Q_a = A_a\, N_p\, G_{ta} \times \frac{3{,}600\ s}{h} \times \frac{365\ days}{year} \tag{3.17}$$

Both these calculations use the yearly averages for solar insulation on a tilted surface (G_{ta}) in kWh/m^2/day. These values are then used in Eq. (3.18) and Eq. (3.19) to find the total efficiency of the solar array for gross area (η_c) and aperture area (η_a) respectively.

$$\eta_c = \frac{Q_u}{Q_c} \tag{3.18}$$

$$\eta_a = \frac{Q_u}{Q_a} \tag{3.19}$$

These efficiencies are then divided by the load factor to find the average efficiency of the panels in the array based on gross area (η_{cp}) and aperture area (η_{ap}) shown in Equation (3.20) and Equation (3.21).

$$\eta_{cp} = \frac{\eta_c}{L_f} \tag{3.20}$$

$$\eta_{ap} = \frac{\eta_a}{L_f} \tag{3.21}$$

Values for panel efficiency are more readily available than the performance variables $F_R(\tau\alpha)$ and F_RU_L, so these calculated efficiencies could be compared to published, calculated, or measured efficiencies to verify and adjust the performance variables. A large online catalogue of test results for various flat plate and evacuated tube collectors is available from the Swiss institute SPF (2012) to compare the efficiency calculated by the model to test results. The catalogue also gives panel dimensions, aperture area, and panel weight, which could aid in obtaining model inputs or preliminary designs for a solar array. SPF (2012) tested each of these panels and reports values for η_o, a_1 (W/m^{2}K), and a_2 (W/m^{2}K^2) based on panel aperture area. The panel efficiency using SPF (2012) data (η_{spf}) is found using Eq. (3.22) and Eq. (3.23).

$$\eta_{spf} = \eta_o - a_1 T_m^* - a_2 G T_m^{*2} \quad (3.22)$$

$$T_m^* = \frac{(T_m - T_a)}{G} \quad (3.23)$$

The mean temperature of the working fluid (T_m) should be larger than the average inlet temp (T_i) set by the user. The irradiation G (W/m^2) can be found using Eq. (3.24) and available solar resource data.

$$G = \frac{G_{ta} \times 1{,}000\frac{W}{kW}}{H_{day}} \quad (3.24)$$

This method was used to verify the panel parameters used. The average values for η_o, a_1 (W/m^2K), and a_2 (W/m^2K^2) from SPF test data are shown in Table 3.1, which are averages found by IEA's Solar Heating and Cooling Programme (IEA SHC) conference proceedings (2004). The values were verified by comparing current values on the SPF website (2012) and the averages still agree with current values on the SPF site. Using these values, the collector efficiency was calculated for a flat plate collector with values for $F_R(\tau\alpha)$ of 0.72 and F_RU_L of 4.5 and an evacuated tube collector with values for $F_R(\tau\alpha)$ of 0.59 and F_RU_L of 1.5. The flat plate collector aperture area was assumed to be 95% of the gross area and the evacuated tube aperture area was assumed to be 80% of the gross collector area. Both the tested plate efficiencies (η_{spf}) and the calculated model

Table 3.1: Average values from SPF test data for the efficiency coefficients of flat plate and evacuated tube solar collectors (IEA SHC 2004).

Average Efficiency Values for Solar Thermal Collectors		
	Flat Plate	Evacuated Tube
η_o	0.79	0.76
a_1	3.2	1.2
a_2	0.015	0.008

efficiencies (η_{ap}) were the same when T_m was set to about 10°C above T_i. This verifies that the model gives accurate estimates of panel efficiency compared to measured efficiencies of panels in the commercial market.

Model outputs for the solar calculations are shown in Figure 3.10. The total useful energy per year in MMBtu (Q_{ut}) is calculated by dividing the useful energy by the

Solar Outputs	
Solar Energy Received on Surface of Array, Q_c (MJ/yr)	
Solar Energy Received on Aperture Surface of Array, Q_a (MJ/yr)	
Useful Solar Thermal Energy, Q_u (MJ/yr)	
Useful Solar Energy, Q_{ut} (MMBtu/yr)	
Solar Array Efficiency, η_c (Gross Area)	
Solar Array Efficiency, η_a (Aperture Area)	
Solar Panel Efficiency, η_{cp} (Gross Area)	
Solar Panel Efficiency, η_{ap} (Aperture Area)	
Percent Shift From Natural Gas to Solar, $\%S_s$	
Percent Shift From Natural Gas to Solar (makeup water), $\%S_{MW}$	

Figure 3.10: Solar outputs of the model

standard conversion factor 1055 J/MMBtu. Equation (3.24) calculates the percent shift from natural gas heating to solar heating ($\%S_s$), and Equation (3.25) calculates the percent shift from natural gas heating to solar thermal heating of the boiler makeup water ($\%S_{MW}$).

$$\%S_s = \frac{Q_u}{Q_{total}} \tag{3.24}$$

$$\%S_{MW} = \frac{Q_u}{PC \times Q_{MW}} \tag{3.25}$$

3.6 Project Costs and Savings

The main concern for any business owner is the ability to make a profit so the business can continue to operate. Implementation costs and payback periods usually trump the good press a company might receive for installing a renewable energy project. This is especially true of ethanol plants that are currently producing environmentally-friendly fuel to reduce oil consumption. Therefore this model focuses on estimating realistic cost savings and payback periods for wind and solar installations. Some of the logistical issues that may arise when planning or installing both of these projects are discussed below, followed by the financial calculations of the model.

Wind and solar energy production can vary dramatically throughout the year. It will be important to be certain the maximum output of the system will not be too large. Since wind energy and plant energy usage varies throughout the day and year, the turbine may produce more energy than the plant consumes with a large percent shift from conventional electricity to wind power. Most turbines will be grid connected so the excess energy will flow into the grid, but the utility company will most likely pay a reduced rate on this electricity compared to the rate the plant is charged for electricity. This will increase the payback period for the wind turbine. Even if the wind turbine is appropriately sized, utility companies often set up purchase agreements with private turbine owners to buyback the electricity at a fixed or predetermined variable rate. The utility company will guarantee a purchase price for the electricity generated by a project and buy all of the electricity generated instead of charging the company for the difference between the electricity used and the electricity generated. This is called a power purchase agreement (PPA). This generally lowers the value of the electricity generated,

but helps the company better predict future energy costs and savings. It also provides backing for the project to guarantee investors the company will be able to repay loans.

It is very important to size a solar thermal array properly to reduce the risk of the system overheating or wasted energy due to low demand. Due to the constant need for thermal energy, it may seem unlikely that a solar array would produce more energy than an ethanol plant would use, but the position of the array in the process flow may make it possible for excess thermal energy to be produced. If the solar array is strictly used as a preheat system for groundwater, then there is a limit to the water the array has available to heat. The system should be limited to the maximum energy needed to heat ground water on the warmest day of the year. This will prevent overheating and wasted energy. A solar thermal system can store heat in large water tanks, which can also provide overheat protection. Wasted thermal energy reduces the amount of expected natural gas replacement, which could lengthen payback periods.

There are currently government and state incentives to encourage the installation of renewable energy projects. One of the most common incentives is a 30% rebate of the installed cost of the system. This incentive can be included in the model by reducing the installed costs by 30%. The main incentive for wind turbines is the Production Tax Credit (PTC), which pays $0.022 per kWh produced by the turbine for the first 10 years (DSIRE 2012). This credit is set to expire at the end of 2012 and it is uncertain if this credit will be extended. The production tax credit can be accounted for by adding $0.022/kWh to the electricity rate. This will give a good estimate for the first ten years of the turbine operation, but will overestimate savings beyond 10 years.

The yearly cost savings of the wind turbine and solar array can be calculated using several methods depending on the adjustments made to the input values. The spreadsheet field for price inputs is shown in Figure 3.11.

Price Inputs		
	Typical Values	**Input**
Current Average Price of Natural Gas for Industrial Sector, R_{NG} ($/MMBtu)	$4.00 - $14	
Natural Gas Percent Price Increase per Year, n_{NG}	0-5%	
Current Average Price of Electricity for Industrial Sector, R_E ($/kWh)	$0.05 – $0.14	
Electricity Percent Price Increase Per Year, n_E	0-3%	

Figure 3.11: Spreadsheet model price inputs

The natural gas price (R_{NG}) in $/MMBtu can be obtained from utility bills or estimated based on U.S. or state averages. It is important to employ end use prices instead of Henry hub or other pipeline prices. The average U.S. natural gas price for the industrial sector in 2011 was $5.11/ft^3 (EIA 2012c). Using the average energy content of natural gas, 1.023 ft^3/MMBtu, the 2011 rate is $5.00/MMBtu. Natural gas prices for each state are also available on the EIA website (2012c) and are included in Table B.1 in Appendix B. Accurate price data will better model cost savings for a particular location.

The average electricity rate (R_E) in $/kWh can also be obtained from utility bills or available price data. The average industrial end use electricity rate for the U.S. was $6.82/kWh for 2011 (EIA 2012c). Average electricity rates for each state are included in Table B.2 in Appendix B. The U.S. average electricity and natural gas rates will be used for most simulations.

Both natural gas and electricity prices are projected to rise over the next 20 years. The lifespan for wind turbines and solar arrays are 20 years or more, which means the changing prices of energy may have a large effect on the economic feasibility of solar and wind installations. This model can simulate electricity and natural gas price increases over the lifespan of the wind or solar installation. The annual percent increase for natural gas prices (n_{NG}) and annual percent increase for electricity prices (n_E) are entered into the model to account for moderate or severe increases in energy costs and/or inflation.

The EIA (2012a) projects the 2035 price of natural gas to be \$7.73/ft^3 in 2010 dollars or \$7.56/MMBtu. This is a 2.1% price increase per year when the 2011 price is considered. Two other price predictions were included in the EIA report. IHSGI reports a 2035 price of \$7.22/ft^3, and SEER predicts a price of \$9.20/ft^3 in 2010 dollars. These two predictions equate to a yearly price increase of 1.7% and 3.3% respectively. These price increases do not include inflation. Inflation can be considered by adding a yearly inflation rate to the price increase percent. Various price increases are investigated to show changes in payback period and cumulative cost savings due to changes in future energy prices.

EIA projections for the price of electricity over the next 25 years are relatively stable. The 2035 price of electricity is projected to be \$0.071/kWh for the AEO reference case, \$0.076 for EVA estimates, and \$0.081 according to IHSGI (EIA 2012a). All of these predictions result in a yearly rate increase below 1%. This means that inflation will account for most of the price increase of electricity over the next 20 years.

Cost and savings outputs of the model are shown in Figure 3.12. The yearly savings and simple payback period values are for the user input values for natural gas or electricity. The yearly natural gas savings is found using Equation (3.26), and the yearly electricity savings for the entered electricity rate is calculated using Eq. (3.27).

$$S_{NG} = Q_u \, R_{NG} \tag{3.26}$$

$$S_E = E_w \, R_E \tag{3.27}$$

Cost and Savings Outputs	
Natural Gas Cost Savings, S_{NG} ($/yr)	
Electricity Cost Savings, S_E ($/yr)	
Solar Array Installed Cost, SC	
Wind Turbine Installed Cost, WC	
Solar Simple Payback Period, PP_s (years)	
Wind Simple Payback Period, PP_w (years)	

Figure 3.12: Simple cost and savings outputs of the model

Equation (3.28) is used to find the total installed cost of the solar array, and Equation (3.29) gives the total installed cost of the wind turbine.

$$SC = N_p \, A_c \, IC_{sc} \tag{3.28}$$

$$WC = P_C \, IC_{wt} \tag{3.29}$$

The simple payback period is a preliminary measure of the length of time it will take for the cumulative cost savings to exceed the total installed cost of the project. Simple payback times do not consider inflation or rising energy costs. Equation (3.30) is used to find the simple payback period for the solar thermal array, and Equation (3.31) is used to find the simple payback period for the wind turbine.

$$PP_s = \frac{SC}{S_{NG}} \tag{3.30}$$

$$PP_w = \frac{WC}{S_E} \tag{3.31}$$

A more realistic measure of the payback period is found using yearly increases of natural gas and electricity prices. Equation (3.32) is used to find the cumulative cost savings (CS_s) of the solar array after n years. The natural gas rate during year n (R_{NGi}) is calculated using Eq. (3.33). Similarly the cumulative cost savings (CS_w) of the wind turbine is given by Equation (3.34), and the electricity rate for year n (R_{Ei}) is found using Eq. (3.35).

$$CS_s = -SC + \sum_{i=1}^{n} Q_{ut}\, R_{NG_i} \tag{3.32}$$

$$R_{NG\,i} = R_{NG\,i-1} \times (1 + n_{NG}) \tag{3.33}$$

$$CS_w = -WC + \sum_{i=1}^{n} E_w\, R_{E\,i} \tag{3.34}$$

$$R_{E\,i} = R_{E\,i-1} \times (1 + n_E) \tag{3.35}$$

The natural gas and electricity rates for the first year (n = 1) are the user-entered values, R_{NG} and R_E. This model calculates cumulative savings for thirty years, which may be longer than the useful lifespans of the solar array and wind turbine. Typical reported lifespans of wind turbines are 20 to 25 years. Solar arrays have reported lifespans between 20 and 30 years. The cumulative savings is plotted per year to show the crossover point between negative and positive values. This is the payback period in years for the project when increases in energy prices are considered.

Both systems will need regular maintenance with more expensive repairs or equipment replacement as the system gets older. Wiser and Bolinger (2012) report that operational and maintenance (O&M) costs are going down for newer wind turbines.

They report the average O&M costs for 69 projects installed since 2000 at $10/MWh (Wiser and Bolinger 2012). The average maintenance costs can be accounted for in the model by reducing the base electricity rate by the estimated O&M costs. If the electricity rate (R_E) was $0.07/kWh and the O&M costs were $0.01/kWh, then the resulting electricity rate would be $0.06/kWh.

3.7 Evaluations and Comparisons of Ethanol Plant Locations

The model was used to evaluate 18 ethanol plants across the U.S. to determine the feasibility of solar thermal and wind power installations. Plants were chosen in all of the major ethanol producing states as well as states that produce very little ethanol. Many of the locations were chosen based on advantageous wind or solar resources in that region. Figure 3.13 shows the approximate location of each ethanol plants considered for this study. All of the relevant data needed for the model for each location is included in

Figure 3.13: Approximate locations for the 18 ethanol plants considered for this study.

Appendix A. Each location was compared using identical solar and wind installations to evaluate the relative payback periods and cumulative cost savings of different areas of the country. The U.S. average 2011 electricity and natural gas prices were used unless otherwise noted. This may introduce small errors in areas that have high or low energy prices. Some locations were separately evaluated using the average energy prices for the state to illustrate the effect of energy price on payback period. Fluctuations in payback period and cumulative savings were investigated by changing inputs for installed cost, energy rates, and rate increases. Modeling the range of possible installation and future conditions gives a better representation of project feasibility.

Each ethanol plant has its own tab in the spreadsheet model. It includes the resource and meteorological data inputs as well as the monthly and yearly outputs. Users can continue to compare plant locations under different conditions in addition to modeling a new location. This allows users to take advantage of data that has already been collected.

3.8 Summary

A model was developed to determine if solar thermal and/or wind power projects are feasible options for reducing fossil fuel consumption at dry mill ethanol plants. Various location and project specifications are entered into the model, and the model calculates payback periods and cost savings for solar and wind installations.

The model was used to compare and analyze wind and solar opportunities at 18 different ethanol plant locations across the U.S. Changes in the various inputs were also examined to predict the range of possible outcomes for different project conditions.

CHAPTER 4: MODEL RESULTS AND ANALYSIS

4.1 Introduction

The outputs from the model were analyzed to determine how closely they replicate a real project and then the model was used to simulate numerous economic and resource conditions for solar and wind projects. The accuracy of the solar and wind models was verified with experimental and operational data. Project feasibility was analyzed for solar and wind installations at 18 different ethanol plants across the country. The input variables for solar, wind, cost, and price were varied to show their influence on payback period and lifetime costs savings for a solar thermal array and a wind turbine.

4.2 Verifying the Solar Energy Model

The model of a solar thermal collector was calibrated and verified by comparing the calculated efficiency of the model to the experimental efficiency coefficients reported by SPF (2012). First the model outputs for various values for $F_R(\tau\alpha)$ and F_RU_L were evaluated to determine the most realistic combination for a flat plate and an evacuated tube collector. RETScreen (2005) estimates for $F_R(\tau\alpha)$ and F_RU_L were used along with SPF test data (2012) to determine the optimal values for each collector. The average values from SPF, shown in Table 3.1, were used with the solar insolation and average ambient temperature data to calculate the useful solar energy produced each month for a flat plate and evacuated tube collector. These values were used to find the average yearly efficiencies of both collectors. The model uses the temperature of the fluid at the inlet of the panel, while the SPF efficiency calculations use the mean temperature of the fluid in

the panel. It was assumed the mean temperature of the working fluid would be 10°C above the inlet temperature. The aperture area of the flat plate and evacuated tube collectors was assumed to be 95% and 80% of the gross area respectively. The values for $F_R(\tau\alpha)$ and F_RU_L that best followed the SPF efficiencies were 0.72 and 4.5 for a flat plate collector and 0.59 and 1.5 for an evacuated tube collector. The solar insolation and average ambient temperature data for Arthur, IA, shown in Table A.7 in Appendix A, was used to find the yearly efficiency of the solar array at different inlet fluid temperatures using the model and the SPF values. The yearly efficiency found from the model and the efficiency found from the SPF data are both shown in Figure 4.1 for flat plate and evacuated tube collectors at various inlet fluid temperatures. The model and SPF values show the same behavior for the respective panels. The model accurately estimates the energy production of a flat plate and evacuated tube collector. These values are for the panels only and not the entire system. There will be additional losses from the system that can be accounted for by adjusting the load factor (L_f) of the solar array.

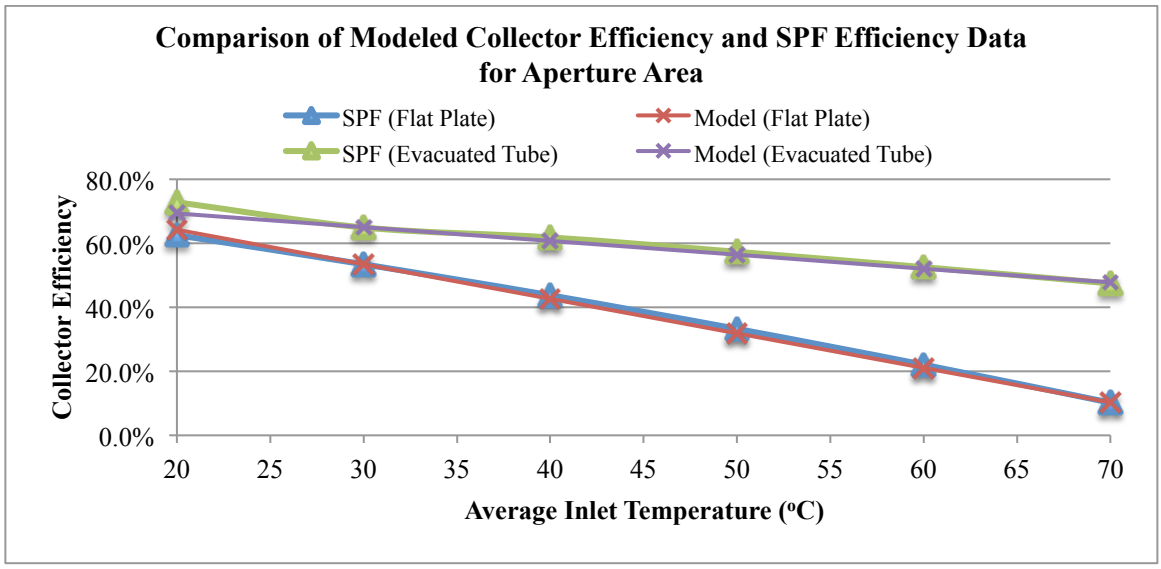

Figure 4.1: Comparison of calculated efficiency values from the model and the SPF (2012) efficiency coefficients for a flat plate and evacuated tube array based on aperture area.

Many solar collector efficiencies are reported according to gross area instead of aperture area. The same data were converted to efficiency values based on gross area and are shown in Figure 4.2. Due to a smaller aperture area, evacuated tubes suffer slightly from gross area efficiency calculations, but they also have significantly high costs per square meter. Regardless of the method of calculation, evacuated tubes would provide more energy for an ethanol plant in Arthur, IA, but the additional cost may not warrant the efficiency increases.

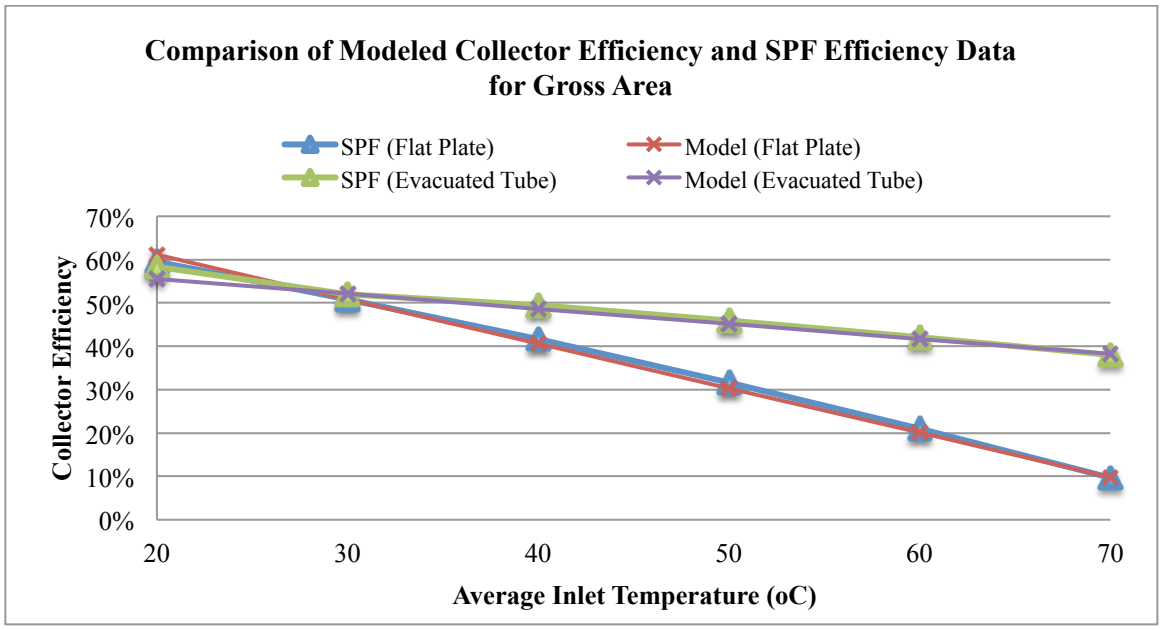

Figure 4.2: Comparison of calculated efficiency values from the model and SPF efficiency coefficients for a flat plate and evacuated tube array based on gross area.

4.3 Evaluating Flat Plate and Evacuated Tube Arrays

The energy production and payback periods for both flat plate and evacuated tube collectors were evaluated for 18 ethanol plant locations. Figure 4.3 shows the annual useful energy production for a 5,000 m^2 solar array of both flat plate collectors and evacuated tube collectors with an average input temperature of 30^{o}C. The load factor

was set at 90% for both collectors. The performance of the flat plate and evacuated tube collectors is very similar for the Midwestern states due to the low inlet temperature.

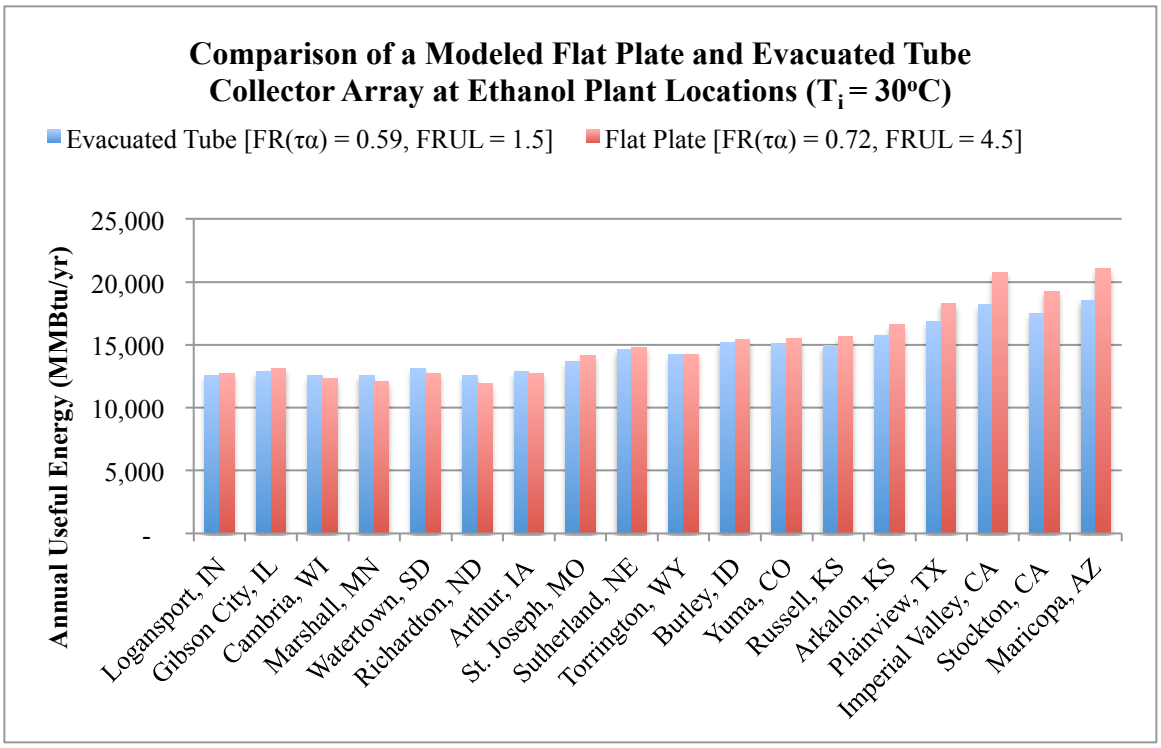

Figure 4.3: Model of a 5,000m^2 gross area flat plate and evacuated tube collector array for solar resources at 18 ethanol plant locations and an average inlet temperature of 30°C.

The flat plate collectors show a slight improvement over the evacuated tube collectors in Texas, California, and Arizona, which have higher ambient temperatures. Figure 4.4 shows the annual useful energy production of the same solar array with an increased inlet temperature of 60°C. The larger inlet temperature significantly reduces the total energy production of the system for all plant locations. Evacuated tubes show much better performance than flat plate collectors with the larger inlet temperature. In most of the Midwestern states the flat plate panels produce less than half the energy that the evacuated tubes produce. It is clear that cold climates greatly benefit from evacuated

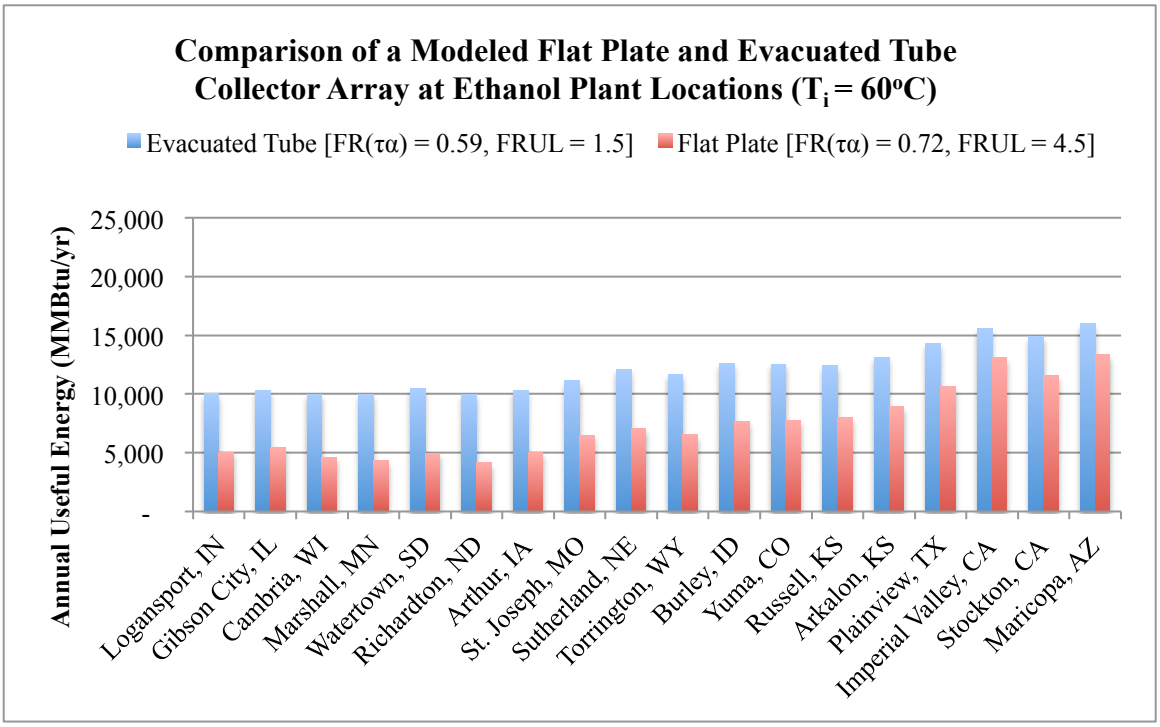

Figure 4.4: Model of a 5,000m^2 gross area flat plate and evacuated tube collector array for solar resources at 18 ethanol plant locations and an average inlet temperature of 60°C.

tube collectors with increased working fluid temperature. Solar resources are very consistent in similar areas of the country, which means conclusions drawn for these particular ethanol plant locations can be applied to nearby locations. Solar resources tend to be consistent for each area of the country.

The model accurately predicts the heat produced by flat plate and evacuated tube collectors. Cold climates and large differences between the working fluid temperature and the ambient temperature favor evacuated tube collectors. The fluid temperature in the solar array has a large impact on the annual useful energy produced by the array. Cold ambient temperatures negatively affect the efficiency of both flat plate and evacuated tube collectors, but flat plate panels suffer a much higher penalty. These are

all proven facts in the solar thermal industry (IEA 2012), but this model demonstrates the magnitude of these differences. Performance of a solar array depends on numerous input variables that can all be changed to show the range of conditions that exist in during actual operation.

4.4 Evaluating Model Results for Solar Thermal Projects

The total percent shift from natural gas heating to solar heating is very low for all four situations considered above. The heating requirement for all of the ethanol plants was assumed to be 29,000 Btu/gal-ethanol. The total percent shift to solar thermal energy for the 5,000 m^2 flat plate array with an inlet temperature of 30^oC ranged between 0.4% and 4.1%. Most of the locations had less than 1% shift to solar energy from natural gas. These are very small percentages and may deter any further investigation, but total percent shift is not a good measure of the total heating that could be accomplished by a non-concentrating solar array.

Percent shift to solar heating for the boiler makeup water gives much more reasonable values. The percent shift to solar heating of the boiler makeup water for the array modeled in Figure 4.3 is shown in Figure 4.5 along with the total production capacity for each ethanol plant. The largest percent shift is for the Torrington, WY plant with an 87% shift. This very large percentage would be oversized for the 12 MGY plant, because peak summer solar heating would most likely far exceed the plant's makeup water heating needs. All of the other plants show a more reasonable percent shift below 50%. Even with the low percent shift to solar heating, this array is quite substantial. The gross area of the collectors is 5,000 m^2 or just under 54,000 ft^2. The actual installed array

would most likely be larger due to installation requirements. This is a large area, but ethanol plants typically are built on many acres of land and have large flat roofs that could be used for installing the solar array. It may be possible to install a larger array depending on available area.

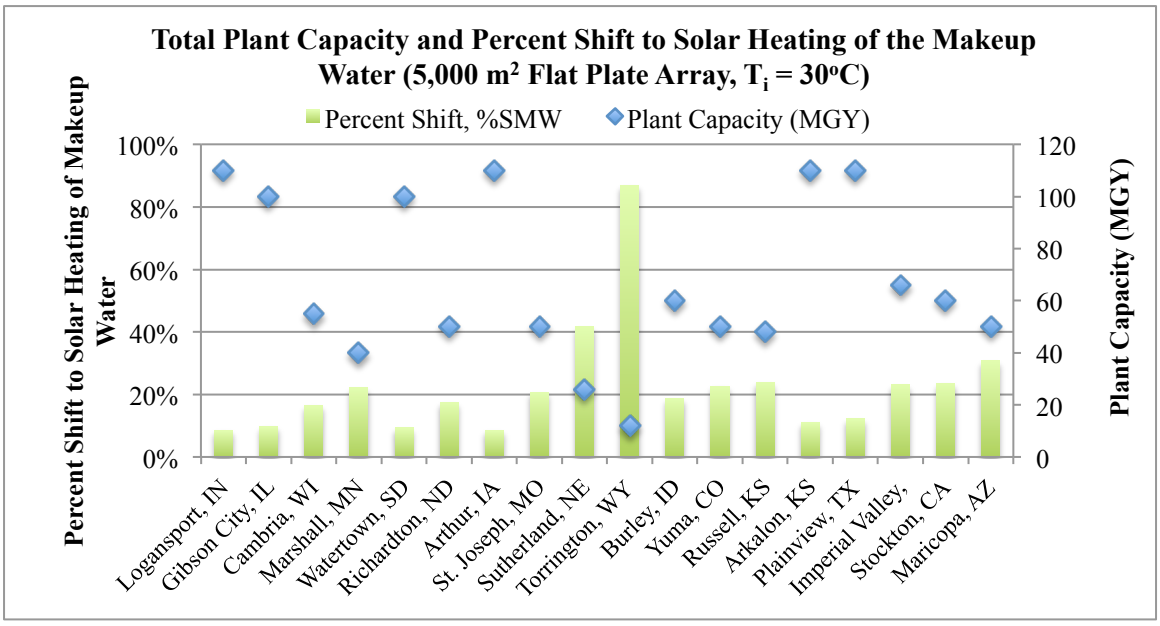

Figure 4.5: Total plant capacity and percent shift to solar heating of the boiler makeup water using a 5,000 m^2 flat plate array at 18 ethanol plants.

The payback periods for a flat plate and an evacuated tube array for all of the ethanol plant locations were compared. Figure 4.6 shows the cumulative cost savings over a lifespan of 30 years for a flat plate solar thermal array for six of the 18 ethanol plants. Some manufacturers claim lifespans for solar thermal panels up to 30 years, but 20 years would be most common (IEA 2012). Thirty years are shown to represent the maximum possible savings, but real operational lifetimes will most likely be shorter. The modeled 5,000 m^2 array had an estimated installed cost of \$314/m^2 with a government rebate of 30%, which brought the installed cost down to \$220/m^2. The average inlet temperature was set to 30°C. The initial natural gas price was set at \$5/MMBtu, and an

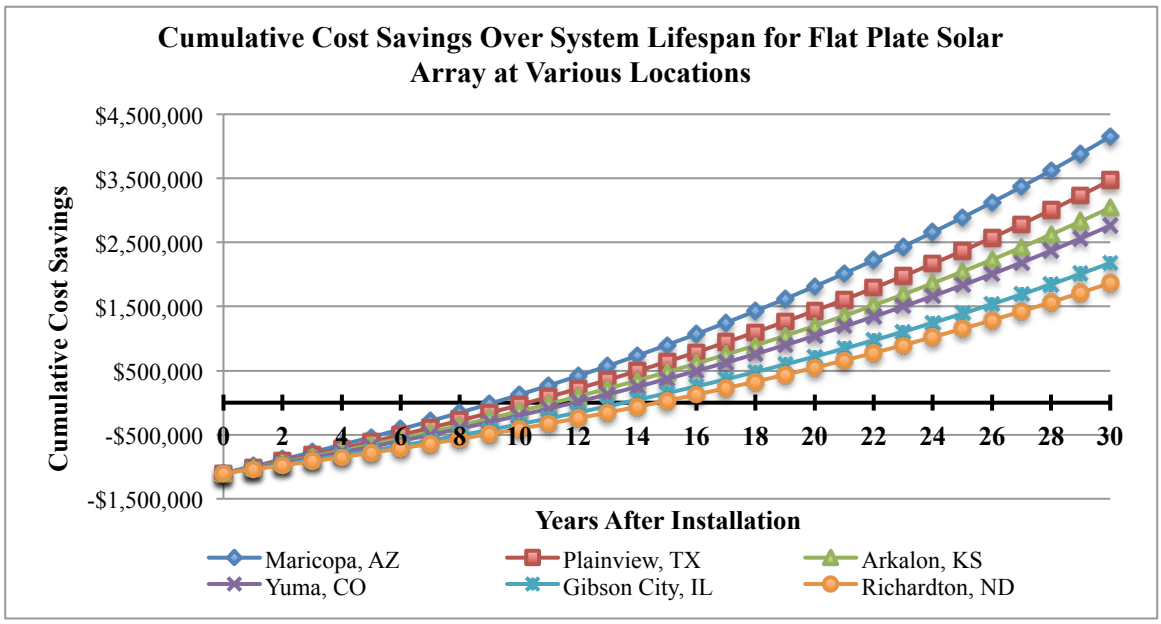

Figure 4.6: Modeled cumulative cost savings of a standard flat plate solar array for selected ethanol plant locations. Model input values: $F_R(\tau\alpha) = 0.72$, $F_R U_L = 4.5$, $T_i = 30^oC$, $R_{NG} = \$5/MMBtu$, $n_{NG} = 3.3\%$, $IC_s = \$220/m^2$.

annual rate increase of 3.3% was chosen. A load factor of 90% was used to account for additional heat losses and inefficiencies in the system. These six locations were chosen to show the spread of the data. All of the plants not shown had payback periods between the two extremes. Maricopa, AZ had the shortest payback period at about 9 years, while Richardton, ND had the longest payback period at about 15 years. The efficiency of the entire array was 58% for Maricopa and 44% for Richardton. This seemingly small difference in efficiency had a large impact on the payback period and cumulative savings of the two projects. The payback periods are quite far above the typical payback period that businesses look for, but all of the solar arrays payback well before an expected lifespan of 20 years and then continue to save energy and costs. The modeled array for Maricopa, AZ provides a net profit of over $4 million with a 30-year lifespan. This is 4

times the initial installed cost. If additional rebates or tax incentives are applied the payback period would decrease and the lifetime savings would increase.

The variation in solar energy throughout the year is another factor to consider when proposing a solar thermal array. Figure 4.7 shows the monthly useful energy output of the flat plate array modeled for Figure 4.3. Only three locations are shown because the other locations show behavior similar to one of these three distributions. Burley, ID has the largest range of energy production with over four times as much energy produced in July compared to January. Imperial Valley, CA had one of the smallest ranges with production in June less than double production in December. Even with the most favorable ethanol plant locations in the U.S., useful energy from a solar array will change significantly throughout the year.

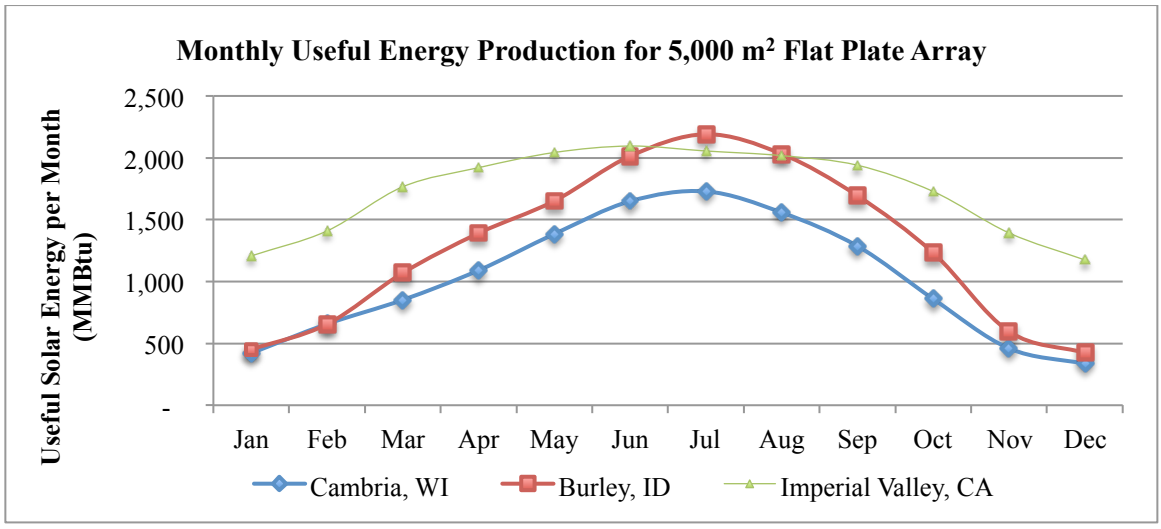

Figure 4.7: Monthly useful energy from a 5,000 m^2 flat plate array for Cambria, WI, Burley, ID, and Imperial Valley, CA.

The price of natural gas varies widely across the country. This can significantly affect the payback period and cumulative cost savings for a solar project. The same flat

plate solar array modeled in Figure 4.6 was used to model the changes in payback period due to adjustments to the natural gas price. All other variables were kept constant. The average natural gas prices for California, Texas, Arizona, and Missouri for 2011 from Table B.1 were used to more accurately model the payback period for solar arrays in these states. The model results for both the U.S. average natural gas price of $5.00/MMBtu and the average state natural gas prices for Imperial Valley, CA and Plainview, TX are shown in Figure 4.8. The natural gas price for Texas is $4.11/MMBtu, and the average price is $6.88/MMBtu for California. The payback periods and cumulative cost savings for the Texas and California plants were very close for the average U.S. gas price, but diverge when using the state gas rates. The payback period for California went from just over 9 years to less than 7 years. The cumulative cost savings increased by nearly $2 million. The lower natural gas rate in Texas increased the payback period by two years and decreased the cumulative savings by over $800

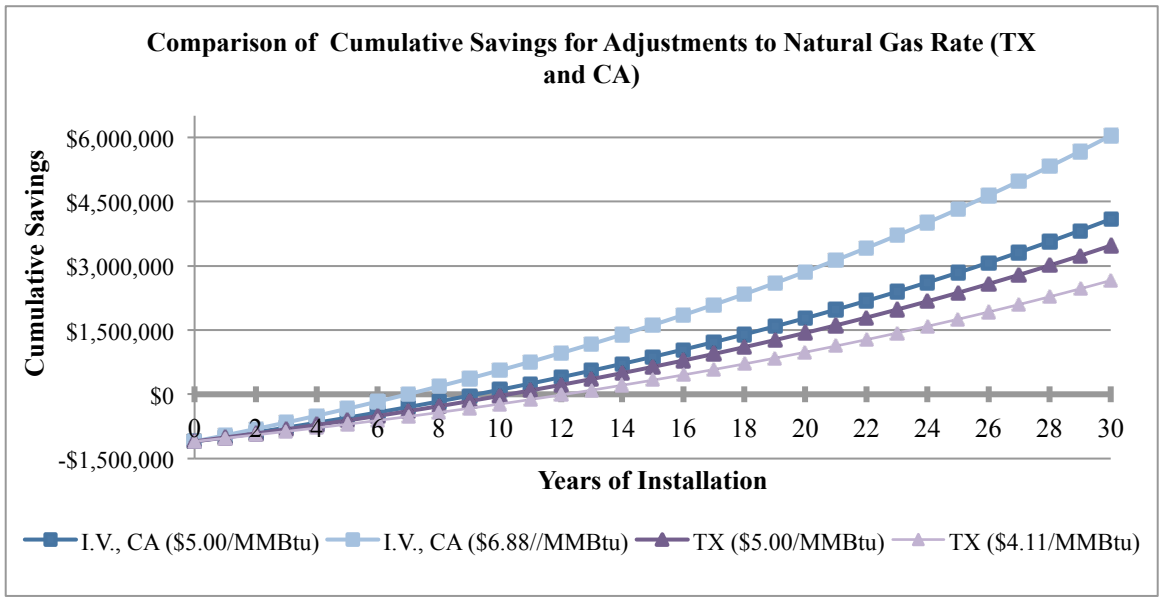

Figure 4.8: Modeled cumulative cost savings and payback period for Texas and California ethanol plants using the national and state natural gas prices. Model input values: $F_R(\tau\alpha) = 0.72$, $F_RU_L = 4.5$, $T_i = 30^oC$, $n_{NG} = 3.3\%$, $IC_s = \$220/m^2$.

thousand. The actual rate an ethanol plant pays for their natural gas use will be one of the main determining factors in the profitability of a solar thermal array.

The rate paid for natural gas can makeup for sizeable differences in solar resources. The modeled flat plate array in Figure 4.3 in Arizona produced over 30% more energy than the same array in Missouri. By using the average natural gas prices in Missouri and Arizona, the solar installation in Missouri is nearly as economical as the installation in Arizona. Figure 4.9 shows the model results for the payback period and cumulative savings for the national average natural gas rate and the state gas rate for the solar array in Missouri and Arizona. The increased gas price of $8.24/MMBtu decreased the payback period to less than 9 years, which is 4 years less than the payback period using the national rate of $5/MMBtu. The cumulative savings increased by over $2 million as well. These values are all more favorable than the Arizona solar array using the national gas rate. This shows that natural gas price can be a more important factor

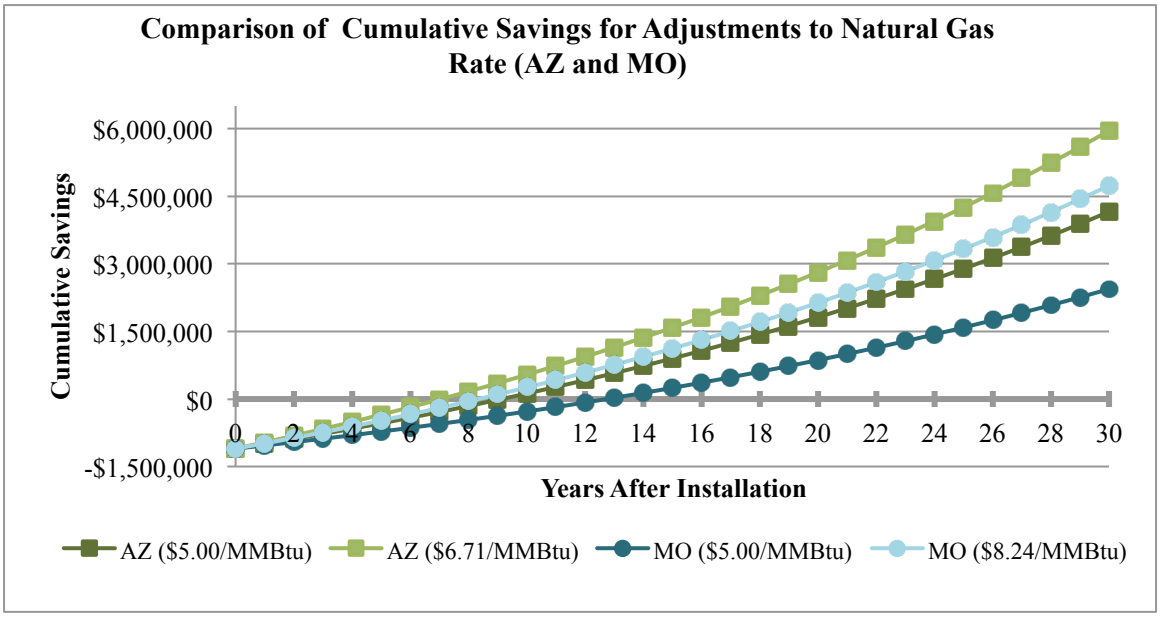

Figure 4.9: Modeled cumulative cost savings and payback period for Arizona and Missouri ethanol plants using the national and state natural gas prices. Model input values: $F_R(\tau\alpha) = 0.72$, $F_R U_L = 4.5$, $T_i = 30^oC$, $n_{NG} = 3.3\%$, $IC_s = \$220/m^2$.

than solar resource in determining the economic feasibility of a solar thermal project. The modeled array for Arizona becomes even more promising when the state gas rate of $6.71/MMBtu is used. The payback period decreased to just over 7 years, which is a reduction of 2 years. The cumulative savings over a 30-year lifespan of the solar array is nearly $6 million. These results clearly show that accurate natural gas rates are extremely important in determining the financial outcomes of a solar thermal project.

The cumulative savings can be slightly misleading because as the system ages it will need more maintenance and replacement equipment. Some of the cost savings will be used to maintain the system and make upgrades, but these costs should be significantly less than the total savings per year. It is also not guaranteed that the system will still be operating at an acceptable level after 30 years. It is likely that the efficiency of the system will decrease slightly as the materials age as well. This will reduce the cost savings predicted by the model. These are all factors to consider when planning for the potential savings of a solar array.

The percent increase of natural gas prices will have a large influence on the cumulative savings from a solar project, but does not reduce the payback period significantly. Figure 4.10 shows the same flat plate array described for Figure 4.6 for Maricopa, AZ with four different percent increases of the natural gas rate. The payback period and cumulative cost savings are shown for a steady natural gas price of $6.71/MMBtu over a 25 year lifespan as well as yearly rate increases of 2%, 3.33%, and 5%. The payback periods for the steady rate, 2% and 3.33% are all between 7 and 8 years, and the 5% rate increase shows a payback period of between 6 and 7 years. The main difference between these rate increases is the total cost savings after about 12 years.

With a 5% rate increase, the cumulative cost savings are $3.2 million more than the steady gas rate. This is almost three times the purchase price of the original system. Very large values for the lifetime savings of a solar array are possible if the price of natural gas increases at a high rate. As discussed previously, a 2% yearly rate increase in current dollars is the most likely future scenario. If inflation were considered, then the 3.33% value would be more realistic. The yearly price increase of natural gas will mostly likely be a secondary consideration when planning a solar project. Its minimal effect on payback period means that it is not essential when considering short timeframes. Future natural gas prices should be considered when the lifetime profitability of a system is analyzed.

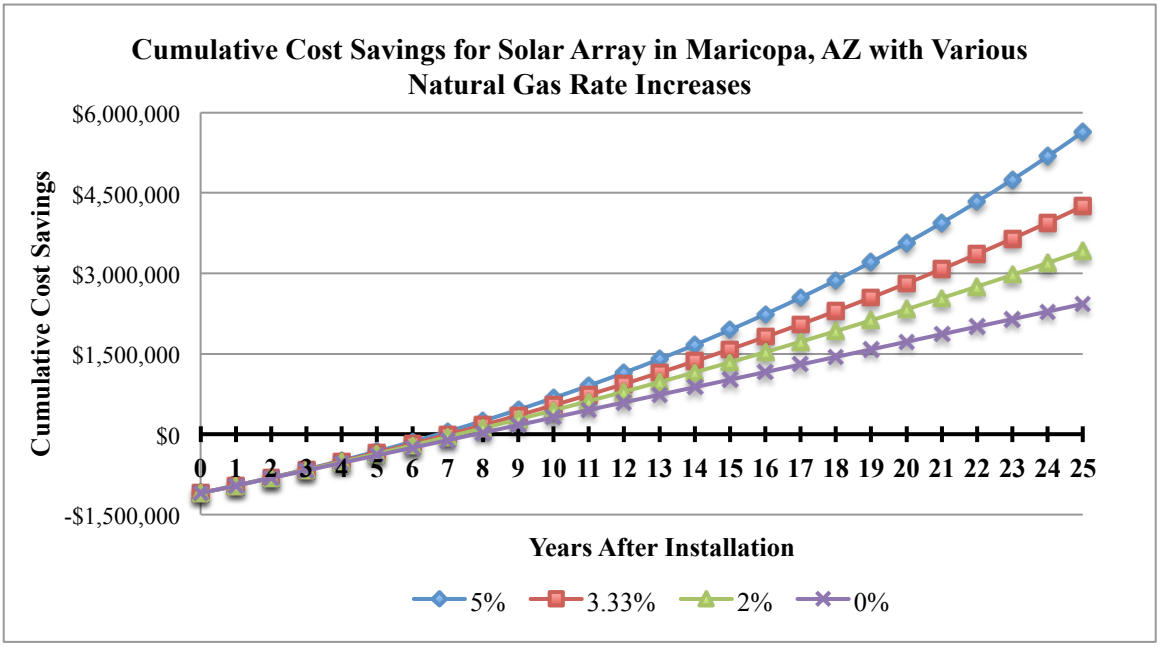

Figure 4.10: Modeled cumulative cost savings and payback period for a flat plate array in Maricopa, AZ with four different percent price increases for natural gas. Model input values: $F_R(\tau\alpha) = 0.72$, $F_R U_L = 4.5$, $T_i = 30^oC$, $IC_s = \$220/m^2$.

All of the simulations of payback periods shown previously used the low installed cost estimate of $\$314/m^2$ for flat plate collectors with a 30% government incentive. The

30% federal government incentive is currently available for solar thermal systems through the year 2016 (DSIRE 2012), so it will be considered for all simulations. Payback periods for the low and high costs of flat plate and evacuated tube collectors are compared for a 5,000 m^2 gross area solar array in Sutherland, NE in Figure 4.11. The input variables for the model are shown in Table 4.1. The load factor for the flat plate

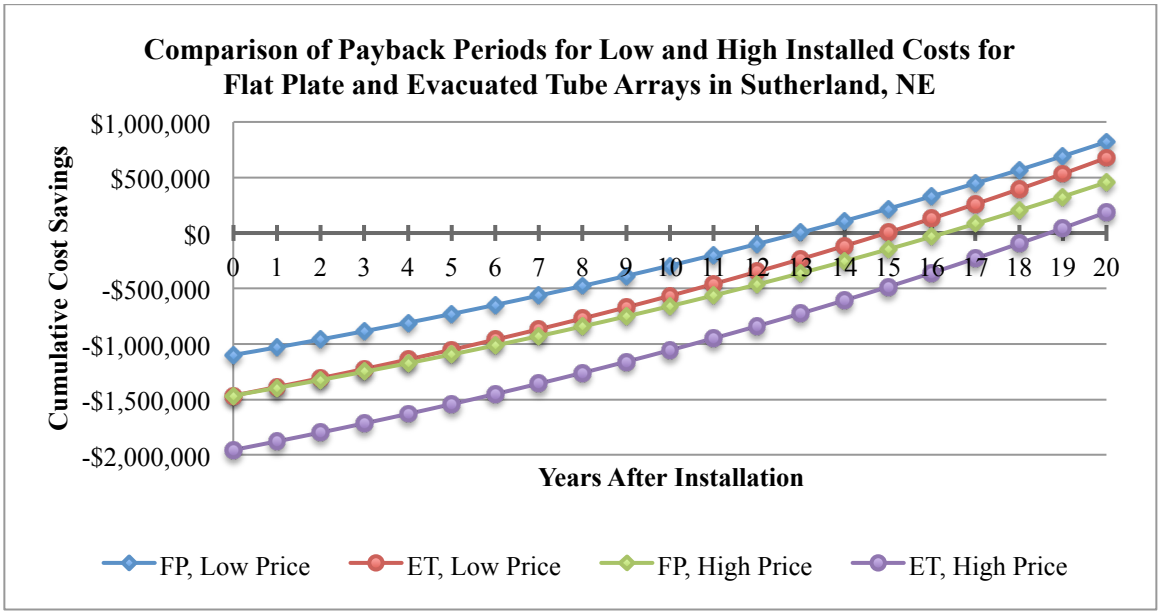

Figure 4.11: Modeled cumulative savings and payback period for low and high installed costs for a standard flat plate and evacuated tube collector array in Sutherland, NE.

Table 4.1: Model inputs for simulation shown in Figure 4.11 for different installed costs

Price Inputs		
	Flat Plate	**Evacuated Tube**
Current Average Price of Natural Gas for Industrial Sector, R_{NG} ($/MMBtu)	5.44	5.44
Natural Gas Percent Price Increase per Year, n_{NG}	0.033	0.033
Solar Inputs		
Total Area of Each Collector, A_T (m^2)	5	5
Number of Panels, N_p	1000	1000
Price per square meter, IC_{sc} ($/$m^2$)	$220 / 293	$293 / 391
$F_R(\tau\alpha)_n$	0.72	0.59
F_RU_L (W/m^2-°C)	4.5	1.5
Input temperature of working fluid, T_i (°C)	35	35
Load Factor, L_f	0.85	0.9

array is 5% lower than the evacuated tube array to account for reduced absorption when the sun is low in the sky. The average natural gas price for Nebraska of $5.44/MMBtu was used. The low-priced flat plate collector had the shortest payback period at 13 years while the low-priced evacuated tube collector was at 15 years, the high priced flat plate collector was at 16 years, and the high priced evacuated tube was at 19 years. All of these payback periods are most likely too long to be considered economically feasible for an ethanol plant. The low-priced evacuated tube collector begins to draw nearer the low-priced flat plate collector as more years pass. The increased solar energy available from the evacuated tube collector begins to make up for the high installed cost, but doesn't reach the cumulative savings of the flat plate collector until after 20 years.

This model can also be used with yearly averages for the solar insolation and ambient air temperature. The model outputs using the monthly data and yearly averages for several plant locations were compared to see the differences between these two methods. Table 4.2 shows the useful energy output of the model for the inputs shown in Table 4.1 with a load factor of 90%. The table shows the model outputs for the yearly and monthly inputs as well as the percent difference in these values. The monthly

Table 4.2: Comparison of model outputs for monthly and yearly data inputs

Location	Useful Energy MMBtu/yr (Yearly Inputs)	Useful Energy MMBtu/yr (Monthly Inputs)	Percent Difference
Marshall, MN	10,376	10,763	3.6%
Gibson City, IL	11,531	11,846	2.7%
St. Joseph, MO	12,606	12,890	2.2%
Arkalon, KS	15,108	15,308	1.3%
Maricopa, AZ	19,577	19,758	0.9%

meteorological data inputs give a slightly higher value for useful energy and the difference increases as the yearly range in air temperature and solar energy increases. The model only shows small differences for monthly and yearly data inputs and should not have a substantial effect on the final output values.

The payback period for a realistic flat plate array was modeled using the individual state natural gas prices for all of the ethanol plant locations. All of the input values for the flat plate collector from Table 4.1 were used except the load factor. The load factor was increased to 90% to model a well-designed system with minimal losses. The lower installed cost of \$220/m^2 was used because the size of the system should provide savings in bulk discounts on equipment, and the 30% Investment Tax Credit (ITC) was applied. Table 4.3 shows the natural gas price and the payback period for this

Table 4.3: State natural gas rates and payback period modeled for a realistic flat plate collector

Location	Natural Gas Price ($/MMBtu)	Payback Period	First Year Cost Savings, S_S ($/yr)
Logansport, IN	5.52	14.0	$63,331
Gibson City, IL	6.59	11.8	$78,065
Cambria, WI	6.79	12.2	$74,704
Marshall, MN	5.44	14.9	$58,551
Watertown, SD	5.89	13.3	$67,117
Richardton, ND	4.97	16.1	$52,657
Arthur, IA	5.71	13.6	$65,362
St. Joseph, MO	8.24	9.1	$106,214
Sutherland, NE	5.44	12.4	$73,435
Torrington, WY	4.8	14.1	$62,242
Burley, ID	6.25	10.6	$88,250
Yuma, CO	5.71	11.4	$80,985
Russell, KS	5.38	11.8	$77,542
Arkalon, KS	5.38	11.2	$82,357
Plainview, TX	4.11	12.9	$69,911
Imperial Valley, CA	6.88	7.4	$134,057
Stockton, CA	6.88	7.9	$123,613
Maricopa, AZ	6.71	7.5	$132,576

array for all of the ethanol plant locations. Only three states have payback periods less than ten years, which include Arizona, California, and Missouri. These three states are the best locations to consider a solar thermal array. California and Arizona have ample solar resources with mid-range natural gas prices to provide payback periods less than 8 years. Missouri is a good candidate for a solar array due to moderate solar resources and a high natural gas price. All three states have yearly natural gas cost savings over $100,000 for the first year. Solar thermal systems could be practical in Idaho, Kansas, and Colorado if additional incentives are available through federal and local programs. If substantial financial assistance and backing for solar thermal projects becomes available through additional government programs, then a flat plate array may become feasible for most of the other ethanol plant locations. It is unlikely that any amount of financial assistance would make a solar thermal array practical for an ethanol plant in North Dakota due to the low solar resources and low natural gas price.

The model accurately estimates the payback period and cumulative cost savings for solar thermal projects. Changes to the numerous inputs can model a wide range of project conditions to compare different possibilities. The cost of natural gas has a very large influence on project feasibility while solar resources generally have a smaller influence. Variations in the yearly price increase of natural gas mainly influence the lifetime savings of a project, but do not change the payback period significantly. Continued government incentives are essential to the feasibility of future solar hot water heating projects for ethanol plants.

Solar thermal arrays can be a viable option for ethanol plants to reduce energy costs, fossil fuel consumption, and greenhouse gas emissions. There are some financial

risks due to the large installed cost of the system and the long payback periods. The most profitable solar arrays will be in areas with medium to high solar resources with natural gas rates well above the national average. Expanded government incentives and programs could make solar heating profitable for Midwestern states where most of the corn ethanol is produced. It is unlikely that solar thermal projects will be economically viable for the most northern states due to extreme temperatures and lower solar resources.

4.5 Verifying the Wind Energy Model

The wind model was verified by comparing the electricity generation of the modeled turbines for the various ethanol plant locations to average data from installed projects across the country. The model inputs are shown in Table 4.4 as well as the outputs for the design turbine using a power coefficient (C_{pd}) of 0.5. The design power coefficient was used to find the design turbine power and theoretical electricity generation to determine the actual capacity factor. The model outputs for the electricity generation of this turbine at the various ethanol plant locations is shown in Table 4.5

Table 4.4: Model inputs for a standard wind turbine with the outputs for the design turbine with $C_{pd} = 0.5$.

Wind Inputs	
	Input
Design Wind Speed for Turbine, V_d (m/s)	9.8
Installed Cost of Wind Turbine, IC_{wt} ($/kW)	1800
Diameter of Turbine Blade, D_R (m)	81
Monthly Wind Data	
	Input
Power Coefficient, C_{pa} or C_{pd}	0.45
Capacity Factor, 1 or C_{fa}	0.95
Outputs	**Output**
Design Turbine Power, P_d (MW)	1.5
Theoretical Electricity Generation, E_{wt} (kWh/yr)	13,140,000

along with the calculated actual capacity factor and the electricity cost savings per year using a national average electricity price of $0.067/kWh.

Table 4.5: Model outputs for electricity generation, capacity factor, and electricity cost savings for turbine model inputs shown in Table 4.4.

Location	Electricity Generation, E_w (kWh/yr)	Wind Turbine Capacity Factor, C_{fa}	Electricity Cost Savings, S_E ($/yr)
Logansport, IN	3,638,194	28%	$243,759
Gibson City, IL	3,617,686	28%	$242,385
Cambria, WI	3,230,696	25%	$216,457
Marshall, MN	2,987,391	23%	$200,155
Watertown, SD	4,791,081	37%	$321,002
Richardton, ND	4,684,691	36%	$313,874
Arthur, IA	3,529,384	27%	$236,469
St. Joseph, MO	3,326,208	25%	$222,856
Sutherland, NE	4,003,069	31%	$268,206
Torrington, WY	4,411,415	34%	$295,565
Burley, ID	2,301,014	18%	$154,168
Yuma, CO	4,032,489	31%	$270,177
Russell, KS	5,455,887	42%	$365,544
Arkalon, KS	6,456,334	49%	$432,574
Plainview, TX	5,685,127	44%	$380,903
Imperial Valley, CA	2,099,503	16%	$140,667
Stockton, CA	2,010,593	15%	$134,710
Maricopa, AZ	2,665,997	20%	$178,622

The capacity factors for the modeled turbines range from 15% to 49%. These values closely match the actual capacity factors for 50 wind projects built in 2010, which ranged from 18% to 53% (Wiser and Bolinger 2012). The power coefficient, capacity factor and design wind speed can be adjusted to obtain a desired capacity factor for a particular location. The range of electricity generated is quite large with the same wind turbine generating over 3 times the amount of energy in Arkalon, Kansas than in Stockton, CA. It is slightly unrealistic to use the same design turbine at all of the ethanol plant locations because different turbines would be selected for the precise wind conditions at the project site. This means that a 1.5 MW design turbine in an area with

lower wind speeds might have a 90 m rotor diameter while a 1.5 MW turbine in an area with higher wind speeds could have a rotor diameter of only 75 m. In such a case, the turbine with the larger rotor will most likely cost more and have a longer payback period. These two opposing factors allow the comparison of the same turbine to be valid for areas with differing wind speeds. Comparisons between the locations for the same turbine are meant to be general and a more thorough analysis would require considering different design turbines for different areas.

4.6 Evaluating Model Results for Wind Projects

The wind model can be used to evaluate a large range of project conditions to determine the economic feasibility of installing a wind turbine at an ethanol plant. The 18 ethanol plant locations were evaluated to determine if they provided a favorable opportunity for wind power development. Several input variables were changed to analyze the impact on payback period and cumulative cost savings.

Figure 4.12 shows the annual electricity production values from Table 4.5 for a 1.5 MW turbine and the annual average wind speed at each plant location. The large variation in electricity production for relatively small changes in wind speed can be clearly seen.

Installing a wind turbine can replace a substantial percentage of the total electricity needs of an ethanol plant. For this model an electricity requirement of 0.74 kWh/gal-ethanol was used. The 1.5 MW turbine modeled with input variables shown in Table 4.4 replaces between 4% and 50% of the electricity needs of the various ethanol plants. The percent shift to wind power and the individual plant capacity is shown in

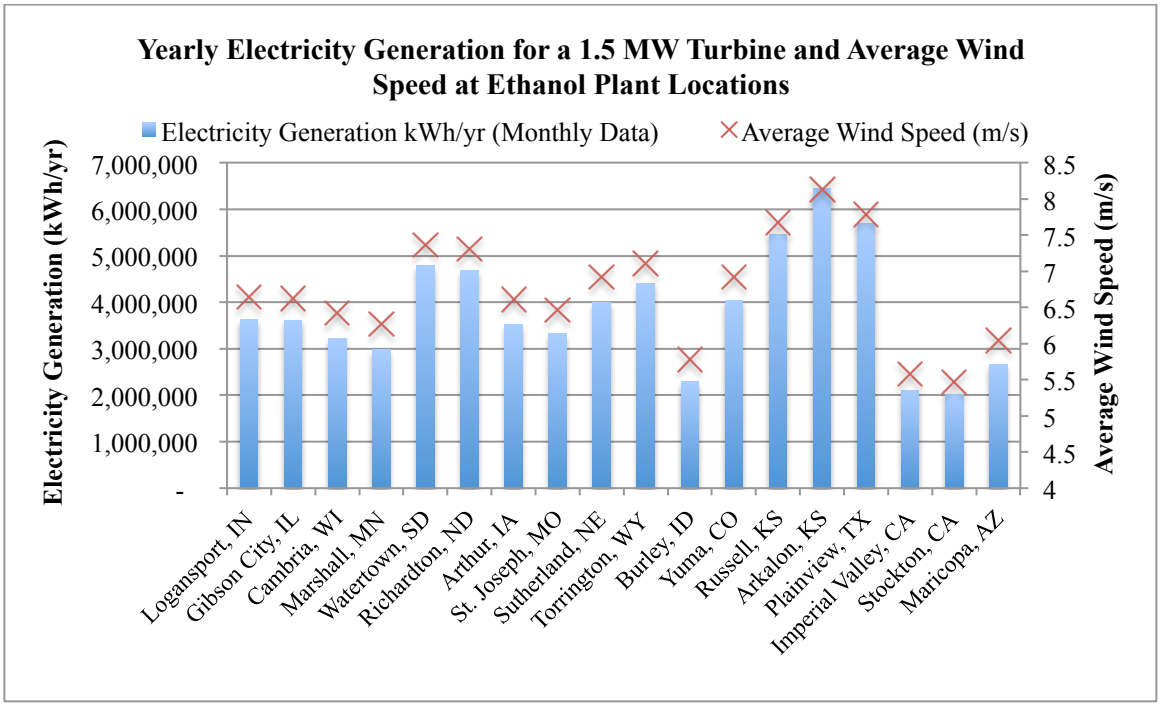

Figure 4.12: Average annual wind speed and electricity generation for a 1.5 MW turbine at different ethanol plant locations.

Figure 4.13 for each ethanol plant. This turbine may be slightly oversized for the Wyoming plant due to the large installed cost, but there is no issue with wasted energy with a wind turbine. The turbine is connected to the electrical grid so the next customers down the line would use any excess energy. To attain a higher percent shift to wind power a larger turbine or multiple turbines could be installed. Contracts with a utility company called a power purchase agreement (PPA) can be settled in which the utility company will purchase all of the electricity generated by the turbine. This means there is no penalty for consuming less energy than is produced by the turbine.

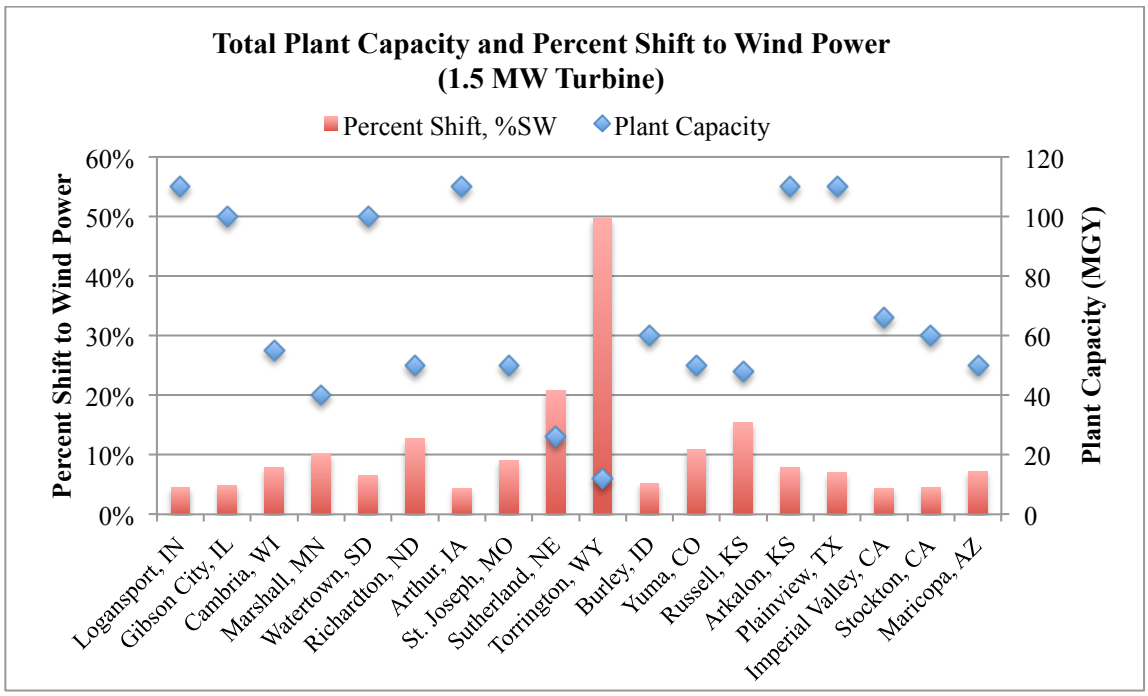

Figure 4.13: Plant capacity and percent shift to wind power for a 1.5 MW turbine for each ethanol plant.

Wind speeds change throughout the year, which will modify the electricity generated by the wind turbine. Typically wind speeds are lower in the summer and higher in the winter. Understanding the differences in electricity generated throughout the year will aid in project planning. Electricity rates are generally higher in the summer, which means electricity generated during peak loads in the summer can be worth much more than the same electricity generated during a winter night. Purchase agreements for the electricity may have varying rates depending when it is generated. This will influence payback periods and cumulative cost savings for the project. Figure 4.14 shows the monthly differences in electricity generation for a 1.5 MW turbine at four ethanol plant locations. All of the locations have lower wind speeds during the summer, but peak wind speeds differ between locations. The wind turbine in Wyoming produces 3 times the energy in January than July, and the turbine in Kansas generates double the

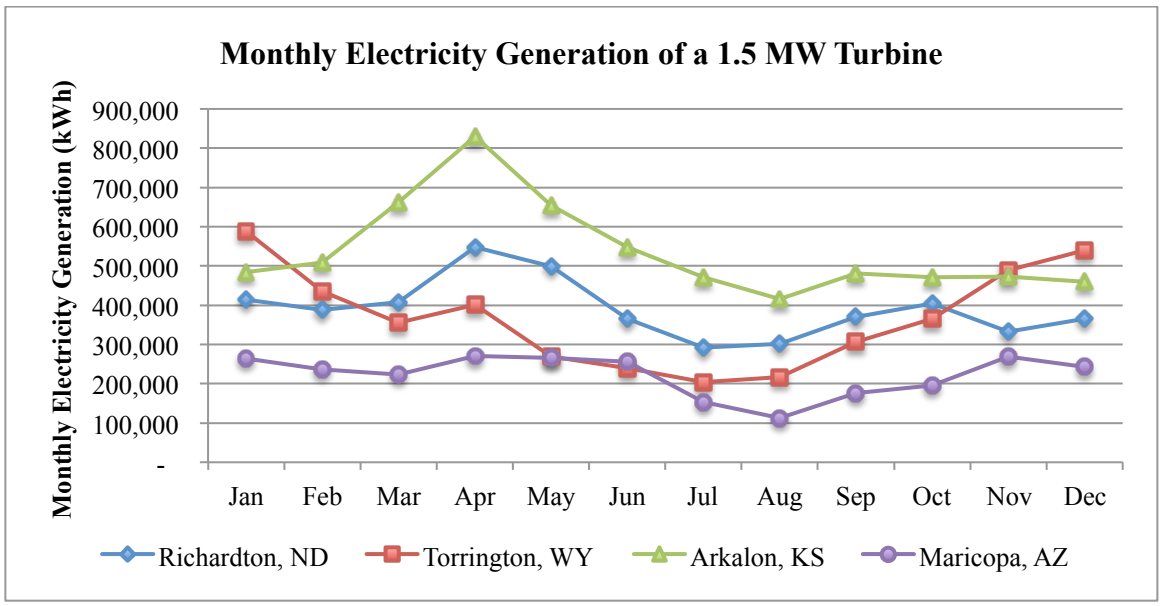

Figure 4.14: Monthly electricity generation for a 1.5 MW turbine in four locations.

energy in April as compared to August. Most of the other locations have monthly electricity variations similar to Kansas. The peak wind speeds occur in April and dip dramatically in July and August. The rate differences between electricity generated during peak demand periods should be considered when moving into secondary stages of wind project planning.

The payback periods and cumulative lifetime savings for the 1.5 MW turbine described in Table 4.4 were compared for all of the ethanol plant locations. The price input variables and the installed cost output are shown in Table 4.6. The average U.S. electricity rate is used along with an installed cost of $1,800/kW. No government incentives were applied to the installed cost or electricity rate. A yearly electricity rate increase of 2% was used to simulate inflation. This results in a total installed cost of $2.7 million. The payback periods ranged from less than 6 to over 16 years. It is clear that there are several locations that are not ideal candidates for wind power. Figure 4.15

shows the cumulative cost savings and payback periods of select locations to demonstrate the range of values. Stockton, CA has the longest payback period of over 16 years, and Arkalon, KS has the shortest payback period of less than 6 years. The Arkalon, KS wind turbine could potentially result in a cumulative cost savings of over $11 million over a 25-year lifespan. This is more than 4 times the purchase price of the original turbine.

Table 4.6: Model price inputs and installed cost output.

Price Inputs	
Current Average Price of Electricity for Industrial Sector, R_E ($/kWh)	0.067
Electricity Percent Price Increase Per Year, n_E	0.02
Wind Inputs	
Installed Cost of Wind Turbine, IC_{wt} ($/kW)	1800
Outputs	
Wind Turbine Installed Cost, WC	$2,700,000

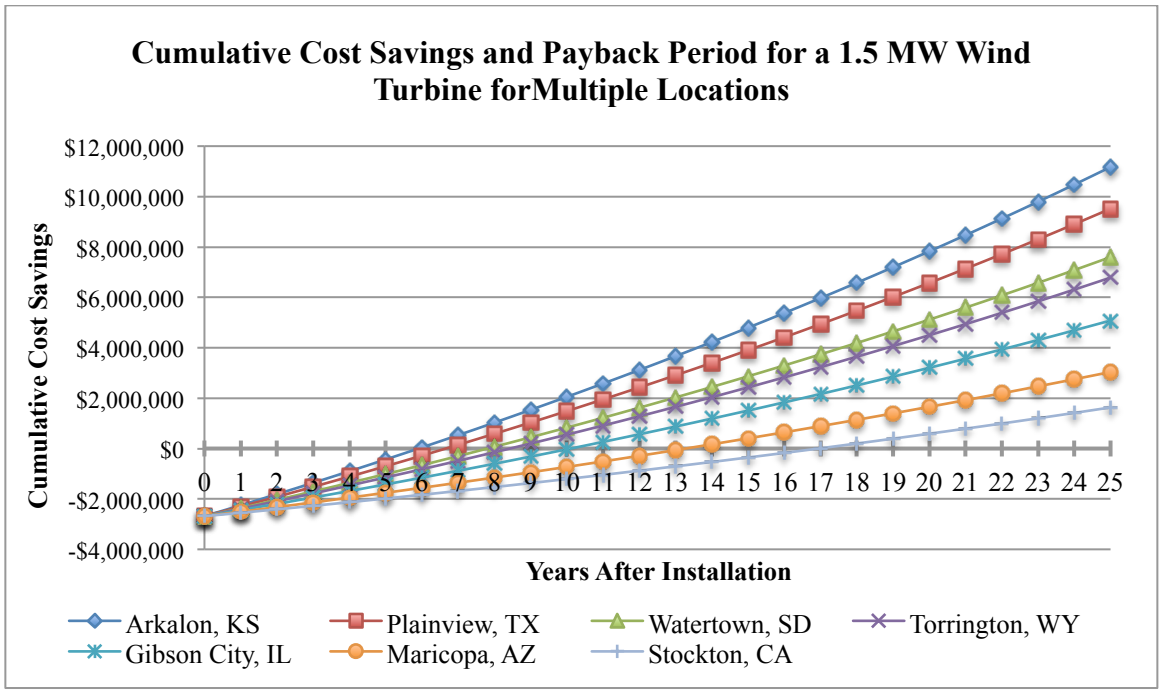

Figure 4.15: Modeled cumulative cost savings and payback period for a 1.5 MW turbine at 7 ethanol plant locations.

The values for payback period and cumulative savings shown in Figure 4.15 were calculated using the average electricity rate $0.067/kWh, but many of the average state rates for electricity differ significantly from this value. The payback period and cumulative cost savings using the state and national rates for electricity were compared for California and Wyoming in Figure 4.16. These two state electricity prices are far from the average, which results in large changes in the economic favorability of these two projects. The green curves show the cost savings for the national electricity rate, and the blue curves show the cost savings for the state prices. Using Wyoming's state electricity rate increased the payback period by two years and the cumulative savings was decreased by over $1.5 million. The payback period for the array in California was reduced by 5 years and the cumulative savings increased by over $2 million by using the average state electricity price. Using the correct state prices, the wind projects in

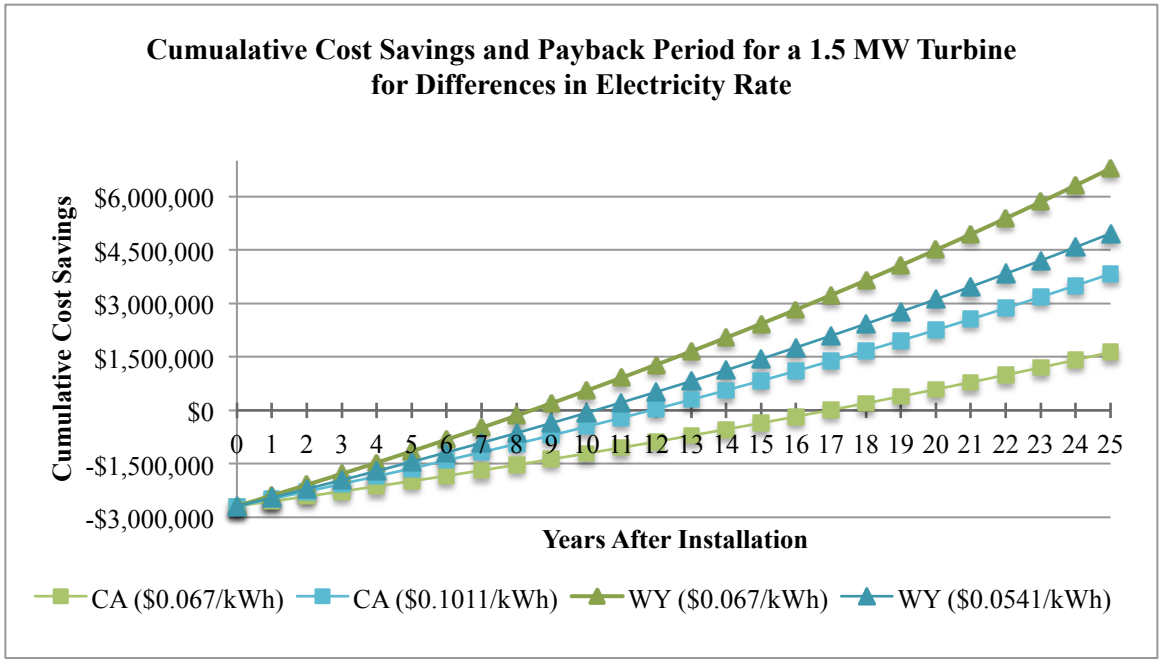

Figure 4.16: Cumulative cost savings and payback period for a 1.5 MW wind turbine for the average state and national electricity rates for Wyoming and California.

Wyoming and California went from opposite ends of the economic spectrum to very similar payback periods and cumulative cost savings. It is clear that state electricity rates play a large role in determining the feasibility of a wind project.

Model inputs can be changed to simulate federal incentives or various percent increases for the electricity rate. The 1.5 MW turbine described by the model inputs in Table 4.4 was used to show the effects of government incentives and electricity price increases for Arkalon, KS. Figure 4.17 shows the changes in payback period and cumulative cost savings for a steady electricity price of $0.0671/kWh, a 2% yearly rate increase, a 2% rate increase with the ITC, and a 2% yearly electricity rate increase and the PTC of $0.022/kWh for the first ten years. Figure 4.18 uses the same standard 1.5 MW turbine and economic conditions as Figure 4.17 for the Cambria, WI location with the average state electricity rate of $0.0733/kWh.

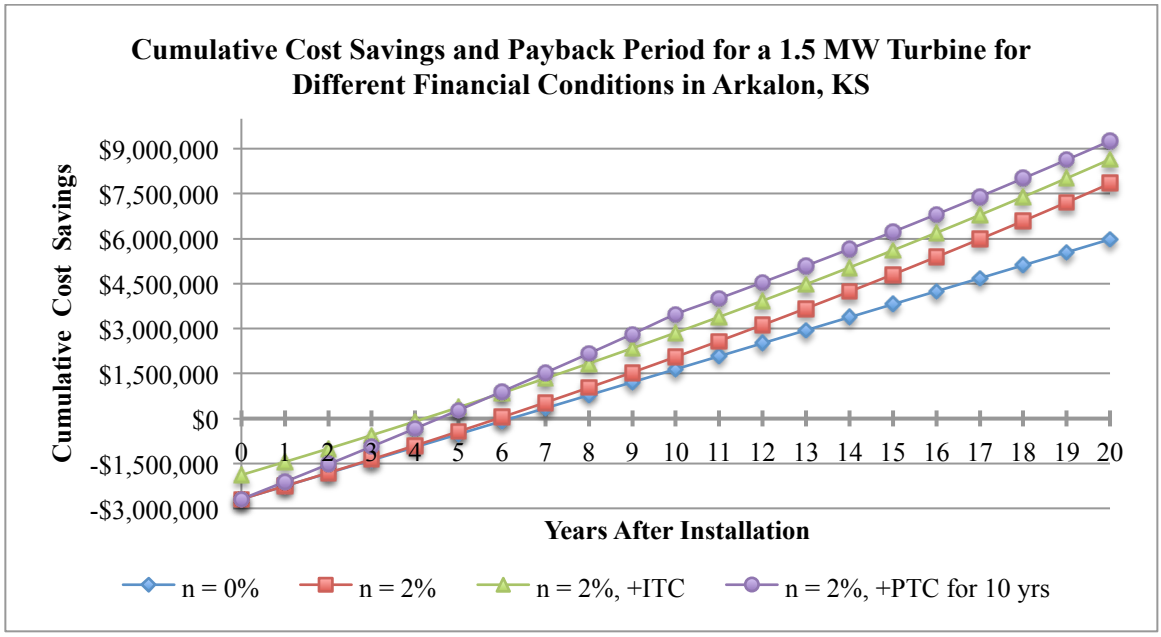

Figure 4.17: Cumulative cost savings and payback period for a 1.5 MW turbine in Arkalon, KS for a steady electricity rate, a 2% yearly rate increase, a 30% installed cost rebate, and a $0.022/kWh tax credit for the first ten years.

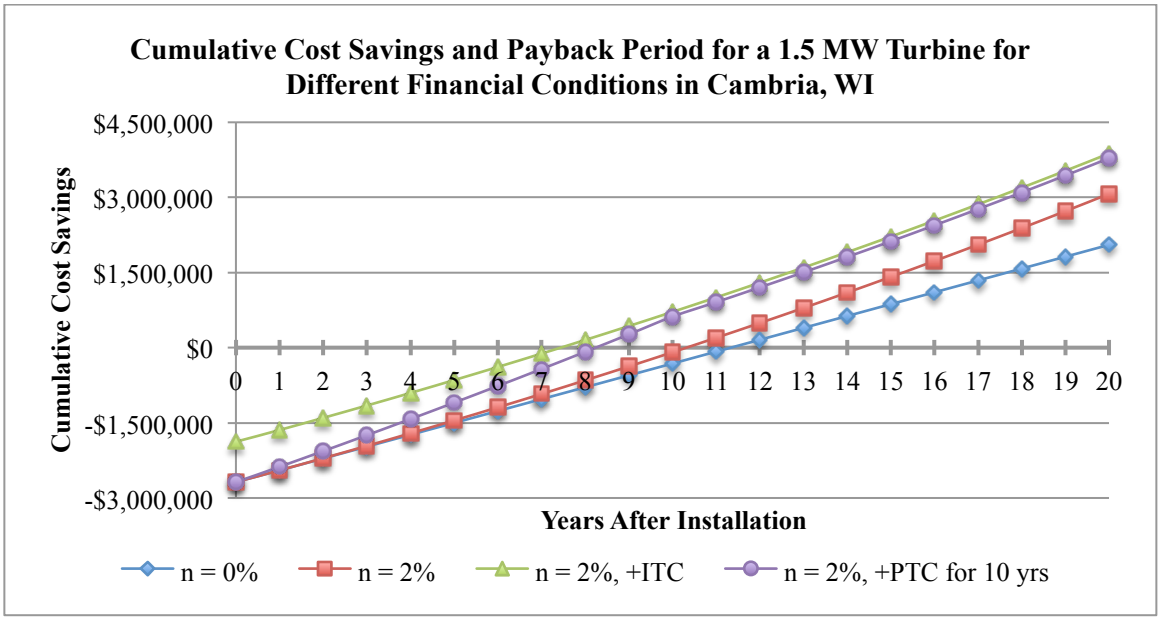

Figure 4.18: Cumulative cost savings and payback period for a 1.5 MW turbine in Cambria, WI for a steady electricity rate, a 2% yearly rate increase, a 30% installed cost rebate, and a $0.022/kWh tax credit for the first ten years.

All of the economic conditions considered in Figure 4.17 and 4.18 had only small effects on payback period with a slightly larger influence on the cumulative cost savings. The Investment Tax Credit (ITC) and Production Tax Credit (PTC) have similar influences on the payback period and cumulative savings. The ITC and PTC reduced the payback period for Arizona by about a year and a half. For the Wisconsin plant, the PTC reduced the payback period by 2 years, and the ITC reduced the payback period by 3 years compared to the 2% yearly electricity rate increase. There was very little difference in payback period for a flat electricity rate and a yearly increase of 2%. The rate increase did raise the cumulative savings by about $1 million for Wisconsin and nearly $1.9 million for Arizona over a 20-year lifespan. Both the PTC and ITC have similar results in reducing payback period and increasing the total profitability of a wind turbine project. The percent increase in electricity rate has only a small influence on reducing payback period, but does increase the total cost savings over the lifespan of a wind turbine.

Extension of the PTC and ITC will help improve the economic feasibility of wind projects, but the elimination of these tax credits will not doom the wind industry. These credits provide an incentive but do not significantly alter the feasibility of a wind project.

One of the largest influences on project viability is the cost of energy. Large differences in payback period and lifetime savings are observed when the average state rate for electricity is used instead of the national rate. The payback period for the state electricity rate was calculated for all of the ethanol plants for a realistic turbine using a moderate yearly price increase of 2%. Table 4.7 shows the state electricity price, the payback period, and the first year cost savings of a standard 1.5 MW wind turbine with inputs shown in Table 4.4 and the ITC applied to reduce the installed costs to $1,260/kW.

Table 4.7: Payback period and yearly cost savings using state electricity rate. Percent difference is from the yearly cost savings when using the average price $0.067/kWh.

Location	State Electricity Rate ($/kWh)	Payback Period (years)	First Year Cost Savings, S_W ($/yr)	Percent Difference
Logansport, IN	$0.0617	7.8	$224,477	-8.6%
Gibson City, IL	$0.0642	7.6	$232,255	-4.4%
Cambria, WI	$0.0733	7.4	$236,810	8.6%
Marshall, MN	$0.0647	9.0	$193,284	-3.6%
Watertown, SD	$0.0620	6.0	$297,047	-8.1%
Richardton, ND	$0.0624	6.1	$292,325	-7.4%
Arthur, IA	$0.0521	9.4	$183,881	-28.6%
St. Joseph, MO	$0.0585	8.9	$194,583	-14.5%
Sutherland, NE	$0.0643	6.9	$257,397	-4.2%
Torrington, WY	$0.0541	7.4	$238,658	-23.8%
Burley, ID	$0.0510	14.0	$117,352	-31.4%
Yuma, CO	$0.0706	6.3	$284,694	5.1%
Russell, KS	$0.0671	4.9	$366,090	0.1%
Arkalon, KS	$0.0671	4.2	$433,220	0.1%
Plainview, TX	$0.0624	5.1	$354,752	-7.4%
Imperial Valley, CA	$0.1011	8.2	$212,260	33.7%
Stockton, CA	$0.1011	8.6	$203,271	33.7%
Maricopa, AZ	$0.0655	9.8	$174,623	-2.3%

The percent difference between the yearly cost savings using the average rate of $0.067/kWh and the state average rate is shown in the last column. These values were chosen to give realistic but advantageous conditions for the installation of a wind turbine at the various ethanol plant locations.

Wind turbines are economically feasible at most ethanol plant locations. All of the ethanol plants except Idaho show payback periods less than 10 years. Texas and Kansas are the ideal locations for wind development due to high wind resources and moderate electricity rates. Both states have payback periods approximately 5 years or less. A 5-year payback period would be in the realm of possibility for most businesses due to lower financial risk. Colorado, North Dakota, and South Dakota are also good locations for wind development. All three states had payback periods less than 6.5 years. Projects in Indiana, Illinois, Wisconsin, and Wyoming would be slightly more risky with payback periods between 7 and 8 years, but would result in significant energy and cost savings for the ethanol plant. Wind projects could be economically feasible at all the other ethanol plant locations if additional incentives are available or electricity rates are higher at the plant's location than the state average. Wind power is a financially responsible choice that can provide energy and cost savings for ethanol plants across the country. The specific economic and wind resource conditions at each ethanol plant will ultimately determine how profitable a wind turbine would be.

This model can use either monthly or yearly wind resource data to provide energy and cost savings estimates. Model outputs for all of the ethanol plants using monthly and yearly data were compared to show if any errors were introduced between the methods. Table 4.8 shows the yearly averaged wind speed, the electricity generation using monthly

Table 4.8: Comparison of model outputs for monthly and yearly data inputs.

Location	Average Wind Speed (m/s)	Electricity Generation kWh/yr (Monthly Data)	Electricity Generation kWh/yr (Yearly Data)	Percent Difference
Logansport, IN	6.64	3,638,194	3,474,397	4.5%
Gibson City, IL	6.63	3,617,686	3,458,724	4.4%
Cambria, WI	6.42	3,230,696	3,140,367	2.8%
Marshall, MN	6.27	2,987,391	2,925,350	2.1%
Watertown, SD	7.36	4,791,081	4,731,607	1.2%
Richardton, ND	7.31	4,684,691	4,635,829	1.0%
Arthur, IA	6.61	3,529,384	3,427,517	2.9%
St. Joseph, MO	6.47	3,326,208	3,214,313	3.4%
Sutherland, NE	6.92	4,003,069	3,932,725	1.8%
Torrington, WY	7.1	4,411,415	4,247,665	3.7%
Burley, ID	5.78	2,301,014	2,291,705	0.4%
Yuma, CO	6.92	4,032,489	3,932,725	2.5%
Russell, KS	7.67	5,455,887	5,355,023	1.8%
Arkalon, KS	8.13	6,456,334	6,377,448	1.2%
Plainview, TX	7.79	5,685,127	5,610,320	1.3%
Imperial Valley, CA	5.58	2,099,503	2,061,949	1.8%
Stockton, CA	5.47	2,010,593	1,942,394	3.4%
Maricopa, AZ	6.04	2,665,997	2,615,087	1.9%

and yearly data, and the percent difference between the values. All the values calculated from monthly data are larger than the values calculated from the yearly average, but the differences are small. The largest percent difference is 4.5% and the smallest is only 0.4%. Yearly wind speeds can be used for this calculation with only small errors introduced. Since all of the calculations slightly underestimate turbine electricity generation, the use of yearly wind speeds will give a more conservative estimate of the power produced from the wind turbine.

This model can accurately estimate the payback period and cumulative cost savings of a wind turbine. Adjustments to turbine parameters and price inputs can show

the wide range of project possibilities. Small adjustments to wind speed and the cost of electricity have a large effect on the profitability of a wind project. The addition of government incentives and yearly electricity rate increases has a small influence on payback periods and a slightly larger effect on the lifetime cost savings of a turbine.

Wind turbines can be a very smart investment for many ethanol plants throughout the country. Payback periods will generally be under 10 years with a few locations under 5 years. Lifetime cost savings of a wind turbine can be 3 times the installed cost or more. Specific conditions at the ethanol plant location will determine how favorable a wind project will be.

4.7 Summary

This model accurately estimates the performance and cost savings of a solar array and a wind turbine. Changes to input variables can model a wide range of project conditions and have differing effects on model outputs. The economic feasibility of a solar array and wind turbine was investigated for 18 ethanol plant locations across the county. Solar thermal arrays and wind turbines are economically favorable for several ethanol plant locations. Wind power is generally more realistic due to a more established market and sufficient wind resources at many of the ethanol facilities across the U.S. Government incentives will continue to play a role in the economics of renewable energy projects.

CHAPTER 5: CONCLUSIONS AND RECOMMENDATIONS

5.1: Conclusions

Ethanol production plants are often in excellent locations for the application of solar thermal and wind projects. The rural setting of most ethanol plants provides ample space for a solar or wind installation with fewer logistical concerns than more populated areas. Corn ethanol production is predicted to increase slightly over the next 20 years to fulfill the RFS requirements, which ensures the market for ethanol will be strong in the foreseeable future. The use of renewable energy sources will reduce the fossil fuel consumption in the production of this renewable fuel. Ethanol's opponents cite the large energy requirements and the use of fossil fuel as two of the main arguments against corn ethanol. Wind and solar energy can help meet the needs of certain ethanol plants across the U.S.

Wind and solar projects can shift a significant amount of the energy burden from conventional fossil fuels to renewable sources. The results of the modeling show that when only the boiler makeup water is considered, a large solar thermal collector array can shift about 10% of this heating requirement for the largest ethanol plants in the country. A utility scale wind turbine can also provide 10% of the electricity requirements of the largest ethanol facilities. Much larger shifts to renewable energy are possible for smaller ethanol plants or larger solar and wind projects.

Solar thermal projects are most profitable in the Southwest, but high natural gas prices can dramatically improve the economics of a solar thermal array. California and Arizona are ideal locations for solar thermal projects, but very few ethanol plants are

located in these states. Missouri is home to a larger number of ethanol plants and has a high natural gas price, which vastly improves the profitability of a solar array in this state. Solar thermal systems in other states are generally only feasible if the actual natural gas rate paid by the plant is well above the state's average rate.

The profitability of solar thermal arrays depends greatly on government incentives. The Investment Tax Credit (ITC) reduces net installed costs, which decreases the payback period and allows solar projects to be more profitable. Payback periods are generally long for solar thermal systems even in areas with high solar resources and anything that can keep these timeframes lower will help build the industry.

Wind turbines are a very attractive option for reducing electricity consumption at ethanol plants. Most of the ethanol plants in the U.S. are located throughout the Midwest, which is where the largest wind resources are available. The wind industry is growing rapidly and is expected to continue this growth for the next 20 years. Installed costs and operation and maintenance costs are coming down, which improves project profitability. Some areas of the country can achieve payback periods less than 5 years for a utility scale turbine using the ITC. Higher electricity rates or larger wind speeds can reduce this payback period further. Even without government incentives, wind turbines can have reasonable payback periods and large lifetime cost savings. Neither the ITC nor the Production Tax Credit (PTC) significantly changed the profitability of the wind projects considered.

The wind resource values used for this model were regional averages and may not accurately represent wind speeds at each ethanol plant location. Wind speed can

dramatically change the economics of a wind project, so accurate values are essential in determining the economic feasibility of a wind project.

The profitability of a wind turbine is much higher than a solar thermal project for almost every ethanol plant location. The only exceptions are California, Arizona, and Idaho. However, these three states contain very few ethanol plants.

Both wind and solar projects are highly sensitive to changes in the price of energy. It is not sufficient to use national averages for industrial electricity and natural gas prices. State averages better represent the economics of a wind or solar project, but the energy prices for a specific plant will give a better estimate of payback period and lifetime savings. The electricity rate an ethanol plant is charged may not be the price they will be paid for electricity generated. Power price agreements (PPA) can be signed to determine how much the utility will pay for the electricity generated by a wind turbine. This value may be more or less (typically less) than what the plant pays for electricity.

The model results show only small differences when monthly and yearly resource inputs are used. Either method will give similar results, but a yearly average of solar insolation or wind speed will not accurately represent the monthly differences in the resource. Resource amounts can vary by up to 400% for some areas of the country. Energy prices may change throughout the year, so it is valuable to know when the solar or wind project will have low and high output.

Rate increases for electricity and natural gas do not have a large effect on payback periods. While predicting the future price of energy is not essential to get an accurate estimate of the payback period of a wind or solar project, energy rate increases can significantly increase the lifetime cost savings of a project.

This model is meant to aid in the beginning stages of a solar thermal or wind project, but is not intended to be a complete representation of all the factors that must be considered when planning a renewable energy project. There are several key aspects that are not addressed by this model. The cost of debt and specifically the interest on loans acquired to install the renewable energy project are not considered in the calculation of payback period or cost savings. This could influence the economics of the project. Operation and maintenance (O&M) costs can be included in the model by reducing the price of energy, but there are no specific methods to account for additional maintenance costs as the system ages or specific inputs to calculate these costs separately. Generally O&M costs are significantly lower than the yearly savings of the system, but these costs may influence payback period and lifetime project savings. The model also does not account for the depreciation of the wind turbine or solar array. A business owner may be able to claim the depreciation of the renewable energy project as a tax deduction, which would improve the finances of the project as a whole.

5.2 Recommendations

This model can provide valuable information to ethanol plants regarding the feasibility of a renewable energy project at their respective locations. Information from this research can be used to initiate a project or merely gain more information about wind and solar energy. Ethanol plants can reduce fossil fuel consumption, greenhouse gas emissions, and improve their public image by installing a renewable energy project. Renewable energy projects are not only good for the environment, but they provide a company reliable cost savings for 20 years or more.

There are some improvements that would make the model more accurate, but some of these changes may not be beneficial. The addition of separate O&M costs would give a broader picture of project costs and improve the accuracy of the model. Additional financial considerations including debt servicing and depreciation may not be appropriate for this type of model. The intended use of this model is a preliminary planning tool. Once the planning process has moved forward then all of the details of the specific location and the financial standing of the company can be considered. These additions may make the model too specific for users that may be just considering the idea of a renewable energy project. The scale of the projects considered would require extensive project planning with outside companies or firms, and they will aid the company with individualized financial calculations.

Government incentives should be continued for solar thermal projects. The ITC can significantly reduce the payback period for a solar thermal installation. This incentive is not set to expire for solar thermal systems until 2016, but if panel prices do not come down significantly in that time, the ITC should be extended. It will be difficult for this industry to grow in the future without continued support or reduced equipment prices.

The profitability of wind power does not depend on government incentives. Many in the wind industry forecast very low sales if the PTC is not extended past 2012. Sales will most likely decrease, but the tax credit does not drastically change the finances of a wind turbine. Wind turbines will be profitable without this tax credit, but eliminating it could stall growth in the near future. Long-term success of the wind industry will not depend on such tax credits.

REFERENCES

Aden, Andy. 2007. "Water Usage for Current and Future Ethanol Production." *Southwest Hydrology* 6, 4: 22-23 http://www.swhydro.arizona.edu/archive/V6_N5/feature4.pdf.

American Coalition for Ethanol (ACE). 2005. "Fuel Economy Study." http://www.ethanol.org/pdf/contentmgmt/ACEFuelEconomyStudy_001.pdf

American Wind Energy Association (AWEA). 2012. "AWEA U.S. Wind Industry Thrid Quarter 2012 Market Report." AWEA Data Services. http://www.awea.org/learnabout/publications/reports/AWEA-US-Wind-Industry-Market-Reports.cfm

Ayompe, L.M., A. Duffy, M. Mc Keever, M. Conlon, S.J. McCormack. 2011. "Comparative field performance study of flat plate and heat pipe evacuated tube collectors (ETCs) for domestic water heating systems in a temperate climate." *Energy* 36: 3370-3378

Clean Fuels Development Coalition (CFDC). 2010. "Ethanol Fact Book: A Compilation of Information About Fuel Ethanol." http://www.cleanfuelsdc.org/pubs/documents/CFDC%202010%20Ethanol%20Fact%20Book.pdf

Database of State Incentives for Renewables & Efficiency (DSIRE). 2012. "Financial Incentives." Accessed Oct 2012. http://dsireusa.org/incentives/index.cfm?EE=1&RE=1&SPV=0&ST=0&sector=Commercial&technology=Wind&sh=1

Edenhofer, Ottmar, Ramon Pichs-Madruga, Youba Sokona, et. al. 2011. "IPCC Special Report on Renewable Energy Sources and Climate Change Mitigation." Intergovernmental Panel on Climate Change (IPCC).

ENERCON GmbH. 2010. "ENERCON Wind Energy Converters-Product Overview." http://www.enercon.de/p/downloads/EN_Productoverview_0710.pdf

Farrell, Alexander E., Richard J. Plevin, Brian T. Turner, Andrew D. Jones, Michael O'Hare, Daniel M. Kammen. 2006. "Ethanol Can Contribute to Energy and Environmental Goals." *Science* 311(5760): 506-508.

Fay, James A. and Dan S. Golomb. 2012. "Energy and the Environment – Scientific and Technological Principles." New York: Oxford University Press.

Global Wind Energy Council (GWEC). 2012. "Interactive Map." Accessed Nov 6 2012 http://www.gwec.net/global-figures/interactive-map/

Institut für Solartechnik SPF (Institute for Solar Technology). 2012. *SPF Online Collector Catalogue*. http://www.solarenergy.ch/Collectors.111.0.html?&L=6

International Energy Agency (IEA). 2012. "Technology Roadmap: Solar Heating and Cooling." http://www.iea.org/publications/freepublications/publication/name,28277,en.html

International Energy Agency's Solar Heating and Cooling Programme (IEA SHC). 2004. "Recommendation: Converting Solar Thermal Collector area into installed capacity (m^2 to kW_{th})." Technical note from meeting proceedings, Gleisdorf, Austria. September 8. http://www.iea.org/publications/freepublications/publication/2012_SolarHeatingCooling_Roadmap_FINAL_WEB.pdf

Keeney, D.R., and T.H. DeLuca. 1992. "Biomass as an Energy Source for the Midwestern U.S." *American Journal of Alternative Agriculture* 7: 137-144

Knoll, Keith, et al. 2009. "Effects of Intermediate Ethanol Blends on Legacy Vehicles and Small Non-road Engines, Report 1 – Updated." NREL: NREL/TP-540-43543

Laylin, Tafline. 2012. "World's Largest (Gargantuan) Solar Thermal Plant Opens in Saudi Arabia." Green Prophet. http://www.greenprophet.com/2012/04/worlds-largest-solar-thermal-plant/

Liska, Adam J. et al. 2009. "Improvements in the Life Cycle Energy Efficiency and Greenhouse Gas Emissions of Corn-Ethanol." *Journal of Industrial Ecology* 13.1: 58-74

Mueller, Steffen. 2010. "Detailed Report: 2008 National Dry Mill Corn Ethanol Survey." University of Illinois at Chicago, Energy Resources Center. http://www.ethanol.org/pdf/contentmgmt/Ethanol_production_efficiency_U_of_IL_spring_2010.pdf.

National Renewable Energy Laboratory (NREL). 2012. http://www.nrel.gov/

Niven, Robert K. 2004. "Ethanol in Gasoline: Environmental Impacts and Sustainability Review Article." *Renewable and Sustainable Energy Reviews* 9: 535-555.

Perlack, Robert D. et al. 2005. "Biomass as Feedstock For Bioenergy and Bioproducts Industry: The Technical Feasibility of a Billion-Ton Annual Supply." DOE, USDA: DOE/GO-102005-2135. http://www1.eere.energy.gov/biomass/pdfs/final_billionton_vision_report2.pdf.

Pimentel, David. 2001. "Ethanol Fuels: Energy Balance, Economics, and Environmental Impacts are Negative." *Natural Resources Research* 12: 127-134.

Ragheb, Magdi and Adam M. Ragheb. 2011. "Wind Turbines Theory - The Betz Equation and Optimal Rotor Tip Speed Ratio, Fundamental and Advanced Topics in Wind Power." Dr. Rupp Carriveau (Ed.), ISBN: 978-953-307-508-2, InTech. http://www.intechopen.com/books/fundamental-and-advanced-topicsin-wind

power/wind-turbines-theory-the-betz-equation-and-optimal-rotor-tip-speed-ratio

Renewable Fuels Association (RFA). 2012a. "2012 Ethanol Industry Outloo*k*." Renewable Fuels Association: Washington DC. http://www.ethanolrfa.org/pages/annual-industry-outlook.

Renewable Fuels Association (RFA). 2012b. http://www.ethanolrfa.org/

RETScreen International. 2005. "RETScreen Software Online User Manual-Solar Water Heating Project Model." Natural Resources, Canada, www.retscreen.net.

RETScreen International. 2012. www.retscreen.net.

Roney, Matthew J. 2012. "Wind Tops 10 Percent Share of Electricity in Five U.S. States." Earth Policy Institute. http://www.earth-policy.org/data_highlights/2012/highlights27

Stackhouse, Paul W. 2012. "Surface Meterorology and Solar Energy-A renewable energy resource web site." NASA, POWER: (release 6.0) http://eosweb.larc.nasa.gov/cgi-bin/sse/sse.cgi?+s01#s01

Shapouri, Hosein, James A. Duffeild, and Michael S. Graboski. 2002. "The Energy Balance of Corn Ethanol: An Update." USDA, AER-813

Swofford, Jeff. 2010. "AWEA Conducts National Wind Energy Survey." Energy Boom. http://www.energyboom.com/wind/awea-conducts-national-wind-energy-survey

Tegen, S., M. Hand, B. Maples, E. Lantz, P. Schwabe, and A. Smith. 2010. "2010 Cost of Wind Energy Review." NREL: NREL/TP-5000-52920

U.S. Department of Agriculture (USDA), National Agricultural Statistics Service. 2012. "Production by Country and Location of Ethanol Plants."

http://www.nass.usda.gov/Charts_and_Maps/Ethanol_Plants/U._S._Ethanol_Plants/index

U.S. Department of Energy (DOE). 2008. "Biofuels & Greenhouse Gas Emissions: Myths versus Facts." http://www.doe.gov/downloads/ethanol-myths-and-facts.

U.S. Department of Energy (DOE). 2012. "U.S. Consumption of Ethanol and MTBE Oxygenates." Alternative Fuels Data Center. http://www.afdc.energy.gov/data/tab/all/data_set/10322.

U.S. Energy Information Administration (EIA). 2011. "International Energy Outlook 2011." DOE,EIA: DOE/EIA-0484(2011).

U.S. Energy Information Administration (EIA). 2012a. "Annual Energy Outlook 2012: With Projections to 2035." DOE, EIA: DOE/EIA-0383(2012).

U.S. Energy Information Administration (EIA). 2012b. "Annual Energy Review 2011." DOE, EIA: DOE/EIA-0384(2011).

U.S. Energy Information Administration (EIA). 2012c. www.eia.gov

U.S. Environmental Protection Agency (EPA). 2012. "E15 (a blend of gasoline and ethanol)." website www.epa.gov/otaq/regs/fuels/additive/e15.

Wang, Michael, May Wu, and Hong Huo. 2007. "Life-cycle Energy and Greenhouse Gas Emission Impacts of Different Corn Ethanol Plant Types." *Environmental Research Letters 2: 024001*

Wiser, Ryan and Mark Bolinger. 2012. "2011 Wind Technologies Market Report." DOE: DOE/GO-102012-3472

APPENDIX A

Meteorological and Resources Date for Ethanol Plant Locations

The following tables show the meteorological and resource data for each ethanol plant location. The data was obtained from NASA's Surface Meteorology and Solar Energy website (Stackhouse 2012) using the latitude and longitude shown in Table A.19. The insolation on a tilted surface (G_t) in kWh/m^2/day is given for the tilt angle shown in Table A.19 for each location. The ambient temperature (T_a) at 10 meters about the earth's surface is in degree Celsius. The average wind (V_{wa}) in m/s is for 80 meters above the earth's surface. The average number of sunlight hours per day (H_{day}) is also given for each month of the year. The production capacity in million gallons of ethanol per year (MGY) for each plant is shown in Table A.19.

Table A.1: Meteorological and resource data for Logansport, IN

	Jan	Feb	Mar	Apr	May	Jun	Jul	Aug	Sep	Oct	Nov	Dec	Annual Average
G_t	2.7	3.3	4.05	4.76	5.21	5.67	5.85	5.38	5.04	4.03	2.68	2.31	4.25
T_a	-3.17	-0.68	4.07	11.2	17.5	22.2	24	22.9	18.9	13	6.28	-0.77	11.3
V_{wa}	7.58	7.27	7.4	7.68	6.73	6.1	5.45	5.24	5.69	6.38	7.02	7.2	6.64
H_{day}	9.61	10.7	11.9	13.2	14.4	15	14.7	13.7	12.5	11.1	9.96	9.33	12.18

Table A.2: Meteorological and resource data for Gibson City, IL

	Jan	Feb	Mar	Apr	May	Jun	Jul	Aug	Sep	Oct	Nov	Dec	Annual Average
G_t	2.76	3.31	4.13	4.84	5.34	5.73	5.94	5.43	5.06	4.12	2.78	2.38	4.32
T_a	-3.63	-0.83	4.43	11.7	18	22.8	24.8	23.7	19.5	13.6	6.17	-1.13	11.6
V_{wa}	7.39	7.18	7.44	7.79	6.77	6.11	5.44	5.24	5.72	6.45	7.01	7.09	6.63
H_{day}	9.65	10.7	11.9	13.2	14.4	15	14.7	13.7	12.5	11.1	9.98	9.35	12.18

Table A.3: Meteorological and resource data for Cambria, WI

	Jan	Feb	Mar	Apr	May	Jun	Jul	Aug	Sep	Oct	Nov	Dec	Annual Average
G_t	3.02	3.84	4.37	4.81	5.31	5.68	5.72	5.26	4.68	3.68	2.73	2.55	4.31
T_a	-8.36	-5.51	0.32	8.02	15	20.7	22.9	21.6	17	10	1.88	-5.43	8.27
V_{wa}	6.88	6.7	6.87	7.46	6.67	6.14	5.51	5.36	5.78	6.42	6.72	6.62	6.42
H_{day}	9.36	10.5	11.9	13.4	14.7	15.3	15	13.9	12.5	11	9.75	9.01	12.19

Table A.4: Meteorological and resource data for Marshall, MN

	Jan	Feb	Mar	Apr	May	Jun	Jul	Aug	Sep	Oct	Nov	Dec	Annual Average
G_t	2.86	3.38	4.16	4.99	5.44	5.78	6.07	5.59	4.77	3.91	2.83	2.41	4.36
T_a	-11.1	-8.05	-1.83	7.03	14.6	19.5	21.6	20.4	15.4	8.07	-1.37	-8.61	6.38
V_{wa}	6.31	6.21	6.7	7.52	6.81	6.14	5.49	5.56	5.98	6.25	6.25	6.01	6.27
H_{day}	9.26	10.5	11.9	13.4	14.7	15.4	15.1	14	12.5	11	9.66	8.91	12.19

Table A.5: Meteorological and resource data for Watertown, SD

	Jan	Feb	Mar	Apr	May	Jun	Jul	Aug	Sep	Oct	Nov	Dec	Annual Average
G_t	2.89	3.48	4.37	5.12	5.62	5.96	6.21	5.86	5.02	4.11	3.04	2.54	4.52
T_a	-10.9	-7.74	-1.67	6.83	14.3	19.1	21.2	20	15	7.56	-1.75	-8.52	6.2
V_{wa}	7.41	7.32	7.72	8.51	7.87	7.15	6.6	6.82	7.17	7.39	7.25	7.1	7.36
H_{day}	9.23	10.4	11.9	13.4	14.8	15.5	15.2	14	12.5	11	9.63	8.88	12.20

Table A.6: Meteorological and resource data for Richardton, ND

	Jan	Feb	Mar	Apr	May	Jun	Jul	Aug	Sep	Oct	Nov	Dec	Annual Average
G_t	2.24	3.35	4.25	5.23	5.76	6.12	6.41	5.92	4.93	3.7	2.59	2.03	4.38
T_a	-10.8	-7.9	-2.54	5.49	12.9	17.7	20.4	19.3	13.3	5.84	-3.19	-8.86	5.22
V_{wa}	7.48	7.32	7.44	8.21	7.96	7.17	6.66	6.73	7.21	7.42	6.95	7.17	7.31
H_{day}	9	10.3	11.9	13.5	15	15.8	15.4	14.2	12.6	10.9	9.43	8.61	12.22

Table A.7: Meteorological and resource data for Arthur, IA

	Jan	Feb	Mar	Apr	May	Jun	Jul	Aug	Sep	Oct	Nov	Dec	Annual Average
G_t	2.84	3.46	4.21	4.87	5.4	5.91	6.03	5.62	4.97	4.09	2.95	2.62	4.42
T_a	-8.35	-5.23	0.93	8.94	15.7	20.5	22.7	21.7	16.9	9.91	0.85	-6.01	8.3
V_{wa}	6.84	6.78	7.25	8	7.11	6.4	5.7	5.68	6.04	6.38	6.65	6.54	6.61
H_{day}	9.46	10.6	11.9	13.3	14.5	15.2	14.9	13.8	12.5	11.1	9.85	9.15	12.19

Table A.8: Meteorological and resource data for St. Joseph, MO

	Jan	Feb	Mar	Apr	May	Jun	Jul	Aug	Sep	Oct	Nov	Dec	Annual Average
G_t	3.14	3.48	4.52	5.04	5.48	5.89	6.09	5.63	5.24	4.35	3.17	2.87	4.58
T_a	-3.45	-0.52	5.32	12.1	17.8	22.4	25	24.4	19.4	13.2	5.15	-1.5	11.70
V_{wa}	6.79	6.85	7.35	7.81	6.74	6.12	5.56	5.43	5.78	6.14	6.55	6.56	6.47
H_{day}	9.69	10.7	11.9	13.2	14.3	14.9	14.6	13.7	12.4	11.2	10	9.41	12.17

Table A.9: Meteorological and resource data for Sutherland, NE

	Jan	Feb	Mar	Apr	May	Jun	Jul	Aug	Sep	Oct	Nov	Dec	Annual Average
G_t	3.25	3.94	4.77	5.46	5.91	6.51	6.61	6.22	5.53	4.6	3.48	3.14	4.96
T_a	-4	-2.13	2.5	8.19	14	18.3	20.8	19.7	15.1	8.44	0.67	-3.76	8.22
V_{wa}	7.66	7.09	7.14	7.55	7	6.4	6.05	6.08	6.73	6.8	7.21	7.38	6.92
H_{day}	9.58	10.6	11.9	13.3	14.4	15	14.8	13.8	12.5	11.1	9.93	9.28	12.1825

Table A.10: Meteorological and resource data for Torrington, WY

	Jan	Feb	Mar	Apr	May	Jun	Jul	Aug	Sep	Oct	Nov	Dec	Annual Average
G_t	3.09	3.74	4.68	5.31	6.01	6.47	6.43	6.07	5.5	4.59	3.31	2.91	4.85
T_a	-3.76	-2.29	2.18	7.11	12.9	17.5	20.9	20	14.8	7.92	0.22	-4	7.86
V_{wa}	8.41	7.61	7.11	7.4	6.48	6.23	5.91	6.03	6.77	7.18	7.91	8.17	7.1
H_{day}	9.5	10.6	11.9	13.3	14.5	15.1	14.9	13.8	12.5	11.1	9.86	9.19	12.19

Table A.11: Meteorological and resource data for Burley, ID

	Jan	Feb	Mar	Apr	May	Jun	Jul	Aug	Sep	Oct	Nov	Dec	Annual Average
G_t	3.03	3.78	4.94	5.77	6.3	6.99	7.09	6.67	6.01	4.92	3.26	2.87	5.14
T_a	-6.42	-4.05	1.6	6.89	12.4	17.9	22.9	21.6	15.2	7.92	-0.36	-5.99	7.55
V_{wa}	5.68	5.65	5.52	5.87	5.83	5.78	5.9	5.83	5.84	5.68	6.02	5.82	5.78
H_{day}	9.44	10.6	11.9	13.3	14.6	15.2	14.9	13.9	12.5	11.1	9.83	9.15	12.20

Table A.12: Meteorological and resource data for Yuma, CO

	Jan	Feb	Mar	Apr	May	Jun	Jul	Aug	Sep	Oct	Nov	Dec	Annual Average
G_t	3.34	3.97	4.95	5.64	6.08	6.69	6.65	6.31	5.71	4.8	3.63	3.22	5.09
T_a	-2.29	-0.76	3.81	8.96	14.3	18.3	20.8	19.7	15.5	9.17	1.71	-2.47	8.95
V_{wa}	7.44	7.28	7.48	8.11	7.47	6.66	6.03	5.95	6.36	6.48	6.77	7.02	6.92
H_{day}	9.68	10.7	11.9	13.2	14.3	14.9	14.7	13.7	12.4	11.2	10	9.38	12.17

Table A.13: Meteorological and resource data for Russell, KS

	Jan	Feb	Mar	Apr	May	Jun	Jul	Aug	Sep	Oct	Nov	Dec	Annual Average
G_t	3.95	4.11	4.96	5.31	5.49	5.68	6.02	5.77	5.48	4.93	4.1	3.77	4.97
T_a	-2.1	0.48	5.73	11.8	17.2	21.6	24.3	23.9	19.3	13.1	4.86	-1	11.6
V_{wa}	7.52	7.65	8.4	9.07	8.22	7.66	7.16	6.93	7.28	7.34	7.45	7.4	7.67
H_{day}	9.78	10.8	11.9	13.2	14.2	14.8	14.6	13.6	12.4	11.2	10.1	9.51	12.17

Table A.14: Meteorological and resource data for Arkalon, KS

	Jan	Feb	Mar	Apr	May	Jun	Jul	Aug	Sep	Oct	Nov	Dec	Annual Average
G_t	4.04	4.31	5.26	5.75	5.84	5.92	6.22	5.9	5.7	5.19	4.32	3.84	5.2
T_a	-0.84	1.52	6.27	12.3	17.1	21	23.6	22.9	18.7	12.6	4.88	-0.42	11.7
V_{wa}	7.88	8.01	8.75	9.43	8.71	8.21	7.81	7.49	7.86	7.81	7.82	7.75	8.13
H_{day}	9.93	10.8	11.9	13.1	14.1	14.6	14.4	13.5	12.4	11.2	10.2	9.68	12.15

Table A.15: Meteorological and resource data for Plainview, TX

	Jan	Feb	Mar	Apr	May	Jun	Jul	Aug	Sep	Oct	Nov	Dec	Annual Average
G_t	4.4	4.76	5.81	6.33	6.07	6.15	6.31	5.96	5.71	5.56	4.66	4.22	5.5
T_a	2.63	5.12	9.46	14.9	18.8	21.8	24.2	23.6	19.8	14.7	7.66	2.36	13.8
V_{wa}	7.52	7.84	8.41	8.89	8.38	8.02	7.41	7.01	7.41	7.49	7.63	7.47	7.79
H_{day}	10.1	11	11.9	13	13.9	14.3	14.2	13.4	12.4	11.3	10.4	9.93	12.15

Table A.16: Meteorological and resource data for Imperial Valley, CA

	Jan	Feb	Mar	Apr	May	Jun	Jul	Aug	Sep	Oct	Nov	Dec	Annual Average
G_t	4.55	5.16	6.14	6.47	6.64	6.57	6.19	6.06	6	5.64	4.93	4.44	5.73
T_a	11.4	12.8	15.7	18.9	22.4	25.6	29	29.2	26.5	21.5	15.2	11.1	20
V_{wa}	5.69	5.63	5.55	5.78	6.33	6.21	5.46	4.99	5.21	4.99	5.61	5.58	5.58
H_{day}	10.2	11	11.9	12.9	13.8	14.2	14	13.3	12.4	11.4	10.5	10	12.13

Table A.17: Meteorological and resource data for Stockton, CA

	Jan	Feb	Mar	Apr	May	Jun	Jul	Aug	Sep	Oct	Nov	Dec	Annual Average
G_t	3.87	4.59	5.73	6.56	6.73	6.83	6.64	6.57	6.33	5.78	4.46	3.63	5.65
T_a	9.89	10.2	11.4	13.8	17	20.2	22	21.6	20.5	17.9	12.9	10	15.6
V_{wa}	4.8	5.28	5.52	5.88	6.33	6.43	6.08	5.59	5.28	4.74	4.83	4.91	5.47
H_{day}	9.86	10.8	11.9	13.1	14.2	14.7	14.5	13.6	12.4	11.2	10.1	9.58	12.16

Table A.18: Meteorological and resource data for Maricopa, AZ

	Jan	Feb	Mar	Apr	May	Jun	Jul	Aug	Sep	Oct	Nov	Dec	Annual Average
G_t	4.89	5.52	6.42	6.81	6.72	6.55	6.06	5.76	6.01	5.8	5.2	4.7	5.87
T_a	8.66	10.2	13.5	17.6	22.7	26.9	29.7	28.5	25.3	19.8	12.6	8.33	18.7
V_{wa}	6.44	6.2	6.09	6.49	6.45	6.38	5.37	4.85	5.63	5.83	6.48	6.26	6.04
H_{day}	10.2	11	11.9	12.9	13.8	14.3	14.1	13.3	12.4	11.3	10.5	10	145.7

Table A.19: Ethanol plant coordinates and solar panel tilt angle used for insolation values

Location	Plant Capacity (MGY)	Latitude	Longitude	Panel Tilt Angle
Logansport, IN	110	40.72	-86.44	25°
Gibson City, IL	100	40.47	-88.4	25°
Cambria, WI	55	43.54	-89.11	28°
Marshall, MN	40	44.47	-95.78	29°
Watertown, SD	100	44.88	-97.11	29°
Richardton, ND	50	46.88	-102.31	31°
Arthur, IA	110	42.32	-95.34	27°
St. Joseph, MO	50	39.74	-94.85	24°
Sutherland, NE	26	41.16	-101.09	26°
Torrington, WY	12	42.04	-104.2	27°
Burley, ID	60	42.52	-113.81	27°
Yuma, CO	50	40.13	-102.68	25°
Russell, KS	48	38.9	-98.85	38°
Arkalon, KS	110	37.08	-100.85	37°
Plainview, TX	110	34.18	-101.63	34°
Imperial Valley, CA	66	32.75	-115.59	32°
Stockton, CA	60	37.94	-121.34	37°
Maricopa, AZ	50	33.03	-112.01	33°

APPENDIX B

Average U.S. Energy Prices by State

Table B.1 gives the average price of natural gas in $/MMBtu for the industrial sector for the U.S. and each state in 2010 and selected states in 2011 (EIA 2012c). Many states did not have values available for 2011. These values were converted from $/ft^3 to $/MMBtu using the average heat content of natural gas in 2011, 1.023 MMBtu/ft^3 (EIA 2012c).

Table B.2 gives the average price of electricity in ¢/kWh for the industrial sector for the U.S., each state, and each region of the country for 2011 (EIA 2012c).

Table B.1: Average Natural Gas Prices for U.S. states in 2010 and 2011 (EIA 2012c)
* prices unavailable

Natural Gas Industrial Retail Prices ($/MMBtu)		
	2010	**2011**
U.S. Average	**5.37**	**5.00**
Alabama	6.52	5.23
Alaska	4.13	3.75
Arizona	7.37	6.71
Arkansas	7.12	*
California	6.86	6.88
Colorado	5.71	*
Connecticut	9.38	*
Delaware	9.95	11.42
Florida	8.14	8.47
Georgia	6.11	5.99
Hawaii	23.56	29.13
Idaho	6.25	*
Illinois	6.97	6.59
Indiana	5.52	*
Iowa	5.96	5.71
Kansas	5.38	*
Kentucky	5.44	5.11
Louisiana	4.57	*
Maine	10.98	*
Maryland	8.85	8.43
Massachusetts	11.28	*
Michigan	9.04	8.07
Minnesota	5.45	5.44
Mississippi	6.05	5.57
Missouri	8.50	8.24
Montana	7.89	*
Nebraska	5.72	5.44
Nevada	10.29	8.78
New Hampshire	11.33	*
New Jersey	9.41	*
New Mexico	6.03	5.78
New York	8.36	*
North Carolina	8.05	7.49
North Dakota	5.10	4.97
Ohio	7.23	6.98
Oklahoma	8.20	7.13
Oregon	6.89	*
Pennsylvania	8.04	*
Rhode Island	11.86	*
South Carolina	5.97	5.44
South Dakota	5.79	5.89
Tennessee	6.49	6.03
Texas	4.51	4.11
Utah	5.44	5.37
Vermont	6.42	*
Virginia	6.53	*
Washington	9.16	*
West Virginia	5.28	4.78
Wisconsin	7.39	6.79
Wyoming	4.80	*

Table B.2: Average electricity rates in 2011 for each state (EIA 2012c)

Average Electricity Industrial Retail Price for 2011 (¢/kWh)			
Location	**Average Industrial Retail Price (Cents/kWh)**	**Location**	**Average Industrial Retail Price (Cents/kWh)**
New England	**12.55**	North Carolina	6.01
Connecticut	13.24	South Carolina	5.94
Maine	8.88	Virginia	6.49
Massachusetts	13.38	West Virginia	6.18
New Hampshire	12.27	**East South Central**	**6.19**
Rhode Island	11.27	Alabama	6.25
Vermont	9.83	Kentucky	5.33
Middle Atlantic	**8.17**	Mississippi	6.53
New Jersey	11.43	Tennessee	7.23
New York	7.83	**West South Central**	**6.00**
Pennsylvania	7.73	Arkansas	5.63
East North Central	**6.53**	Louisiana	5.69
Illinois	6.42	Oklahoma	5.46
Indiana	6.17	Texas	6.24
Michigan	7.32	Mountain	6.08
Ohio	6.12	Arizona	6.55
Wisconsin	7.33	Colorado	7.06
West North Central	**6.08**	Idaho	5.10
Iowa	5.21	Montana	5.27
Kansas	6.71	Nevada	6.65
Minnesota	6.47	New Mexico	6.06
Missouri	5.85	Utah	5.10
Nebraska	6.43	Wyoming	5.41
North Dakota	6.24	**Pacific Contiguous**	**7.62**
South Dakota	6.20	California	10.11
South Atlantic	6.66	Oregon	5.47
Delaware	8.91	Washington	4.09
District of Columbia	6.89	**Pacific Noncontiguous**	**25.02**
Florida	8.55	Alaska	15.71
Georgia	6.60	Hawaii	28.40
Maryland	8.76	**U.S. Total**	**6.82**